

Diffraction optics: An old subject teaches new tricks

Kwangje Woo
Dimitrios Koukis
Sinan Selcuk
Art Hebard

Stacy Wise
Volker Quetschke
Guidp Mueller
Dave Reitze

UF Physics

Sergei Shabanov
Paul Holloway
Chuck Schau
Andrei Borisov

UF Math
UF Materials Science
Raytheon
CNRS

G. McGuire
O. Shenderova

International Technology Center



Outline

1. “White light” optical cavities

- The diffraction of light affects optical path only



Outline

1. “White light” optical cavities
 - The diffraction of light affects optical path only
2. Enhanced transmission of light by sub-wavelength hole arrays
 - If $r < \lambda$, no light is transmitted by a hole



Outline

1. “White light” optical cavities
 - The diffraction of light affects optical path only
2. Enhanced transmission of light by sub-wavelength hole arrays
 - If $r < \lambda$, no light is transmitted by a hole
3. Beaming of light by structures around a single hole
 - If $r < \lambda$, the transmitted light is scattered into 90°



Outline

1. “White light” optical cavities
 - The diffraction of light affects optical path only
2. Enhanced transmission of light by sub-wavelength hole arrays
 - If $r < \lambda$, no light is transmitted by a hole
3. Beaming of light by structures around a single hole
 - If $r < \lambda$, the transmitted light is scattered into 90°
4. Imaging by “photon sieves” (a bunch of holes)
 - Images require curved glass or curved mirror surfaces



White light cavities

- The grating pulse compressor/expander
- Idea: white light cavities from two parallel gratings
- It doesn't work!
- Phase shift by gratings

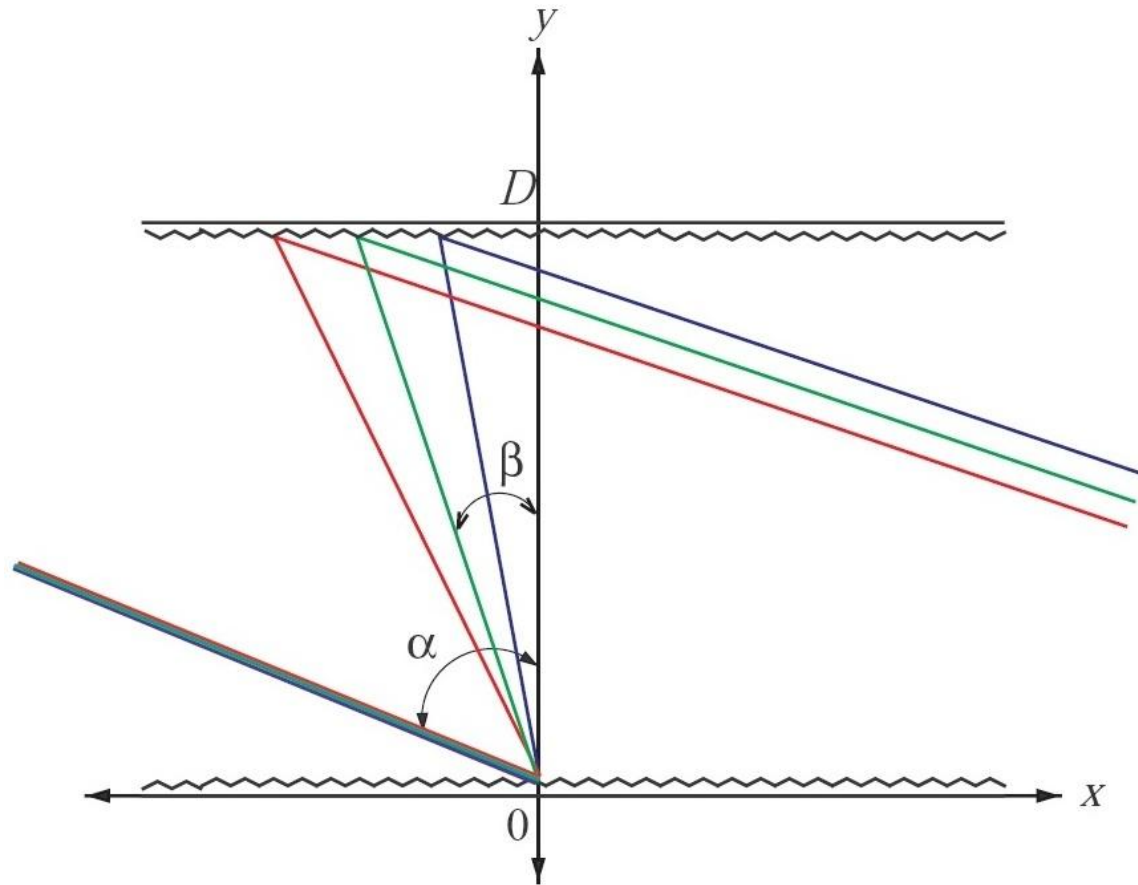
Question 1: What is the (wavelength dependent) phase change arising from diffraction by a grating?

Question 2: What effect occurs when a grating is moved *parallel to its surface*?

Question 3: What are the implications for the use of gratings in some advanced GW detector?



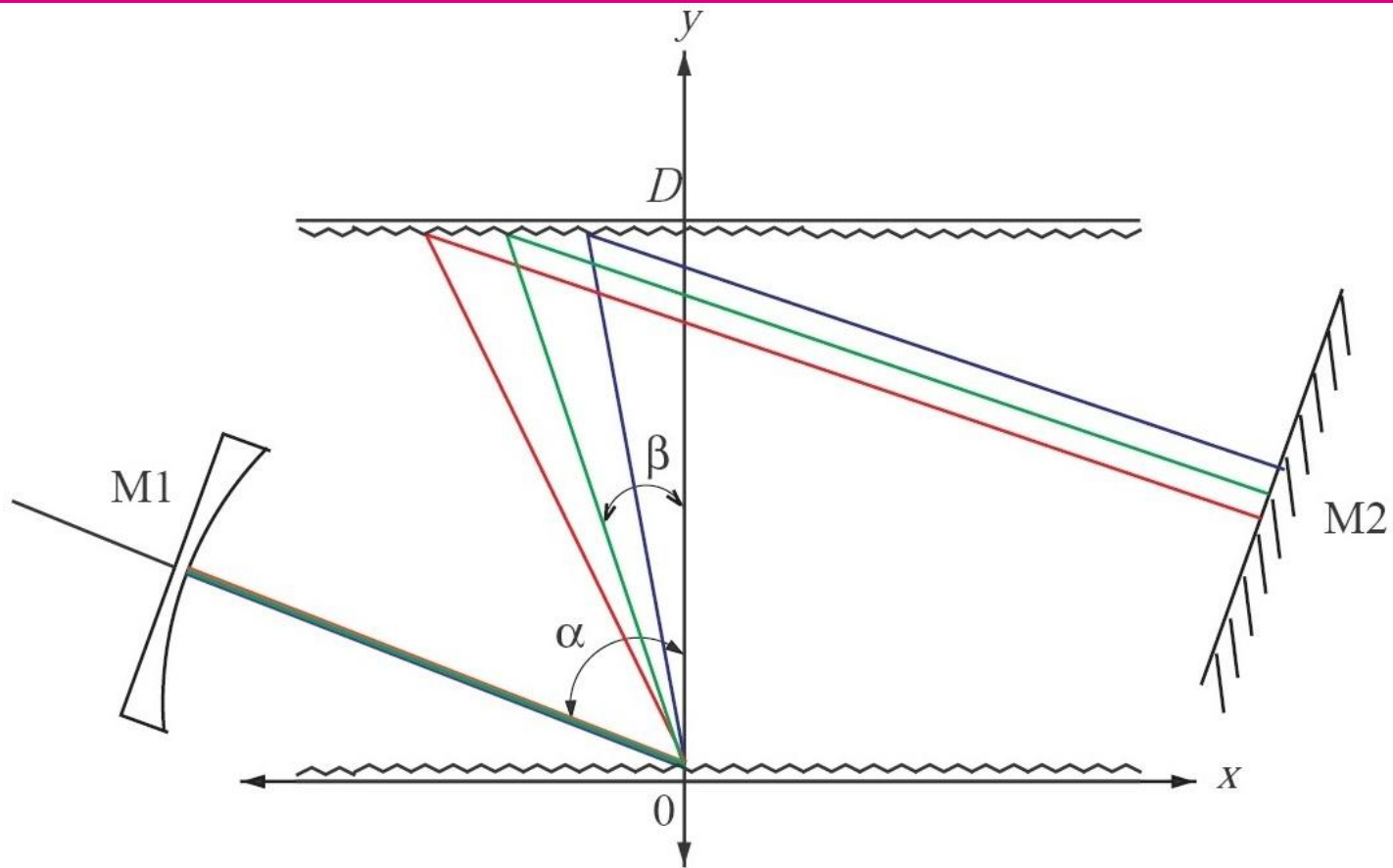
The grating pulse compressor/expander



$$n\lambda = d(\sin \alpha + \sin \beta)$$



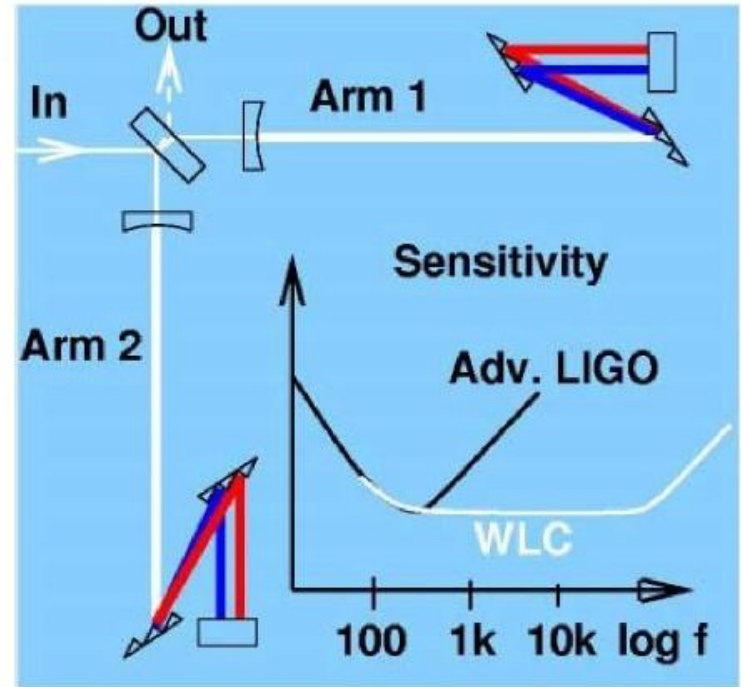
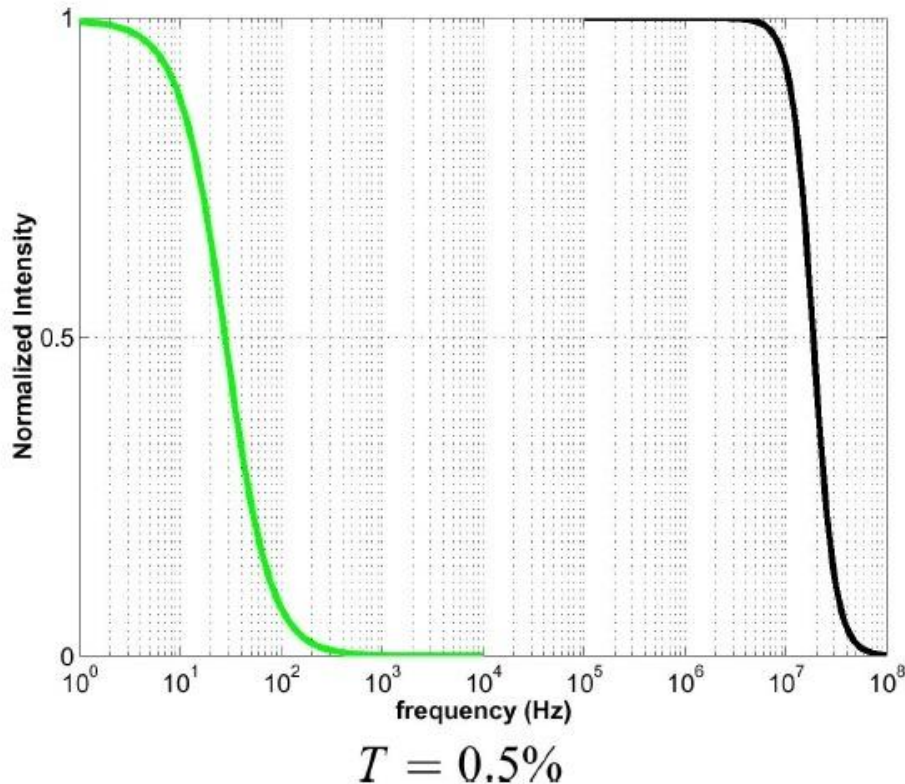
Add mirrors at each end: Fabry-Perot cavity



- $L_{red} > L_{green} > L_{blue}$
- Adjust D such that $L_{red}/\lambda_{red} = L_{green}/\lambda_{green} = L_{blue}/\lambda_{blue}$



Were this true....



one could incorporate these gratings into the arms of a km-scale interferometer and get better high frequency performance (or turn up the finesse, and get greater sensitivity).



Experiment: No increase in bandwidth

- Yanbei's solution:

Gratings bestow a phase factor on the light of

$$e^{ikG(x)} = \sum_m C_m e^{imgx} \approx e^{-igx} \quad \text{and} \quad e^{-ig(x-x_o)}$$

where $G(x)$ is the periodic grating profile, $g = 2\pi/d$, $m = -1$, $C_{-1} = 1$, and x_o is the offset of the second grating wrt the first.

- → shift theory in Fourier transforms

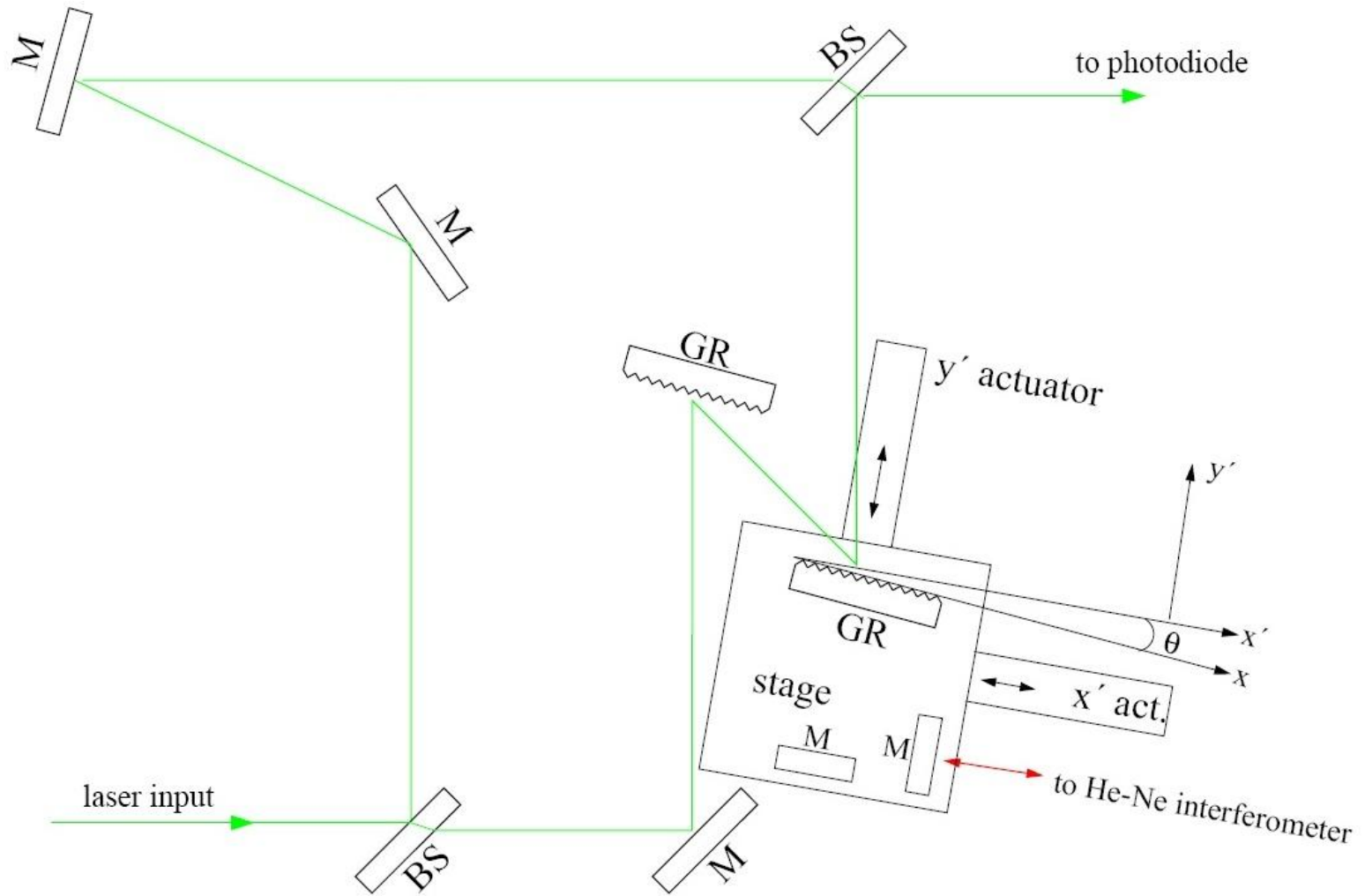
The phase $\Phi(\omega, x, y)$ is

$$\Phi = \frac{\omega}{c} [x \sin \alpha - (y - D) \cos \alpha + D \cos \beta] - gx_o$$

- Phase is linear in the displacement



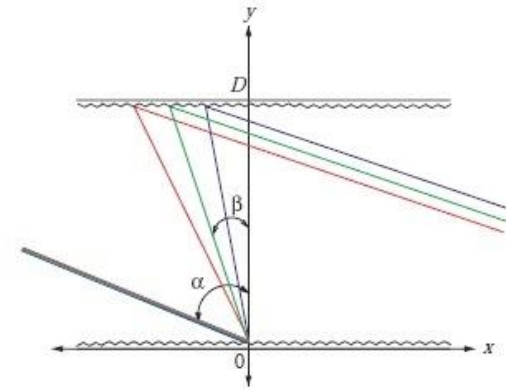
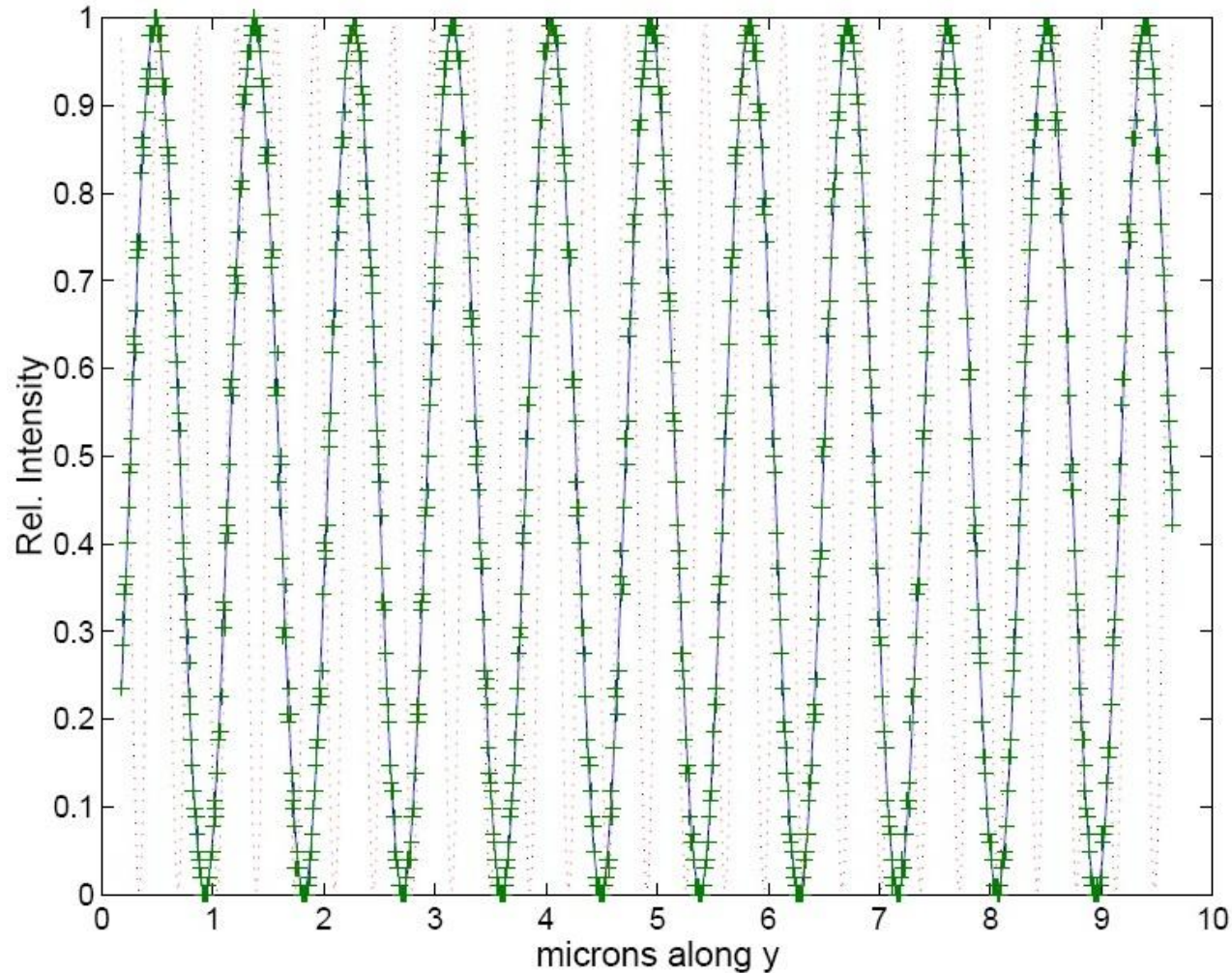
Measuring the phase



$$\theta \sim 0.2^\circ \pm 0.2^\circ$$



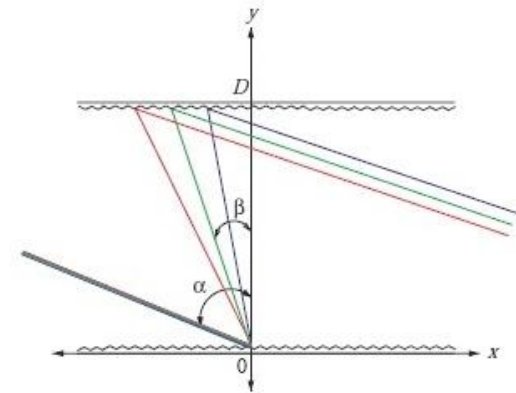
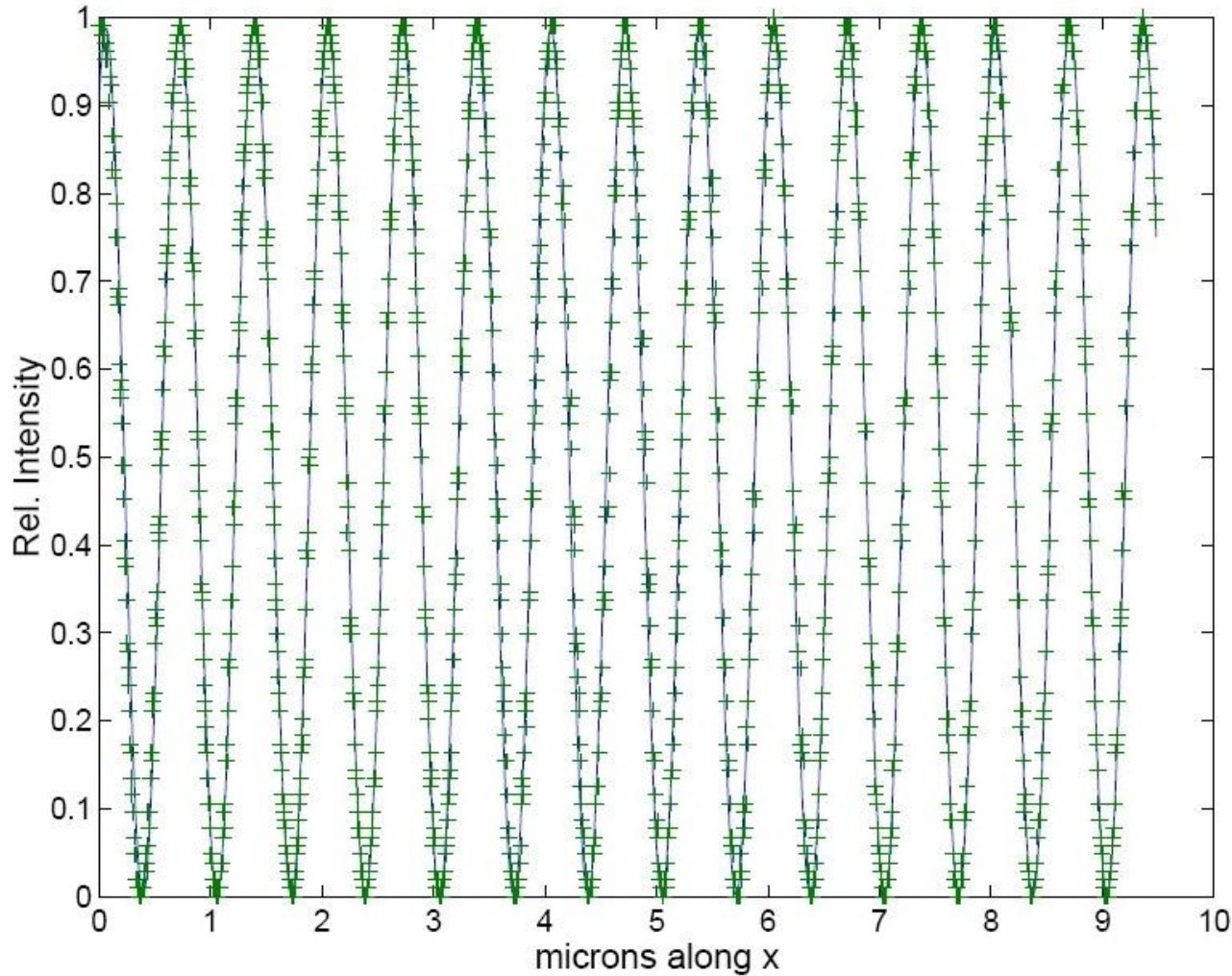
Perpendicular motion



Motion along y
Period is λ



Parallel motion



Motion along x
Period is δ



Gain*bandwidth is preserved

- The phase of light diffracted from a grating can not be deduced from the diffraction equation and geometry alone.
- Such a derivation neglects the curious fact that the absolute phase is proportional to the distance along the grating face at which the light strikes.



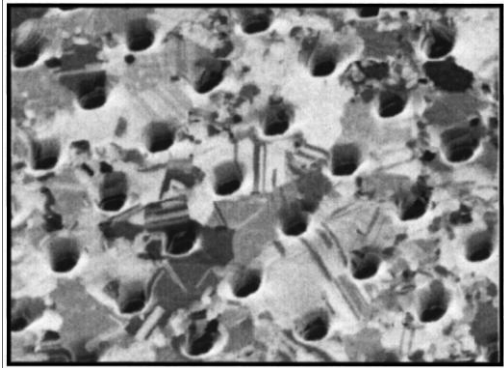
“Enhanced transmission”

- Enhanced transmission by periodic (period D_g) sub-wavelength hole arrays has been known for 14 years (Ebbeson et al, 1998)
 - $T \sim 75\%$ for holes with 25% open area
 - Surprise, as most people would have said the array should be nearly opaque, estimating less than 1% transmission, on account of diffraction when $\lambda \gg D_g$
- Capability to control light could yield applications: “plasmonics.”
- Have been two competing explanations
 - SPP: Surface plasmon polariton ($k_{sp} + 2\pi/D_g = k_{light}$; requires metallic dielectric function)
 - CDEW: Coherent diffracted evanescent waves (scalar diffraction, with $\pi/2$ phase shift, adding coherently in the transmitted direction)
- We showed scaling: spectrum is unchanged when wavelength scaled by product of hole spacing and refractive index of substrate.
 - Novel computational algorithm (vector diffraction) produces computed results in good agreement with measurements
 - Closer to CDEW than SPP explanation
 - Would get enhanced transmission even for perfect metal.



Ebbesen's experiment

[*Nature* **391**, 667(1998)]



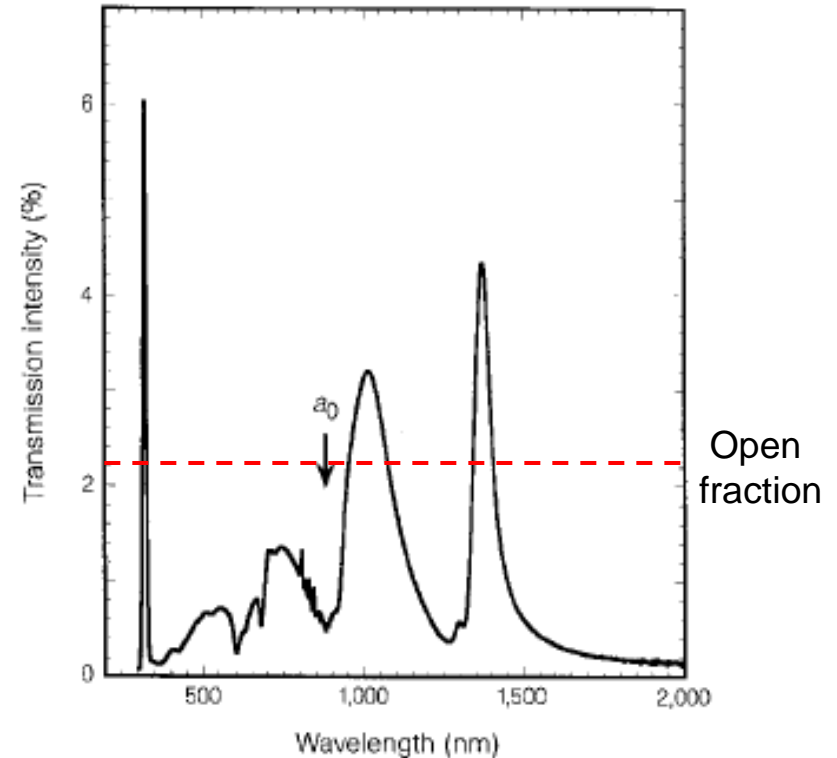
H. F. Ghaemi et al., *PRB* **58**, 6779 (1998)

Period = 900 nm

Hole diameter = 150 nm

Film thickness = 200 nm

Open fraction = 2.18 %



T. W. Ebbesen et al., *Nature* **391**, 667 (1998)



Surface Plasmon

A collective excitation of the electrons at the interface between conductor and insulator

Gives evanescent wave on surface

Dispersion relation of surface plasmon:

$$k_{sp} = k_0 \left(\frac{\epsilon_d \epsilon_m}{\epsilon_d + \epsilon_m} \right)^{1/2} \quad (\text{only for p-pol.})$$

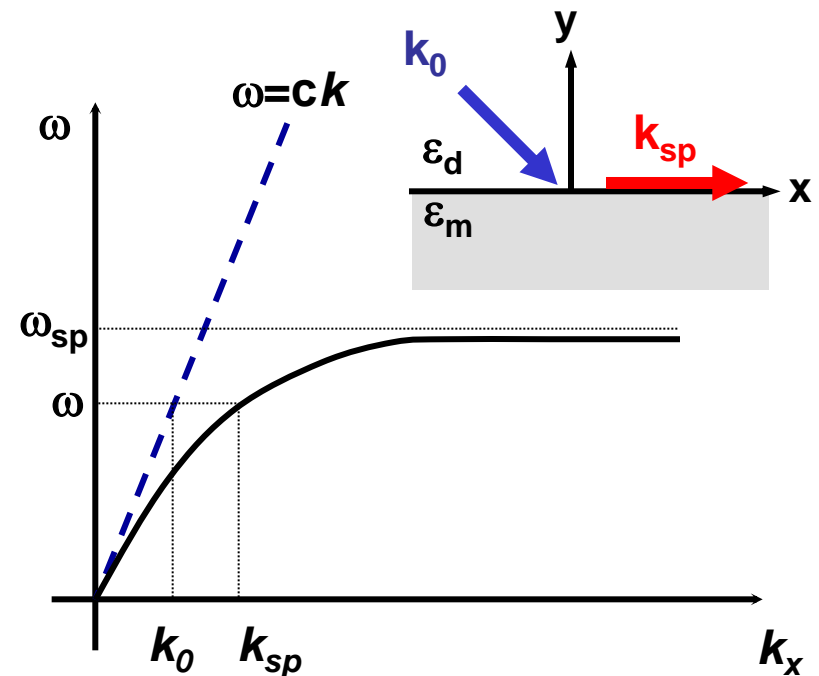
$$k_0 = \frac{\omega}{c} \quad \text{for free space photon}$$

If $k_{sp} \rightarrow \infty$ and $\epsilon_m = 1 - (\omega_p/\omega)^2$

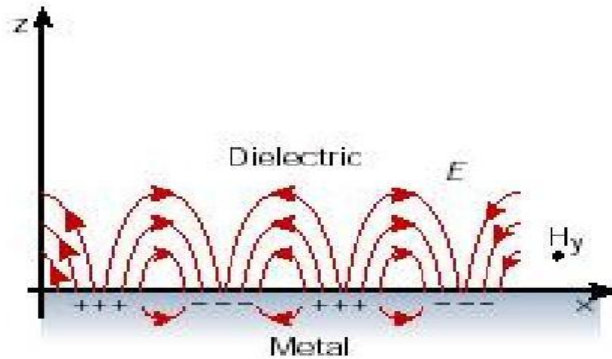
then $\epsilon_d + \epsilon_m = 0$ means

$$\omega_{sp} = \omega_p / (1 + \epsilon_d)^{1/2}$$

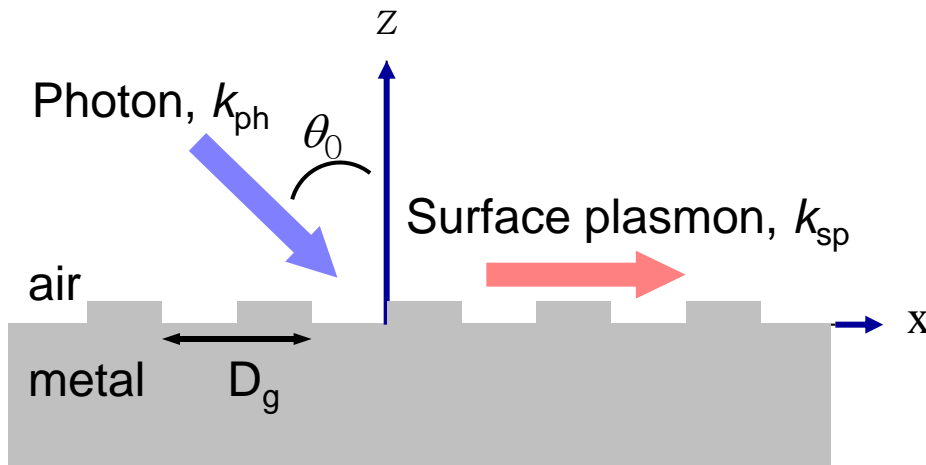
where ω_p is the bulk plasma frequency



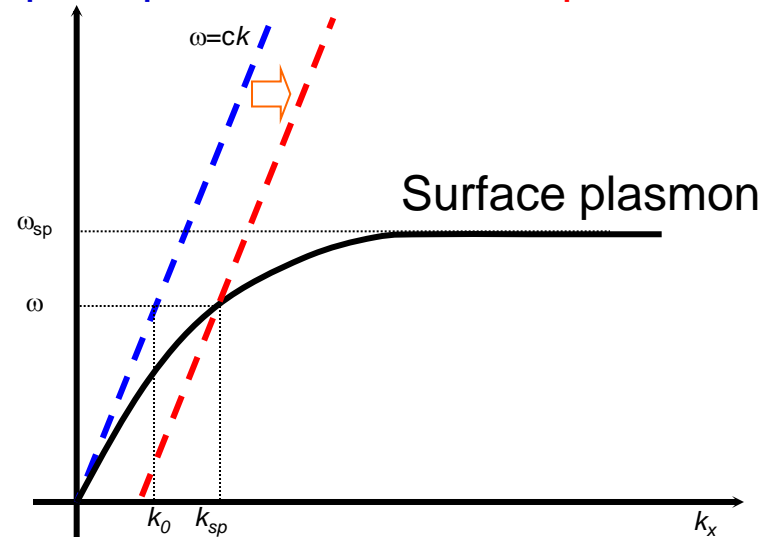
Surface Plasmon Coupling *via* a Grating



Surface plasmon at dielectric-metal interface



Free space photon Scattered photon

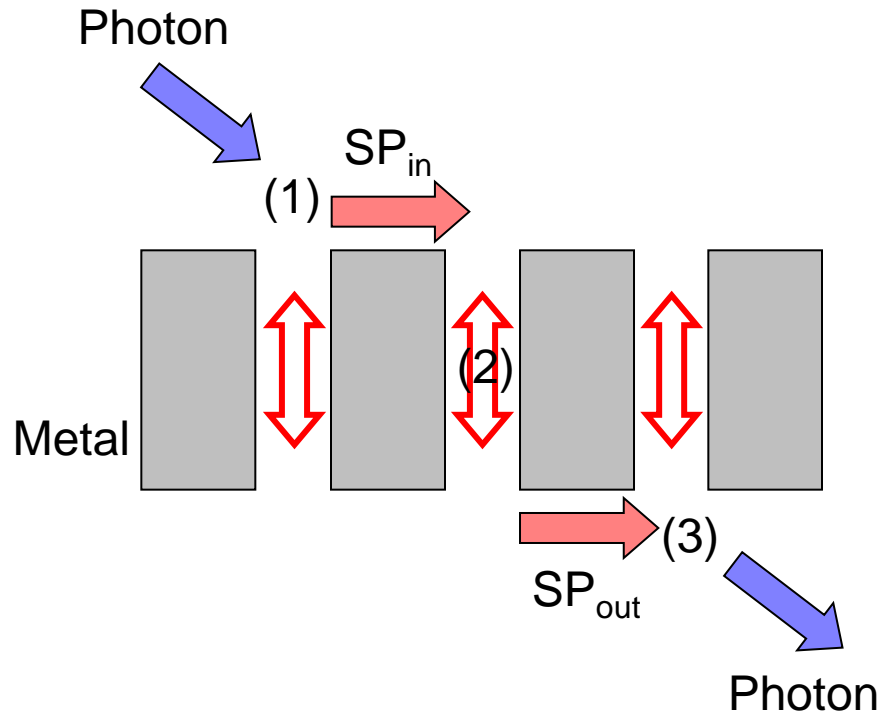


Dispersion curves

$$k_x = \frac{\omega}{c} \sin \theta_0 + m \frac{2\pi}{D_g} = k_{sp}$$



Surface Plasmon Resonant Transmission



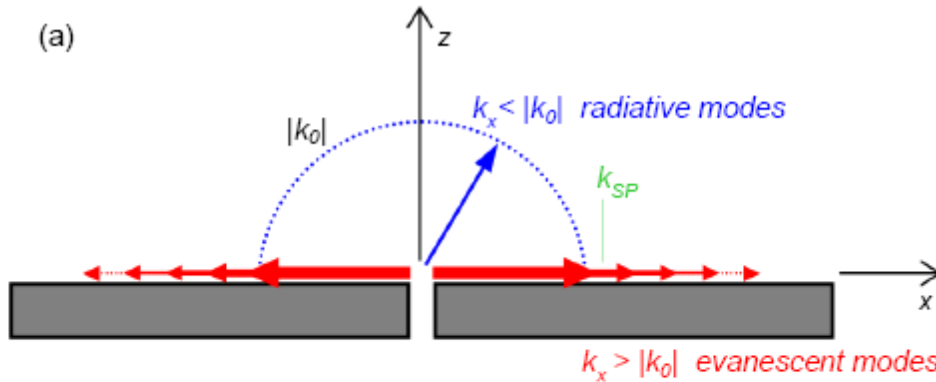
1. Coupling between the incident photons and the SP_{in} on the front side
2. Evanescent coupling between SP_{in} and SP_{out}
3. Decoupling photons from the back side SP_{out} for re-emission



CDEW (Composite Diffractive Evanescent Wave)

CDEW¹:

Superposition of evanescent waves diffracted from a of a single subwavelength surface feature.



Momentum conservation

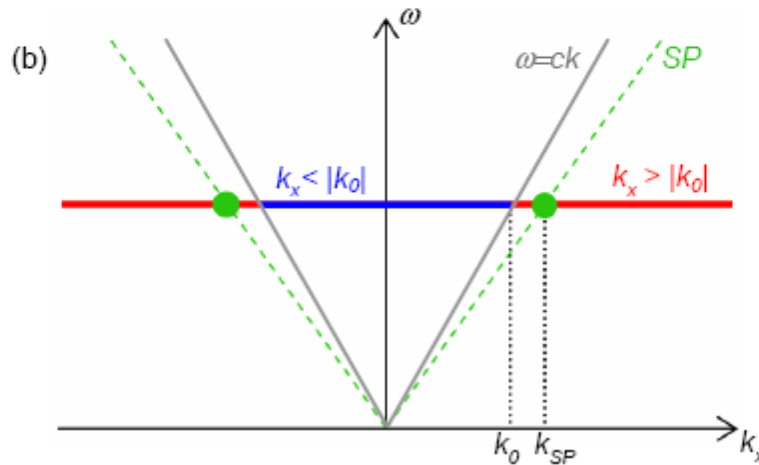
$$\vec{k}_0 = \vec{k}_x + \vec{k}_z$$

$$\text{If } k_x < k_0, k_z = (k_0^2 - k_x^2)^{1/2}$$

=> radiative mode

$$\text{If } k_x > k_0, k_z = i(k_0^2 - k_x^2)^{1/2}$$

=> evanescent mode

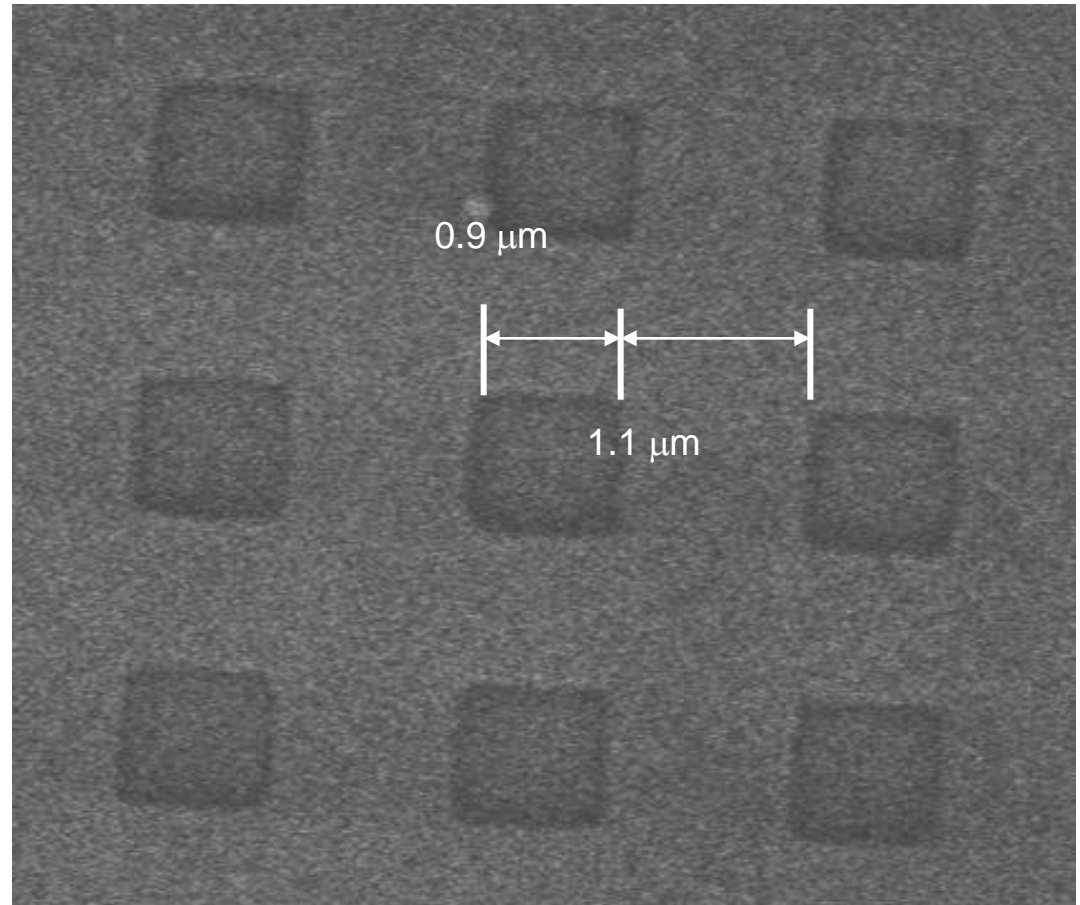


1. H. J. Lezec and T. Thio, *Opt. Exp.* **12**, 3629 (2004)



Samples and spectroscopy

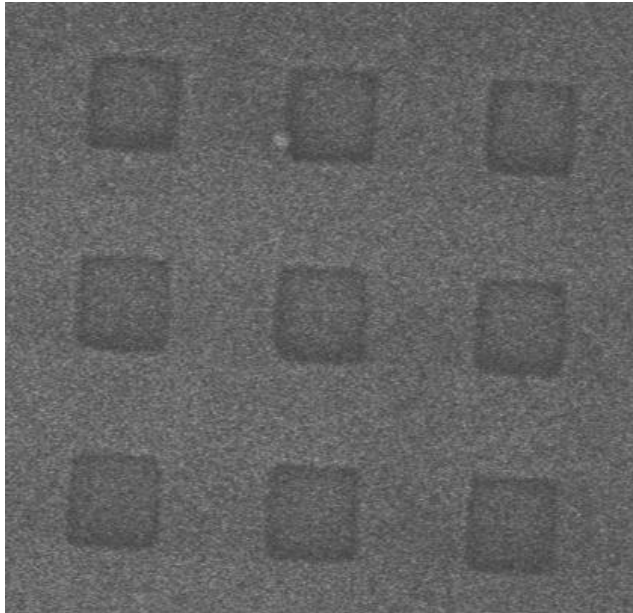
- Silver deposited on silica or ZnSe substrates
- Evaporation from tungsten basket
- E-beam lithography makes the holes
- We made mostly squares, with $0.5 < D_g < 20 \mu\text{m}$
- Also rectangles, slits, coaxial
- Measured transmittance over wavelength range $250 < \lambda < 30,000 \text{ nm}$
- Reference is a hole that just circumscribes the pattern, with no correction for reflection at either interface.



Square hole array in an 150 nm Ag film. $D_g = 2 \mu\text{m}$.



“Transmission enhancement” example

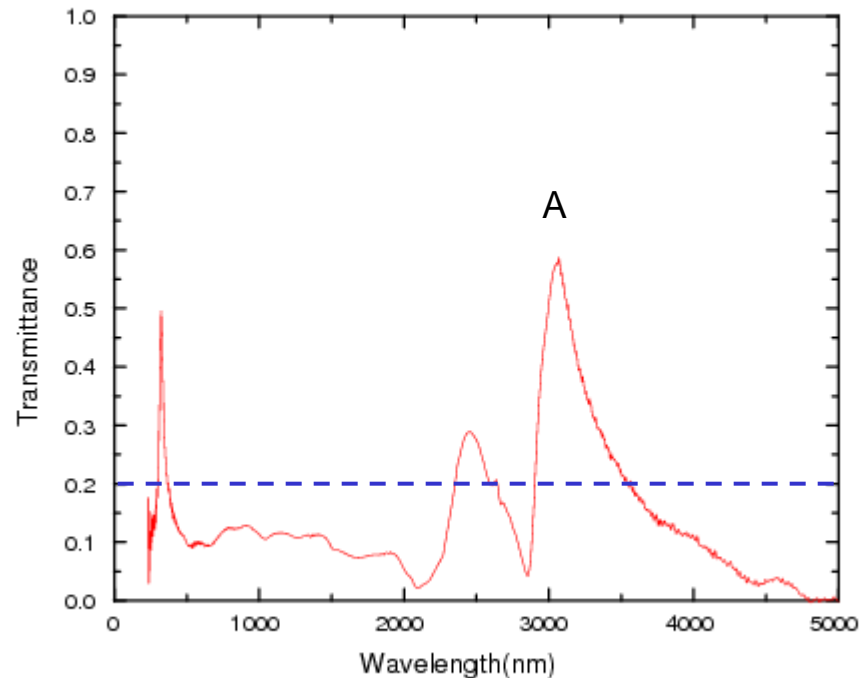


Square hole array in Ag film on quartz substrate

Periodicity, $D_g = 2 \mu\text{m}$

Hole size, $0.9 \mu\text{m} \times 0.9 \mu\text{m}$

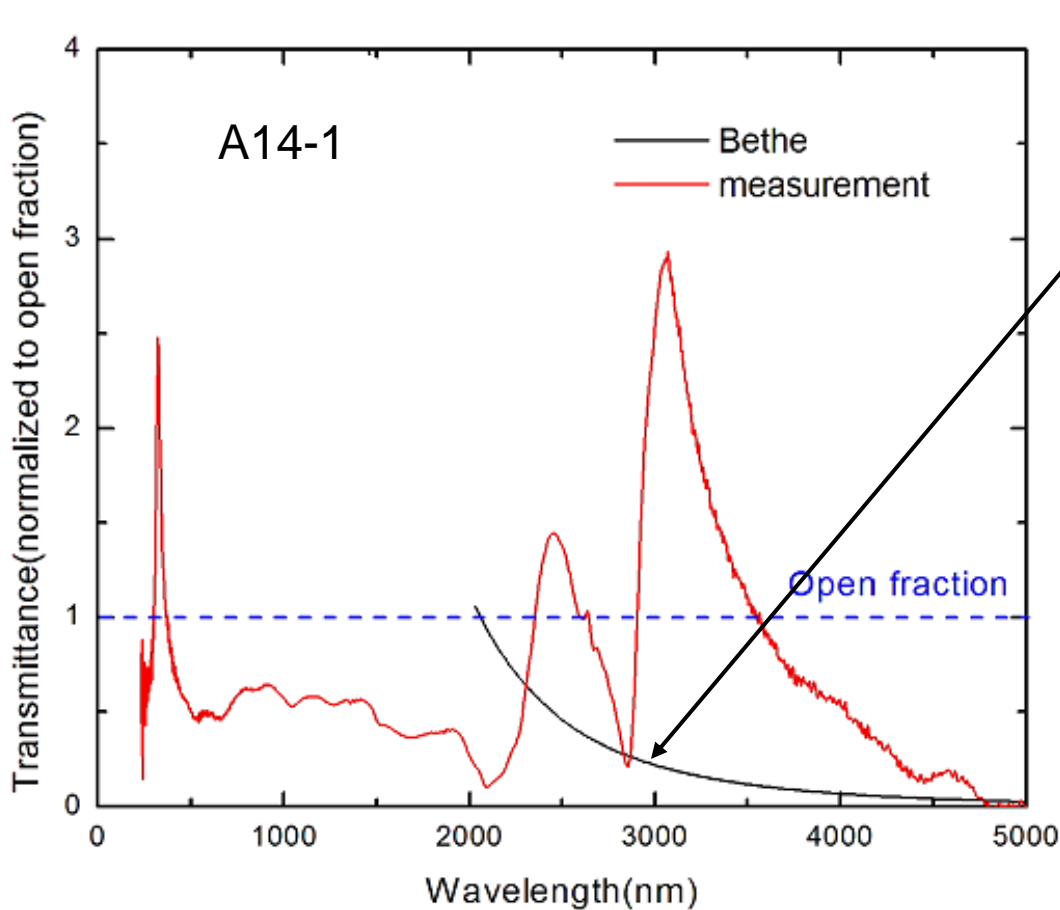
Fraction of open area $f = 20 \%$



- Highest transmission peak (A) is at $\lambda = 3070 \text{ nm}$ for normal incidence.
- Peak A shows $\sim 60\%$ transmission.
- Have observed up to 80% in $f = 20\text{-}25\%$ samples



Superposition of independent holes



Bethe's transmission ($\lambda \gg r_0$)

$$T = \frac{64}{27\pi} \frac{(kr_0)^4}{2^6} \approx 18 \left(\frac{r_0}{\lambda} \right)^4$$

At the peak $\lambda = 3070$ nm, the measured peak intensity is 15 times greater than the calculated one.

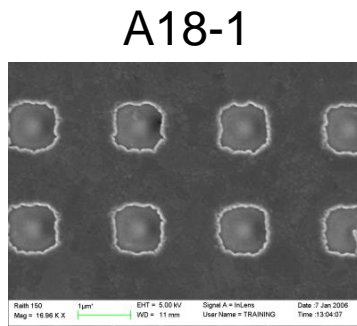


SP prediction of peak positions

For normal incidence ($\theta_0 = 0$)

$$\lambda_{\max} = \frac{D_g}{\sqrt{i^2 + j^2}} \sqrt{\frac{\epsilon_d \epsilon_m}{\epsilon_d + \epsilon_m}}$$

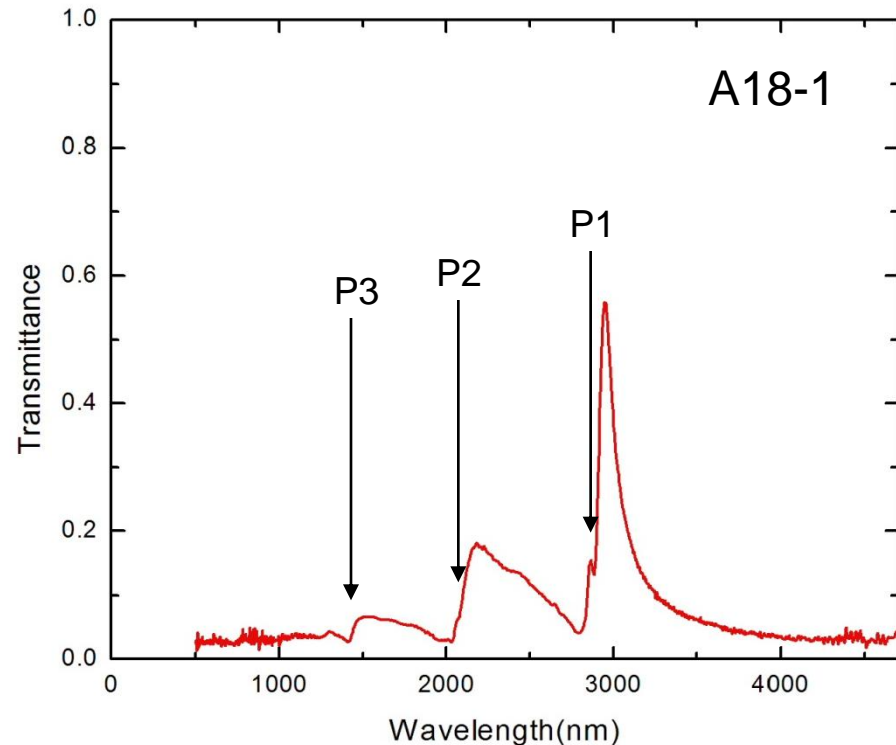
(i, j)	air / metal	fused silica / metal
(0, ± 1), (± 1 , 0)	2020 nm (P2)	2860 nm (P1)
(± 1 , ± 1)	1450 nm (P3)	2040 nm (P2)



Hole size: $0.84 \times 0.84 \mu\text{m}^2$

Period: $2 \mu\text{m}$

Open fraction: 18 %



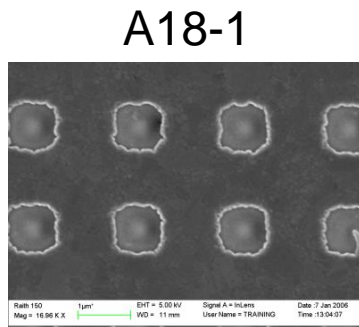
Diffraction condition prediction of dip positions

For normal incidence ($\theta_0 = 0$)

$$\lambda_{\min} = \frac{D^g}{\sqrt{i^2 + j^2}} \sqrt{\epsilon_d}$$

(Grating diffraction equation at $\theta_m = 90^\circ$)

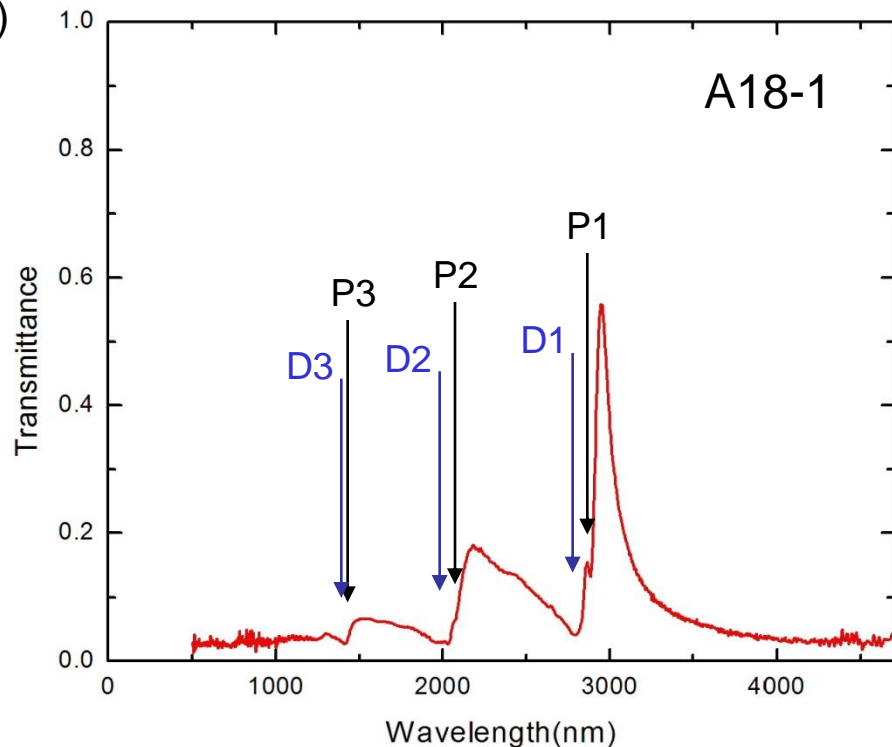
(i, j)	air / metal	fused silica / metal
(0, ±1), (±1, 0)	2000 nm (D2)	2800 nm (D1)
(±1, ±1)	1420 nm (D3)	2000 nm (D2)



Hole size: $0.84 \times 0.84 \mu\text{m}^2$

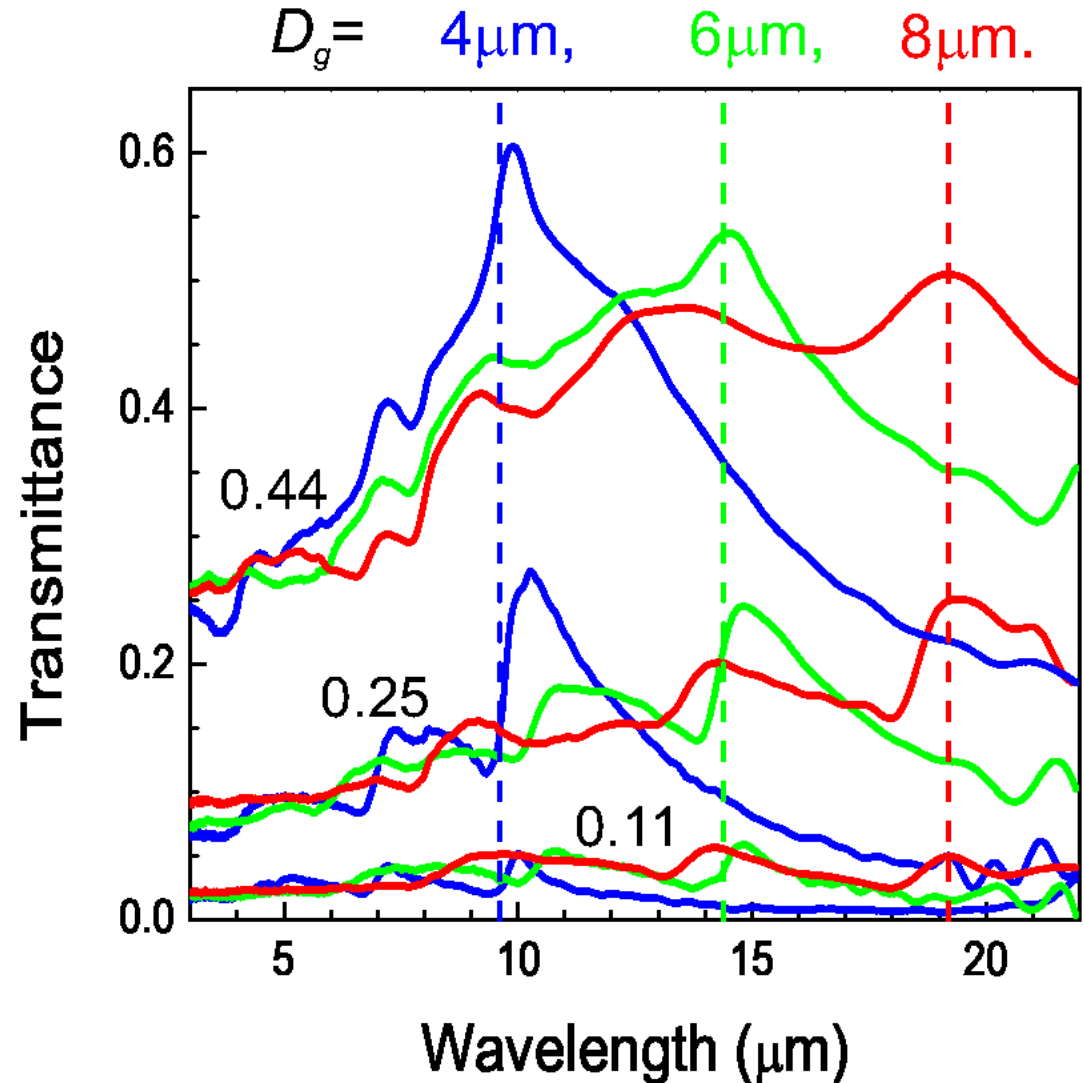
Period: $2 \mu\text{m}$

Open fraction: 18 %



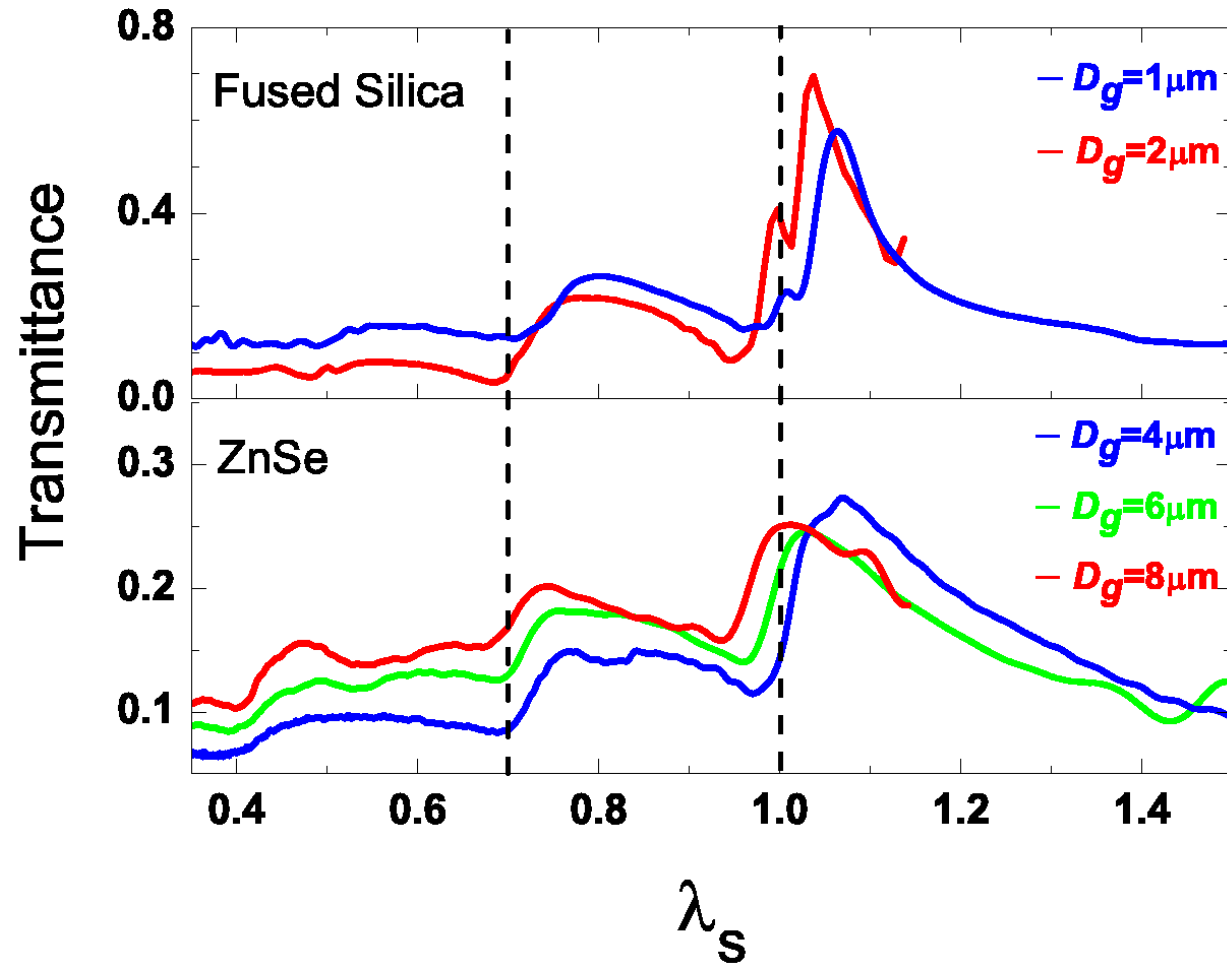
Scaling study

- OAF = open area fraction, varies from 11% to 44%
- Hole period varies from 4 μm to 8 μm
- Max transmission at the longest wavelength peak, a minimum at shorter wavelengths, and characteristic structure above this
- Dashed line shows where diffraction channel opens for film-ZnSe interface



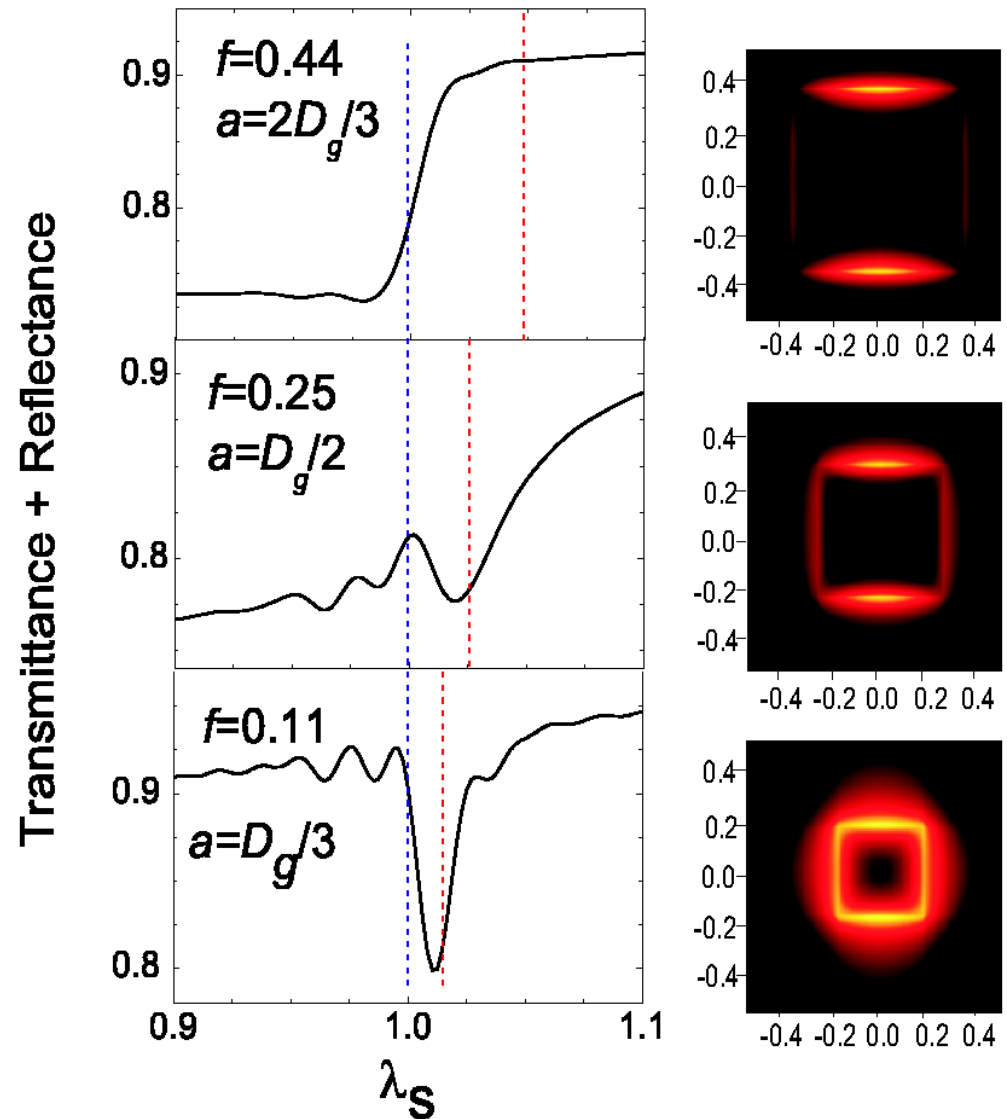
Scaling

- OAF = 25% samples
- Scaling function is
$$\lambda/nD_g \equiv \lambda_s$$
- $n = 1.4$ (quartz)
 $n = 2.8$ (ZnSe)
- Works over wavelength range of a factor of 14.
- The dielectric function varies from
$$\varepsilon = -90 \quad (1.4 \mu)$$
- to
$$\varepsilon = -14,000 \quad (20 \mu)$$



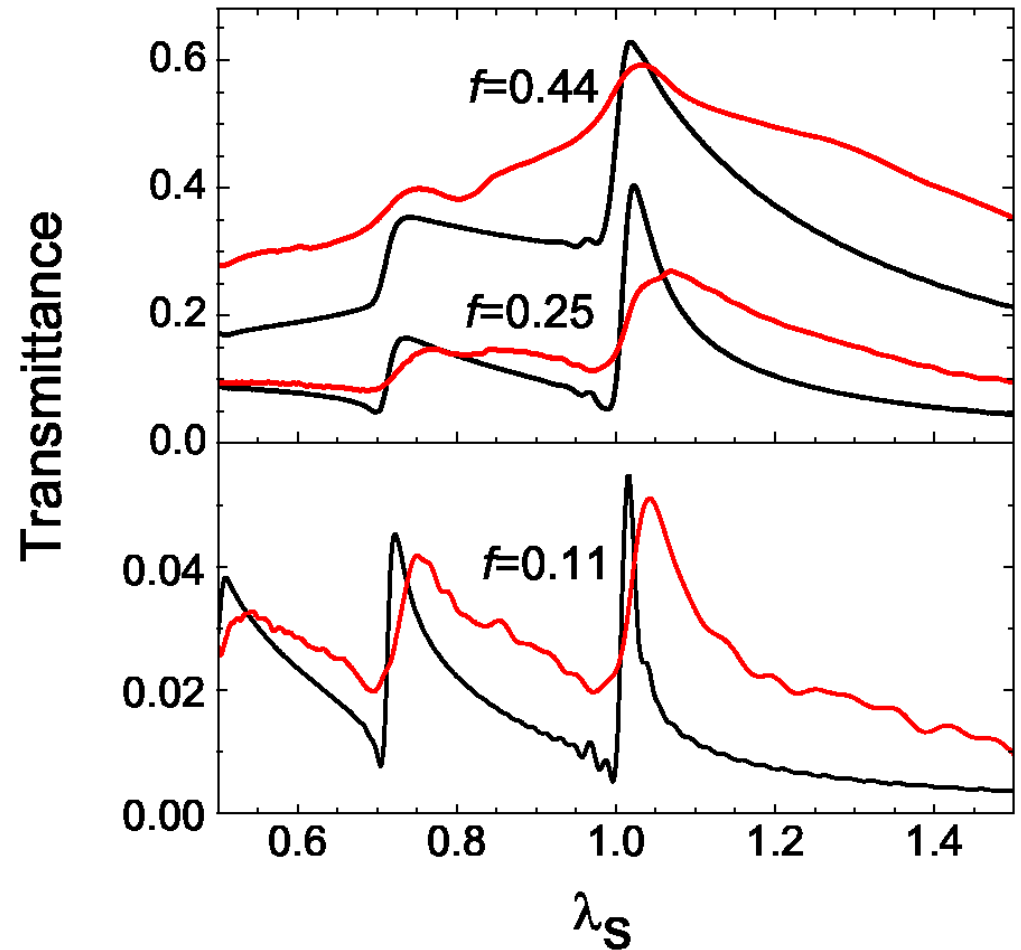
Trapped modes

- Resonant contribution from electromagnetic modes trapped near the film
- Trapped modes slowly decay by emitting radiation
- Modes can exist in structures made from dispersive or non-dispersive materials
- Geometry is the key factor
- Surface plasmons play a minimal role in the enhanced transmission

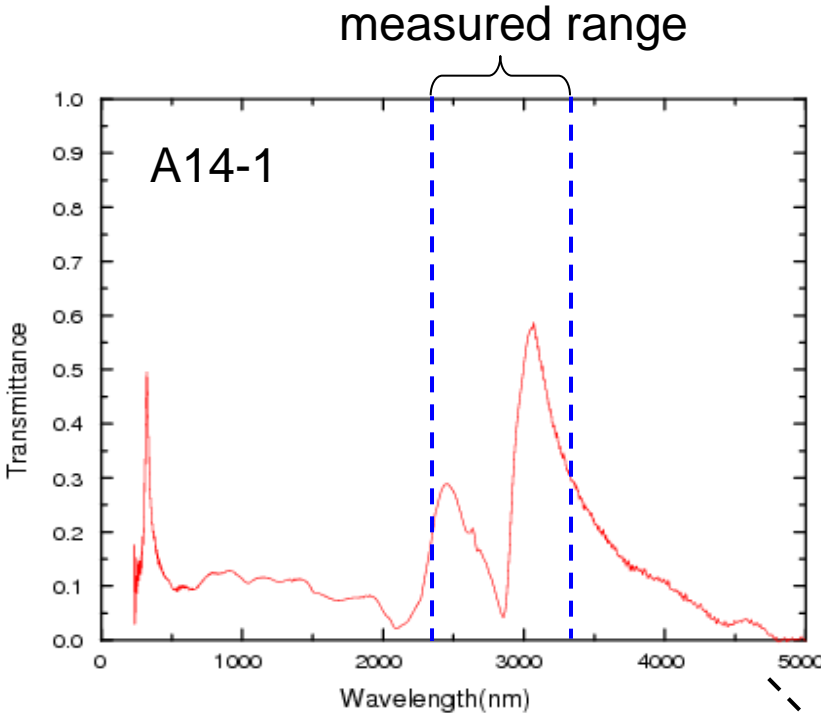


Comparison to simulations

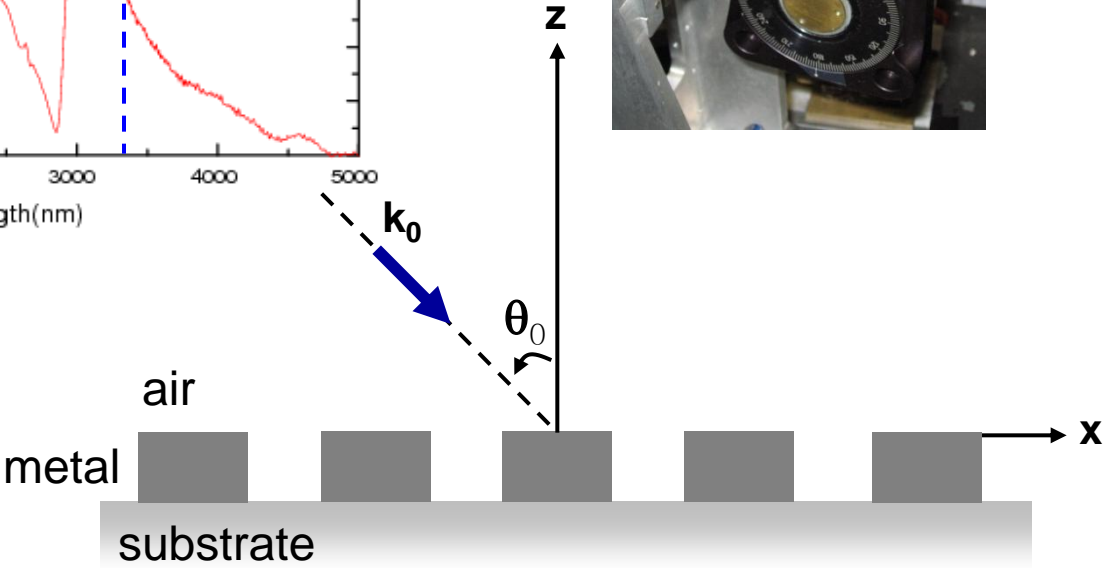
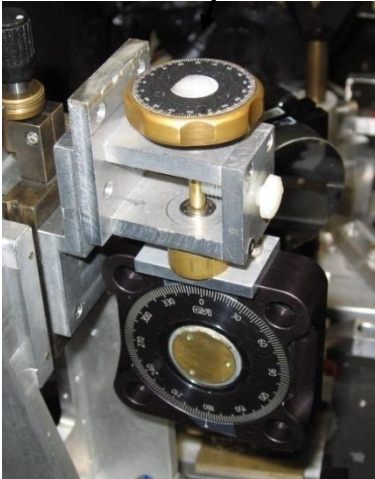
- Simulations (black) based on full Maxwell's theory
- Time domain
- Silver viewed as Drude metal
- No adjustable parameters
- Gives wavelengths of peaks, dips, lineshape, transmittance value



Dependence on the incident angle, polarization

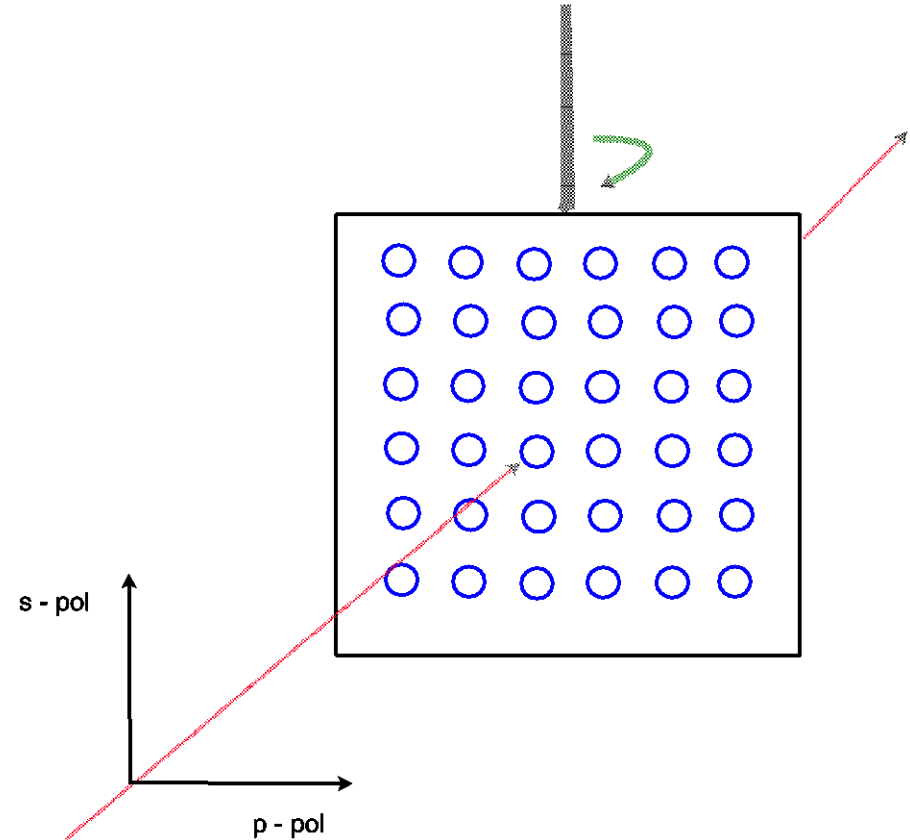


Incident angle rotator

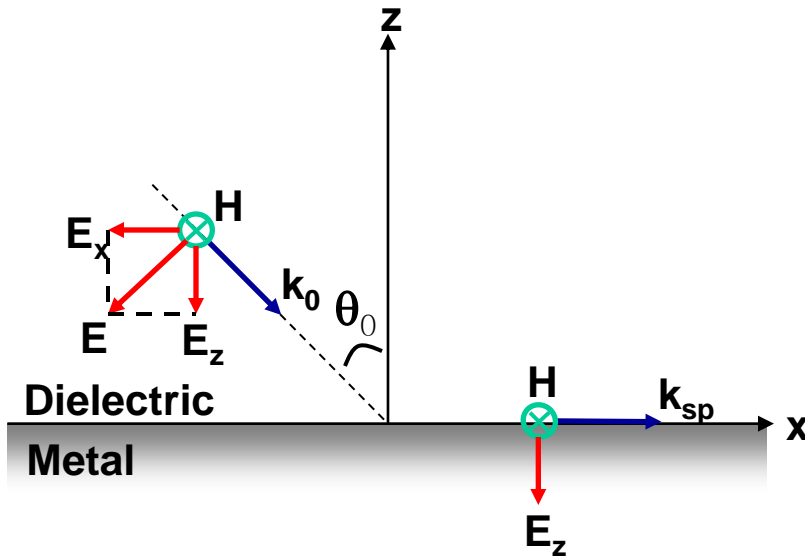


Polarization and angle of incidence

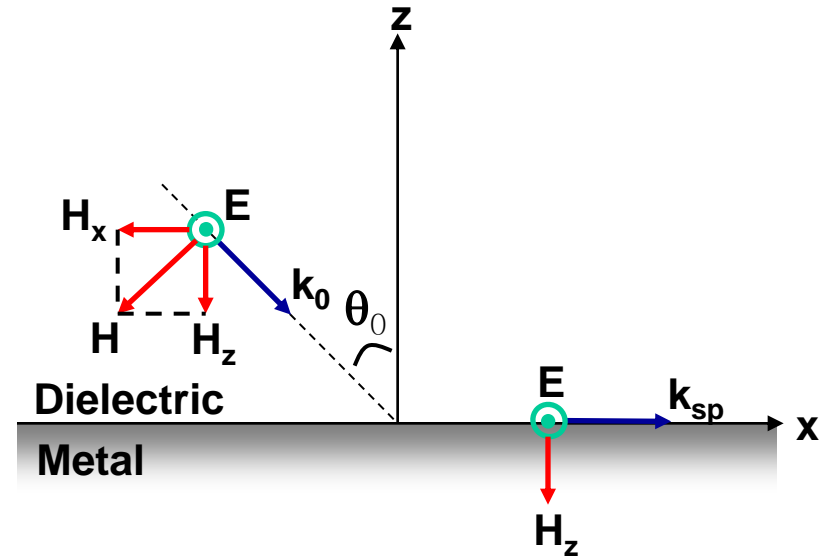
- Use polarized light
- Rotate film about vertical axis
- “Plane of incidence” is the horizontal plane
- s (E \perp plane of incidence)
- p (E \parallel plane of incidence)
- Rotate array around vertical axis
- NB. Surface plasmons are supposed to be restricted to p - polarization



$p = \text{Parallel}; s = \text{Senkrecht}$



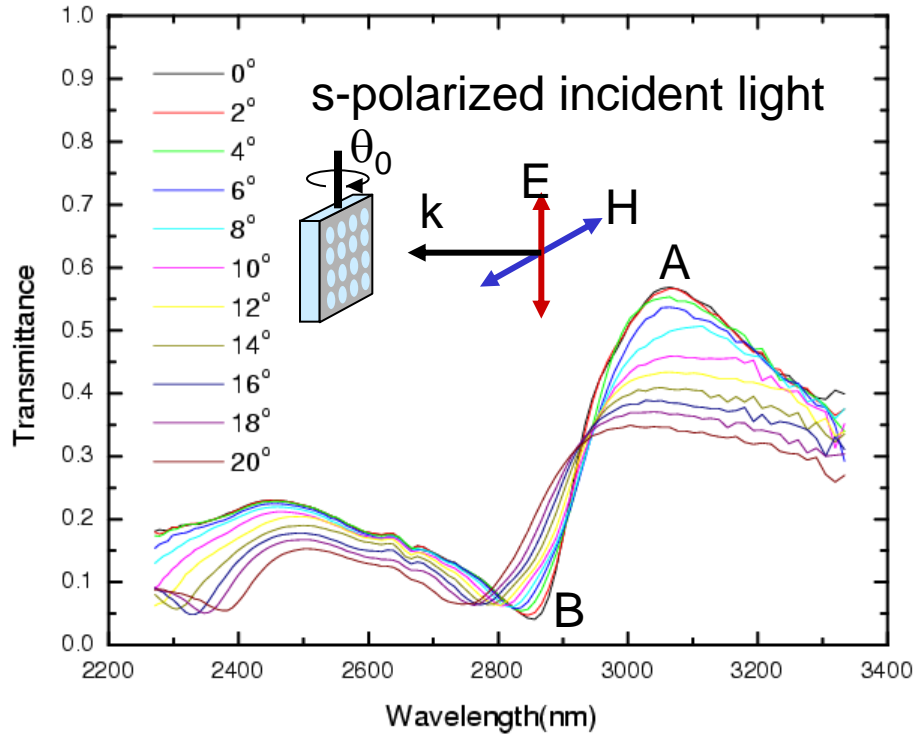
p-polarization (TM)



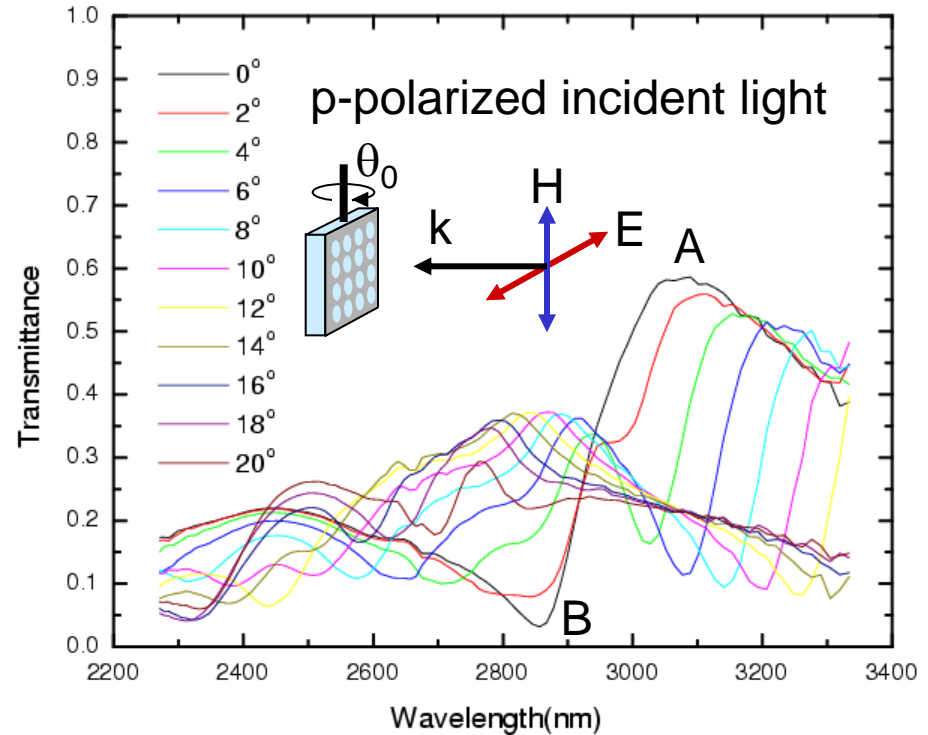
s-polarization (TE)



Transmittance with polarized light



The peak A and the dip B shifts to shorter wavelengths with changing the angle of incidence.

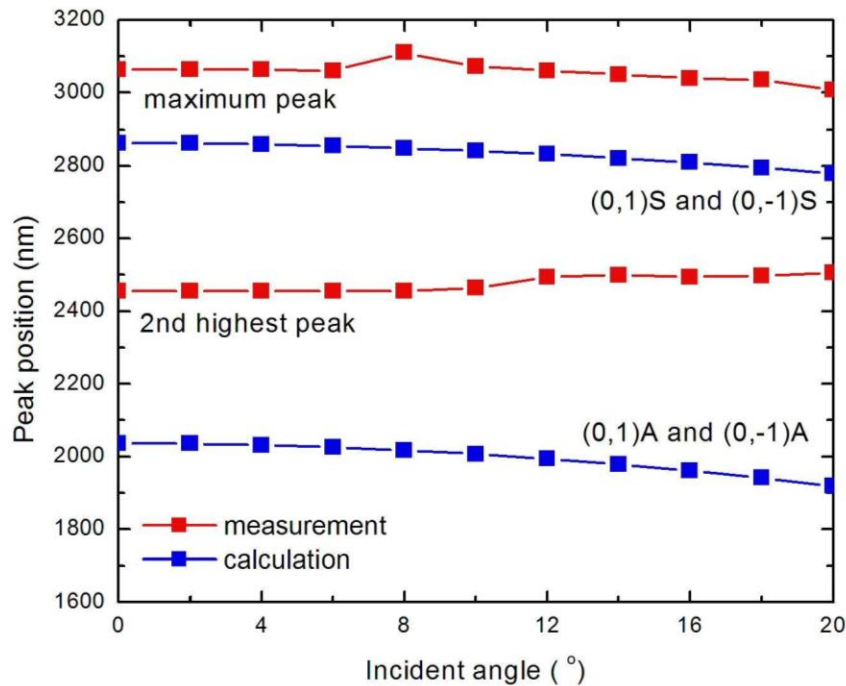


Peak A (dip B) splits into two peaks (two dips) and one shifts to longer wavelengths and the other shifts to shorter wavelengths.

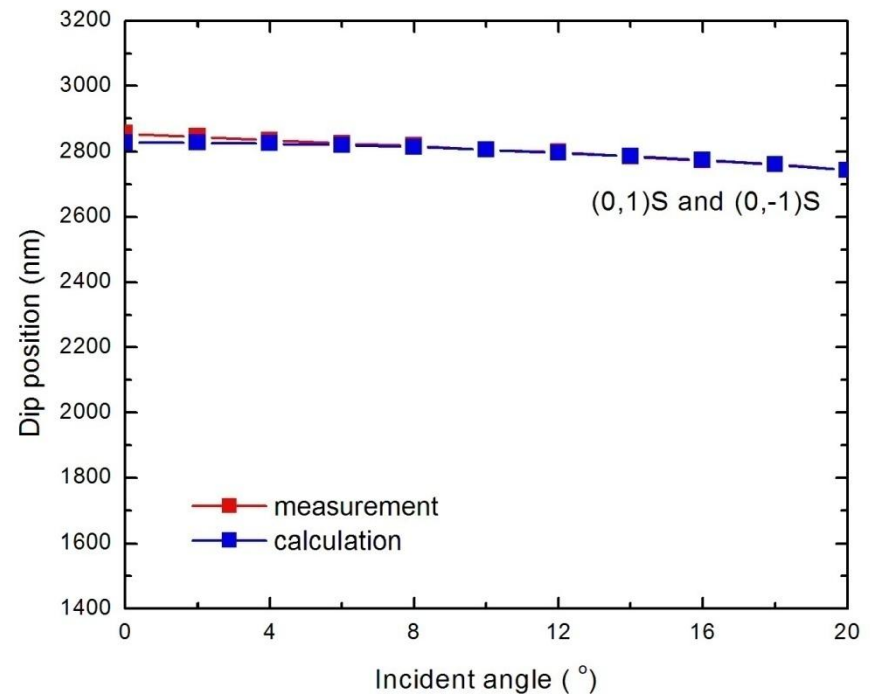


Angle dependence, s-polarization

Fused silica has $n = 1.4$, so the modes at the metal-silica interface are at longer wavelengths than the metal-air interface.



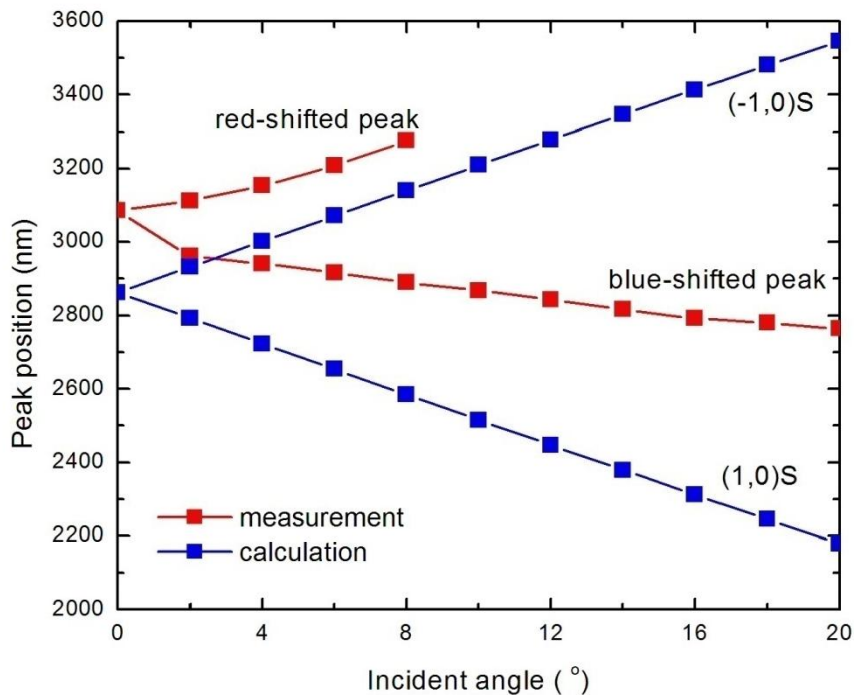
For peaks



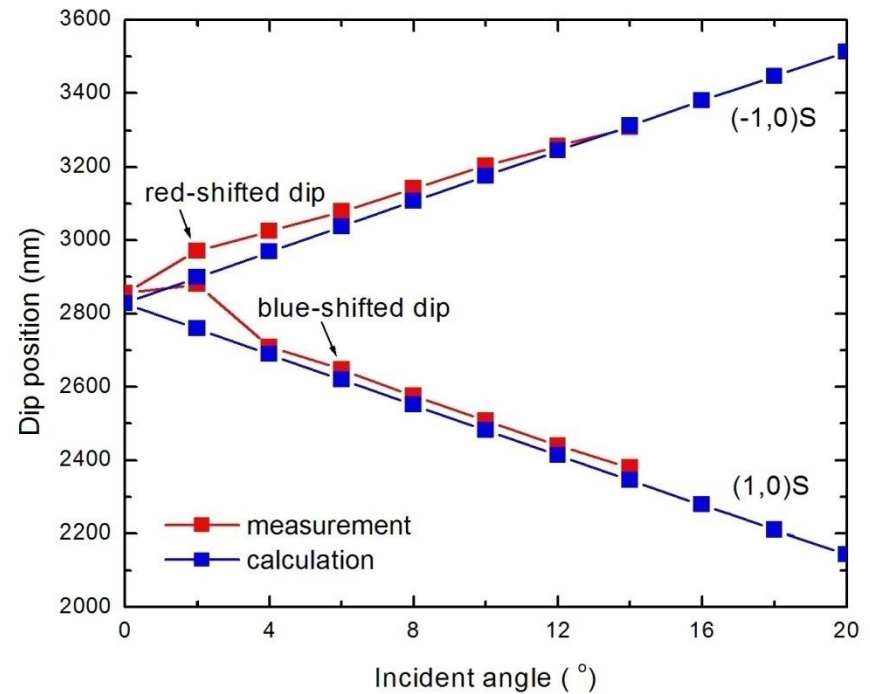
For dips



Angle dependence, p-polarization



For peaks



For dips



Angle dependence summary

- Away from normal incidence, s and p spectra are very different
- A vector theory is clearly needed
- Quantitative disagreement with surface plasmon calculations

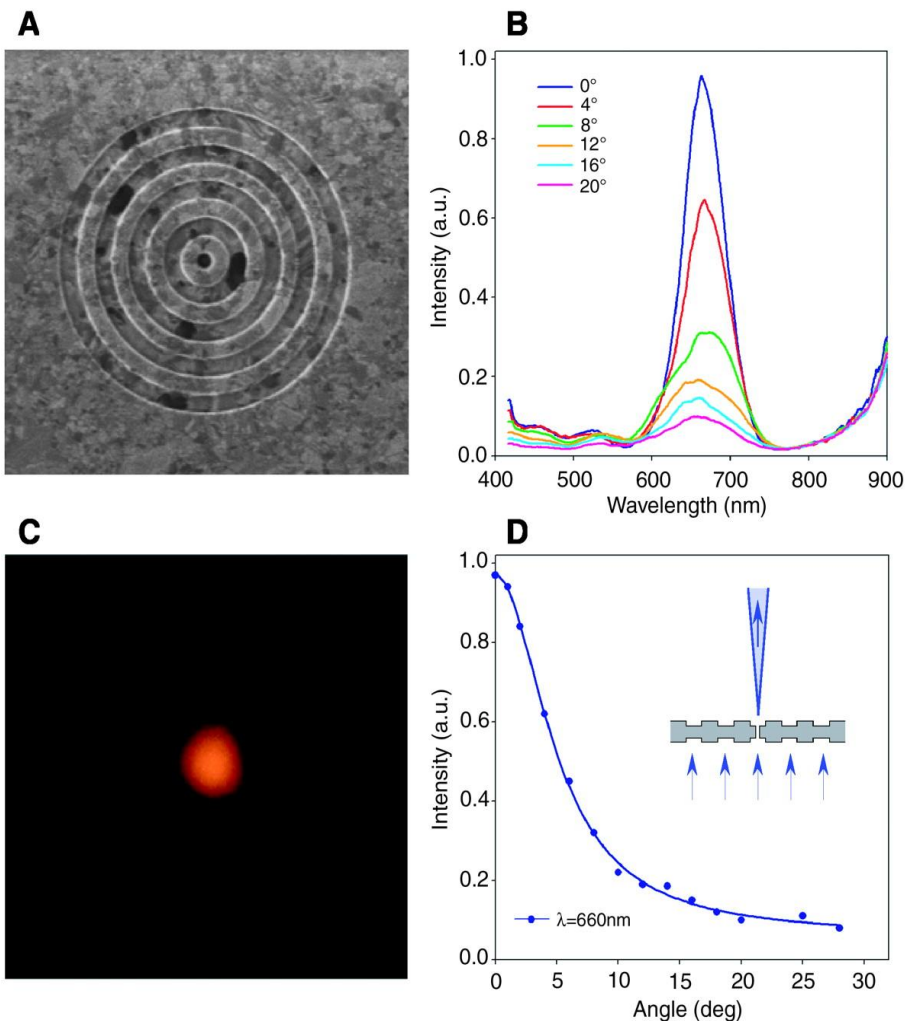


Transmittance of bullseye structures

- Bullseye (or ring pattern)
- Subwavelength hole in center
- Show high transmittance
 - Relative to hole by itself
- Show beaming
 - Hole would diffract light into 2π steradians



Beaming Light From a Subwavelength Aperture



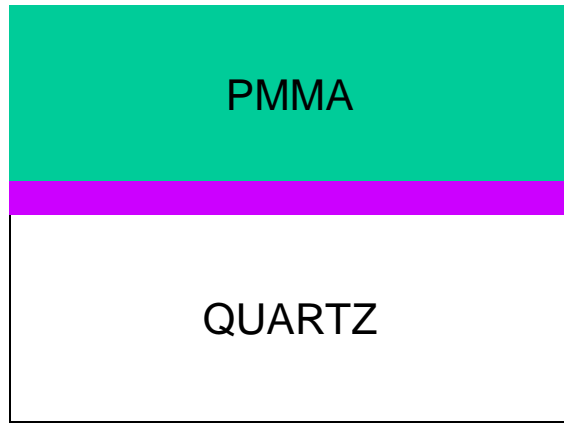
Periodic texture of annular rings surrounding a 250 nm hole causes the transmitted light to emerge with enhanced transmission and small angular divergence ($\pm 3^\circ$).

H.J. Lezec et al., *Science*
297, 820 (2002)



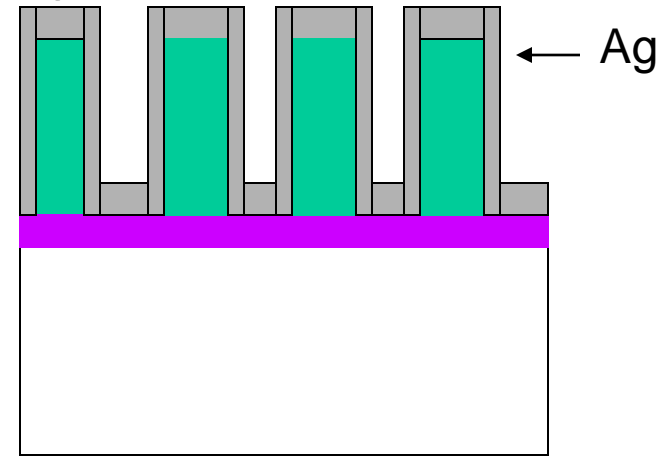
Bullseye Fabrication

I. InO_x and PMMA coating

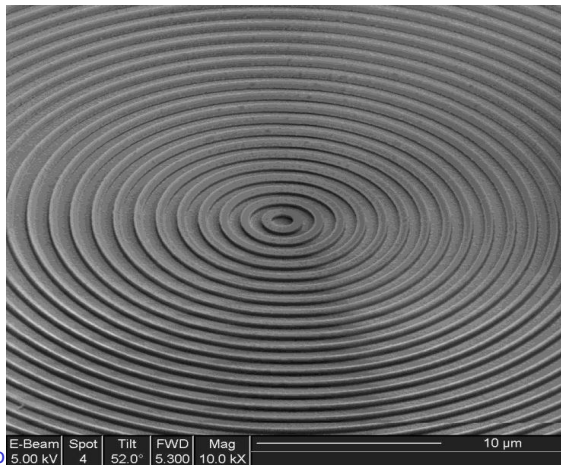


II. E-beam lithography and silver metallization

$$n_{\text{quartz}}=1.46,$$
$$n_{\text{pmma}}=1.44$$

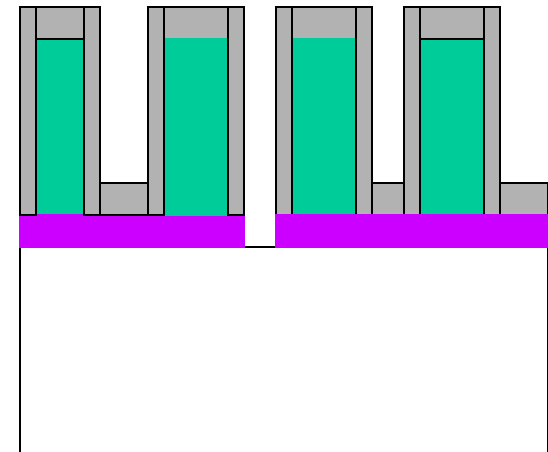


III. Measurement: Without holes Karl-Zeiss Microscope , T₀₀

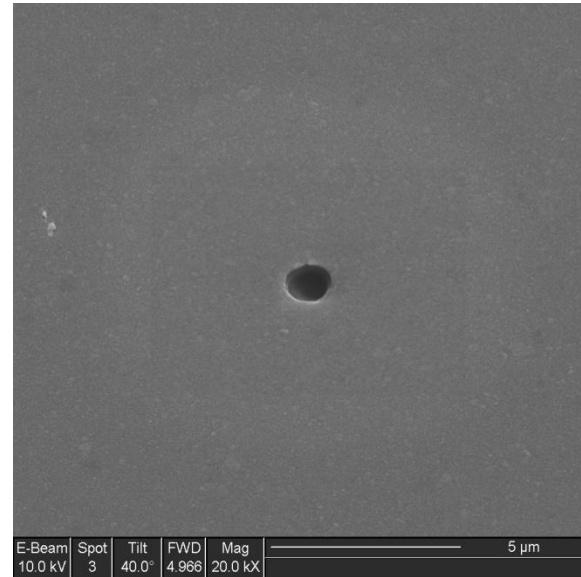
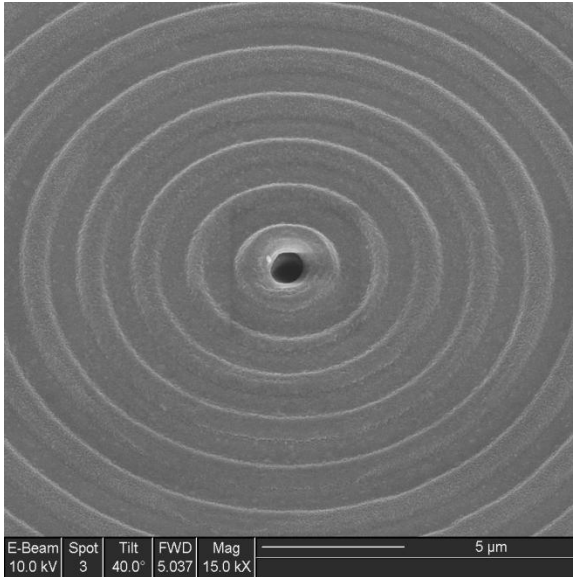


400nm PMMA with
35nm Ag film

IV. Focused Ion Beam



Bullseye Structure



50 grooves around the aperture

Structure big enough to get an appreciable signal from the film



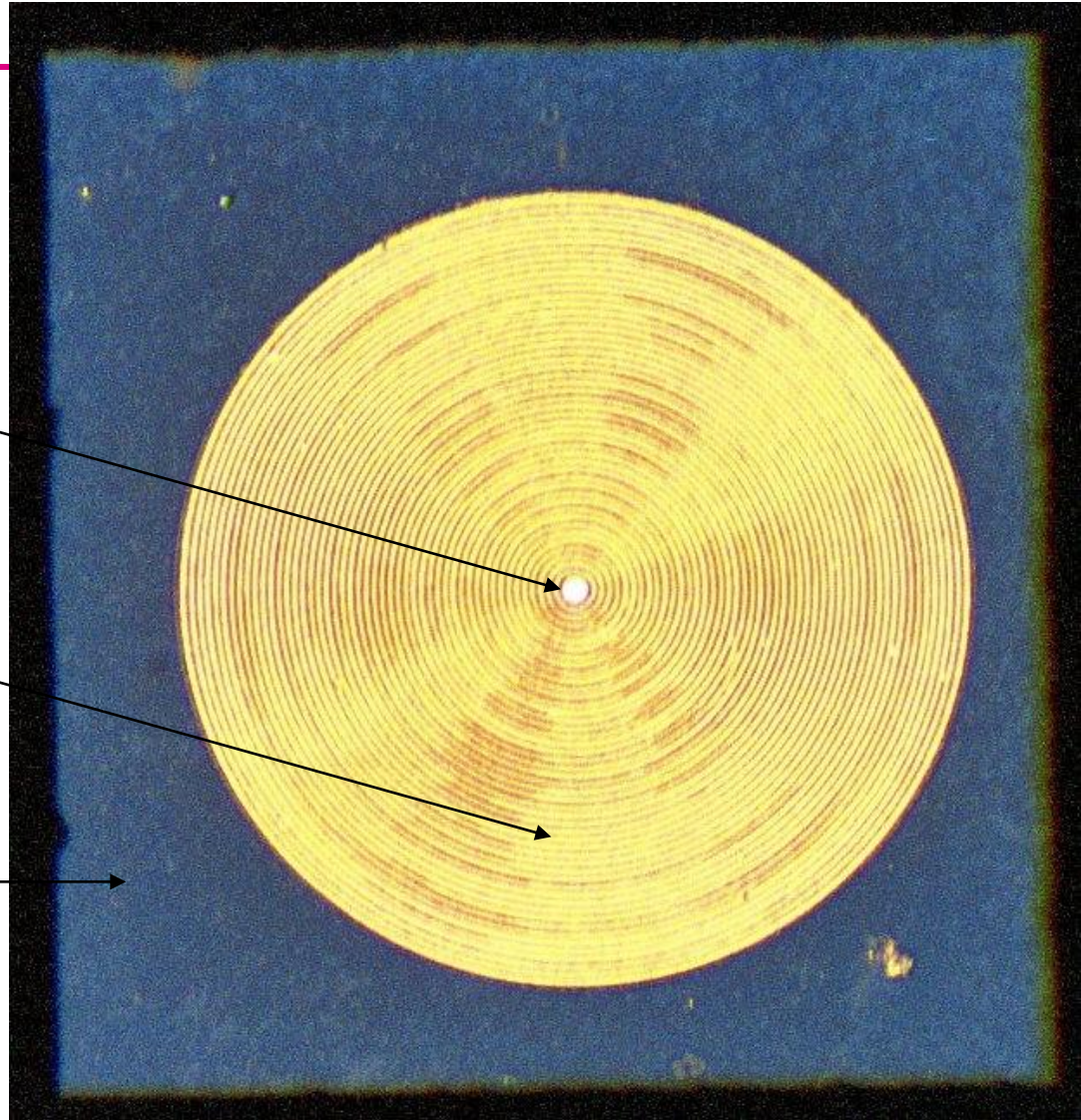
Enhanced Transmission from Bullseye Pattern

Transmission of
'bullseye' patterned
Ag film

$T \sim 20\%$;

Light through center
hole may interfere
constructively or
destructively with light
through patterned
area

Transmission of Ag
film $< 2\%$ in the blue,
 $< 0.1\%$ in red and IR

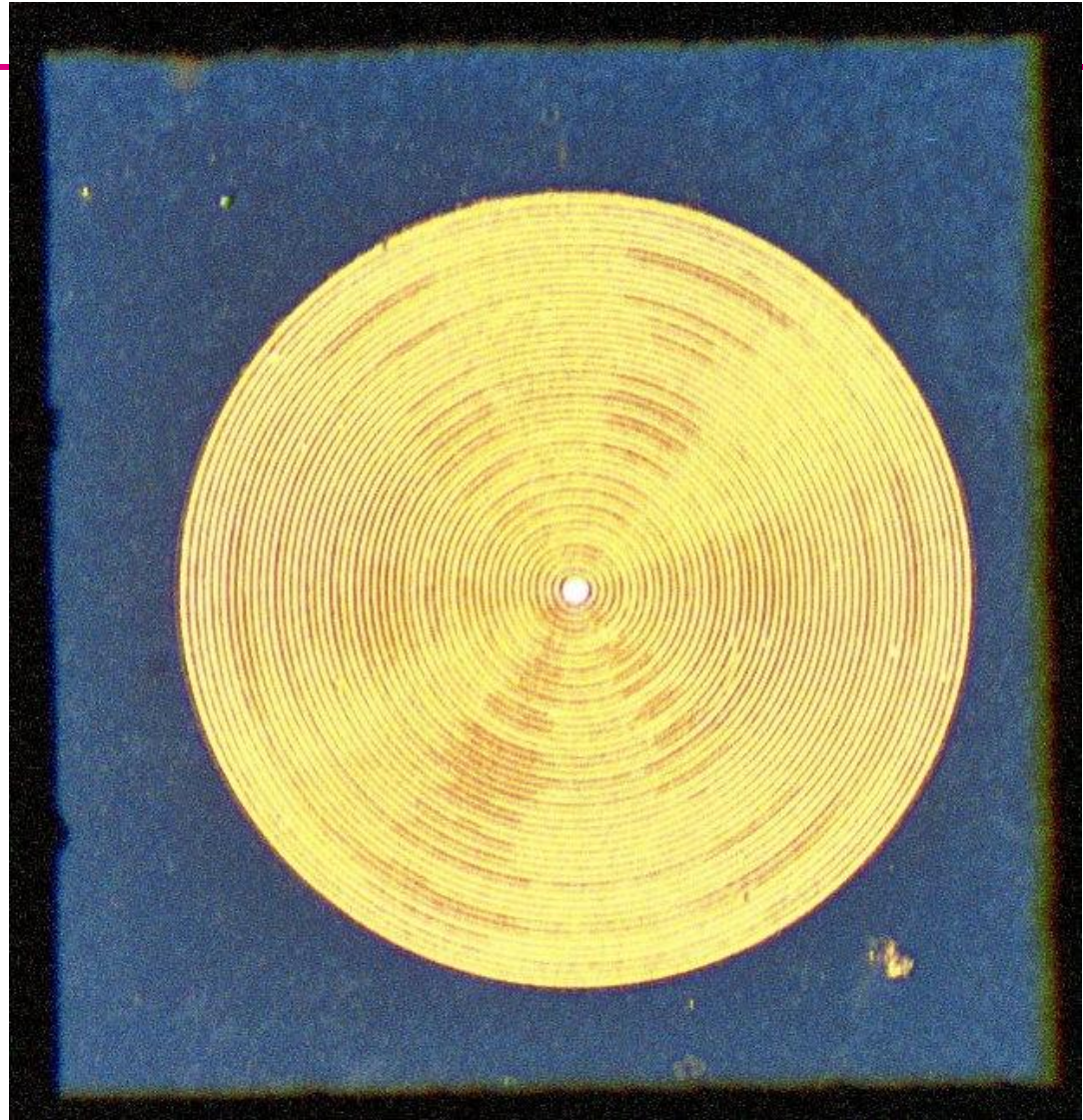
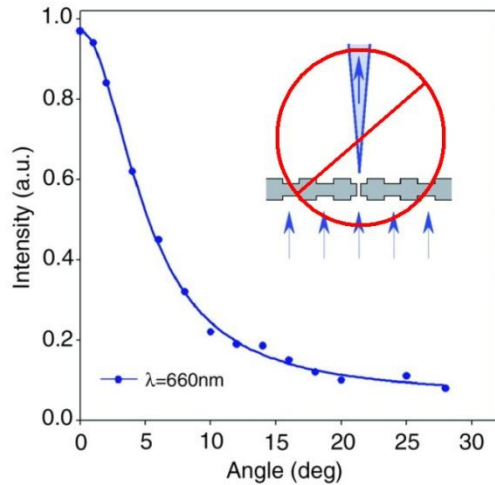


The *entire pattern*
lights up



Enhanced Transmission from Bullseye Pattern

Transmission of
'bullseye' patterned
Ag film

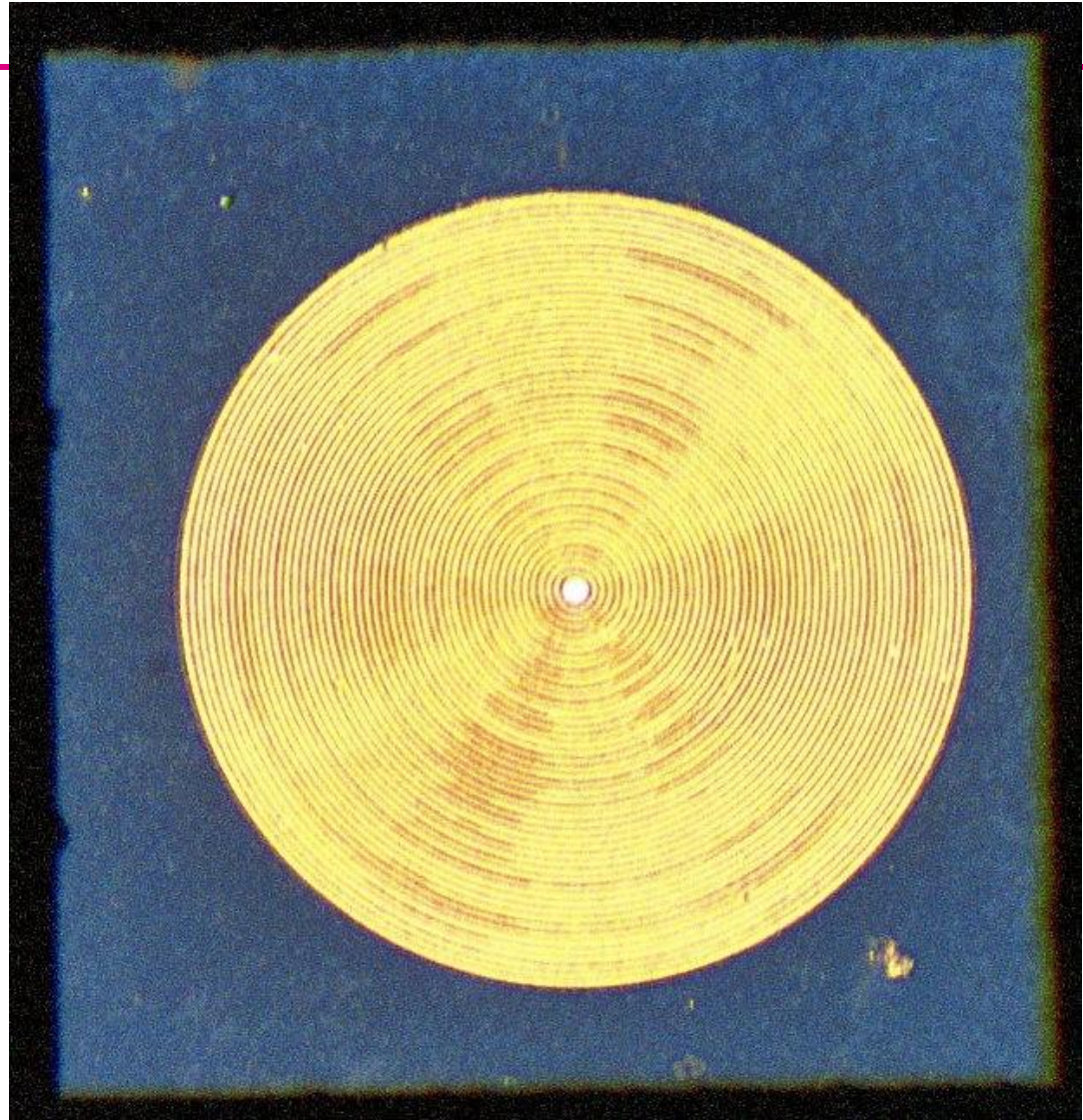
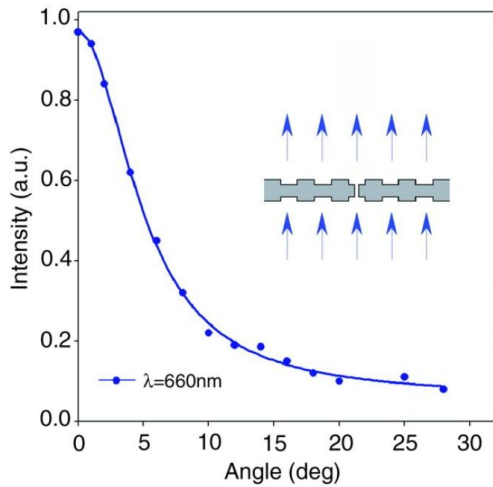


*The entire pattern
lights up*



Enhanced Transmission from Bullseye Pattern

Transmission of
'bullseye' patterned
Ag film

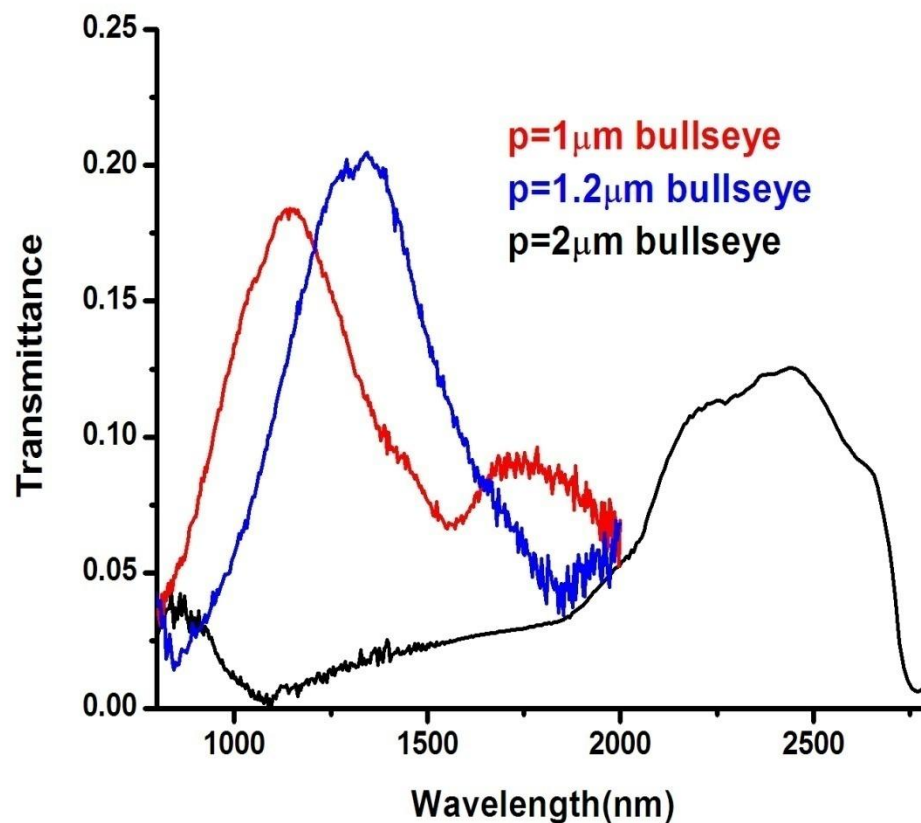
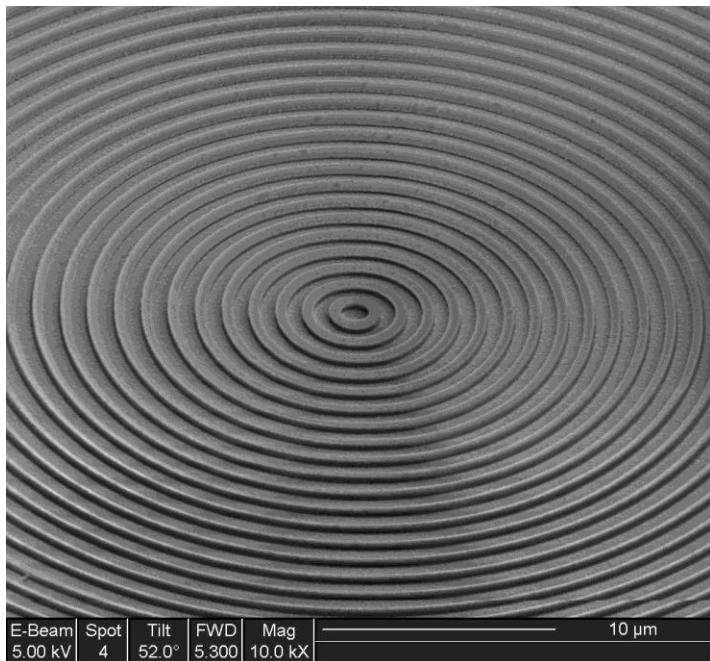


*The entire pattern
lights up*



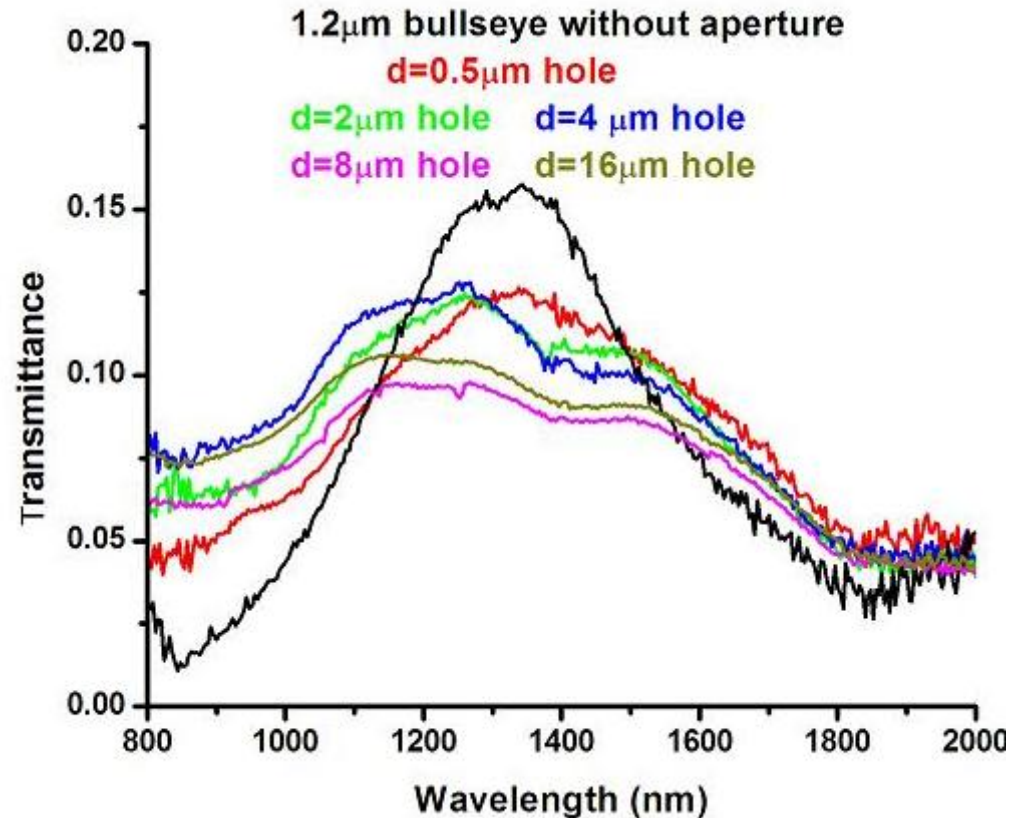
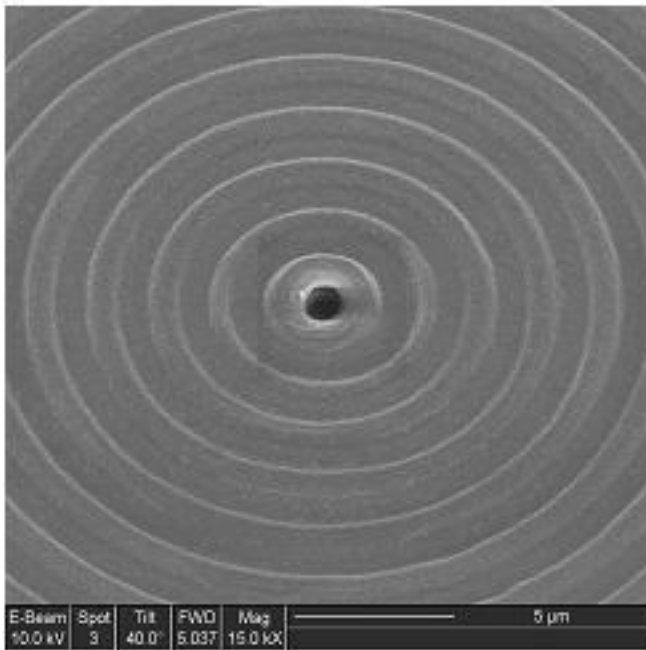
Scaling in bullseye structure

- Silver bullseye on fused silica.
- Transmits up to 20% of the light even with no center hole
- Wavelength of maximum scales with ring spacing

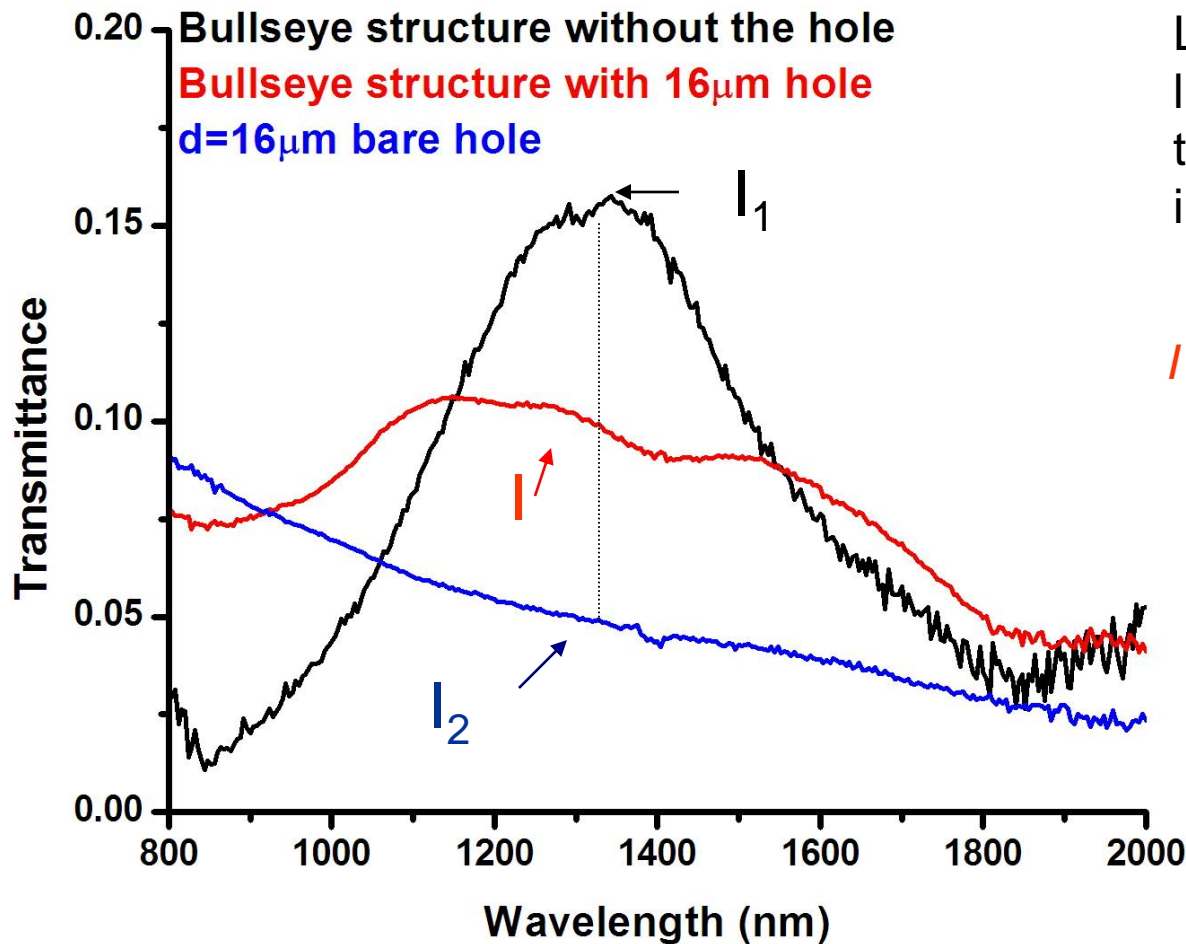


Interference effect in bullseye

- Silver on fused silica
- Light from hole interferes destructively with light from ring pattern, reducing transmittance
- Eventually, hole is big enough to dominate transmittance



Phase Difference



Light from the aperture and light attenuated from the bullseye structure interferes destructively,

$$I = I_1 + I_2 + 2(I_1 I_2)^{1/2} \cos(\delta)$$

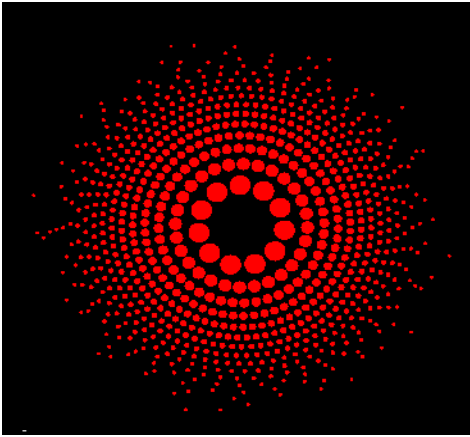
δ =Phase Difference

$$\delta \approx 2\pi/3$$



Imaging with sieves and zone plates

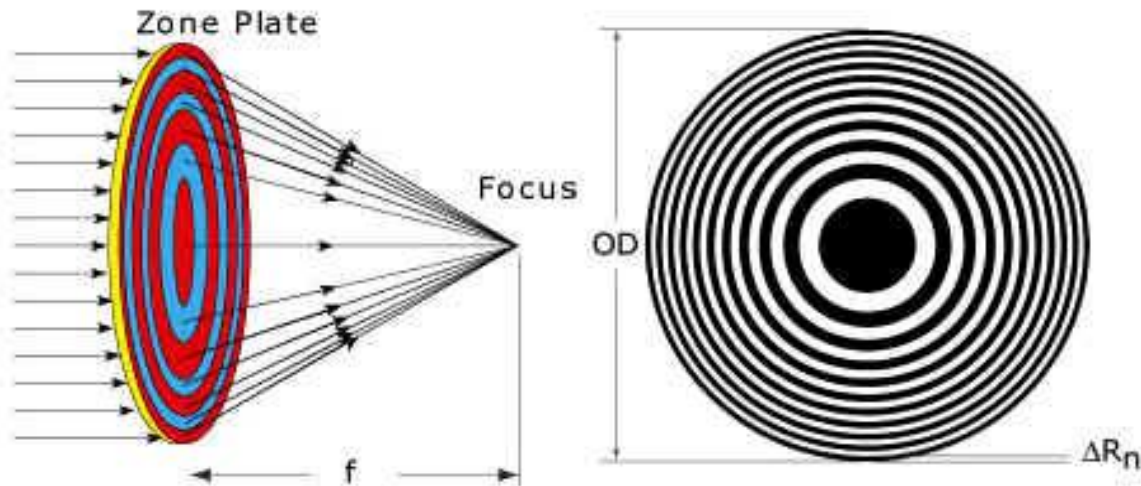
- Photo with sieve



- 100 nm silver film
- 3 mm diameter
- 50 mm focal length



Fresnel zone plate



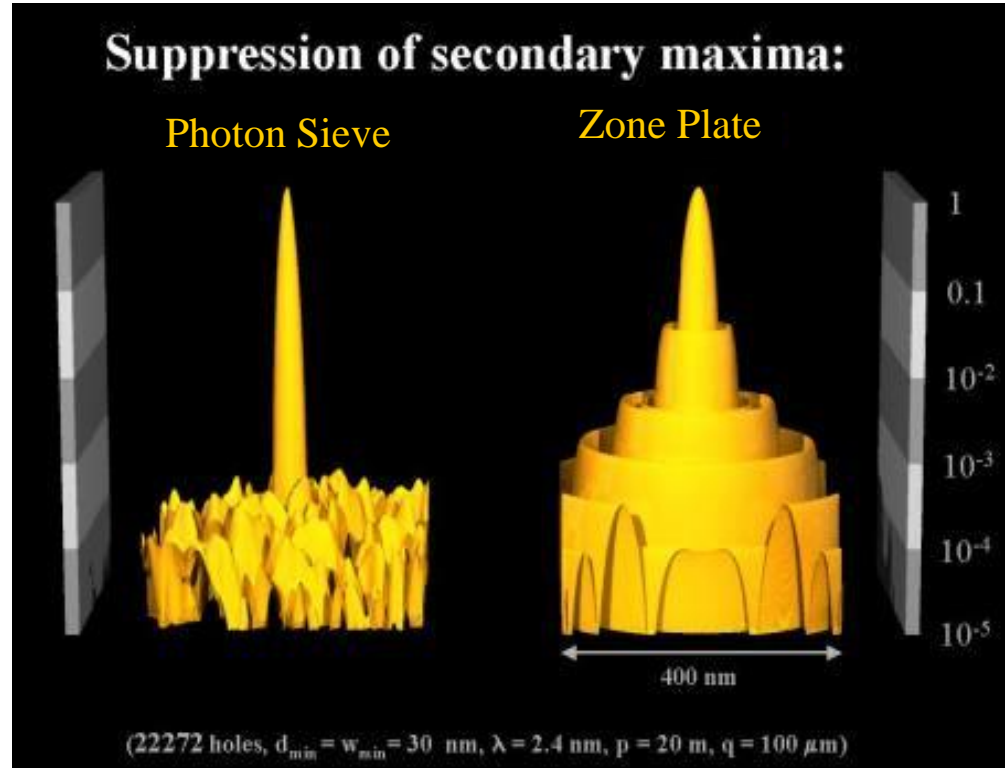
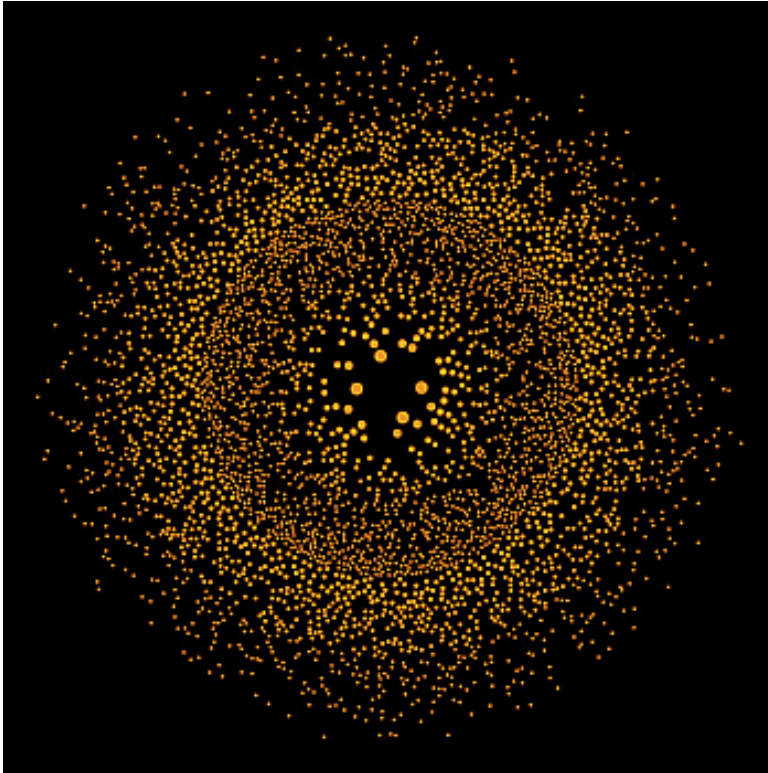
- Focusing device, made of a set of radially symmetric rings which alternate between opaque and transparent
- Zone plates use constructive interference of light rays from adjacent zones to form a focus
- The focal length f of a zone plate is a function of its diameter OD, its outermost zone width ΔR_n and the wavelength λ :

$$f = OD \cdot \Delta R_n / \lambda$$



Photon Sieve: a diffractive lens

Kipp L. *et al.*,
Nature 414, 2001

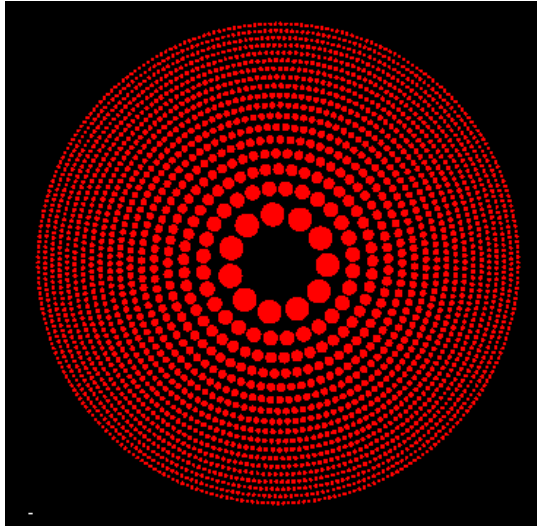


- Resolution better than FZP
- Contrast better than FZP



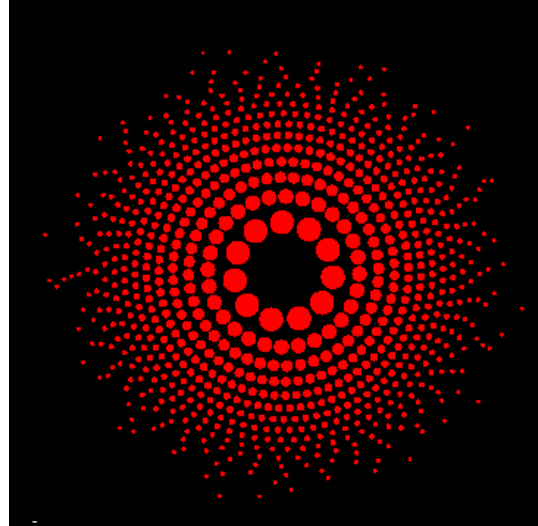
Characteristics of PS: Effect of Apodization

Unapodized



2,722 pinholes,
transmission 55.8%

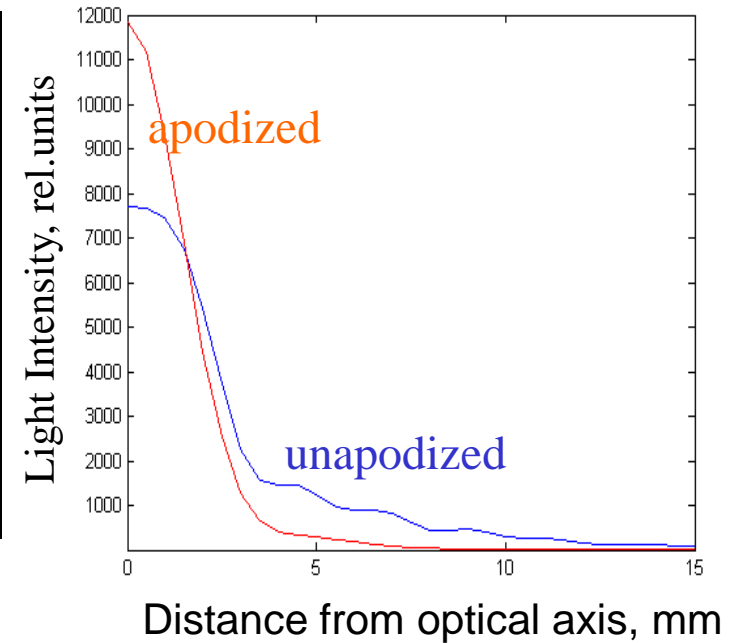
Apodized



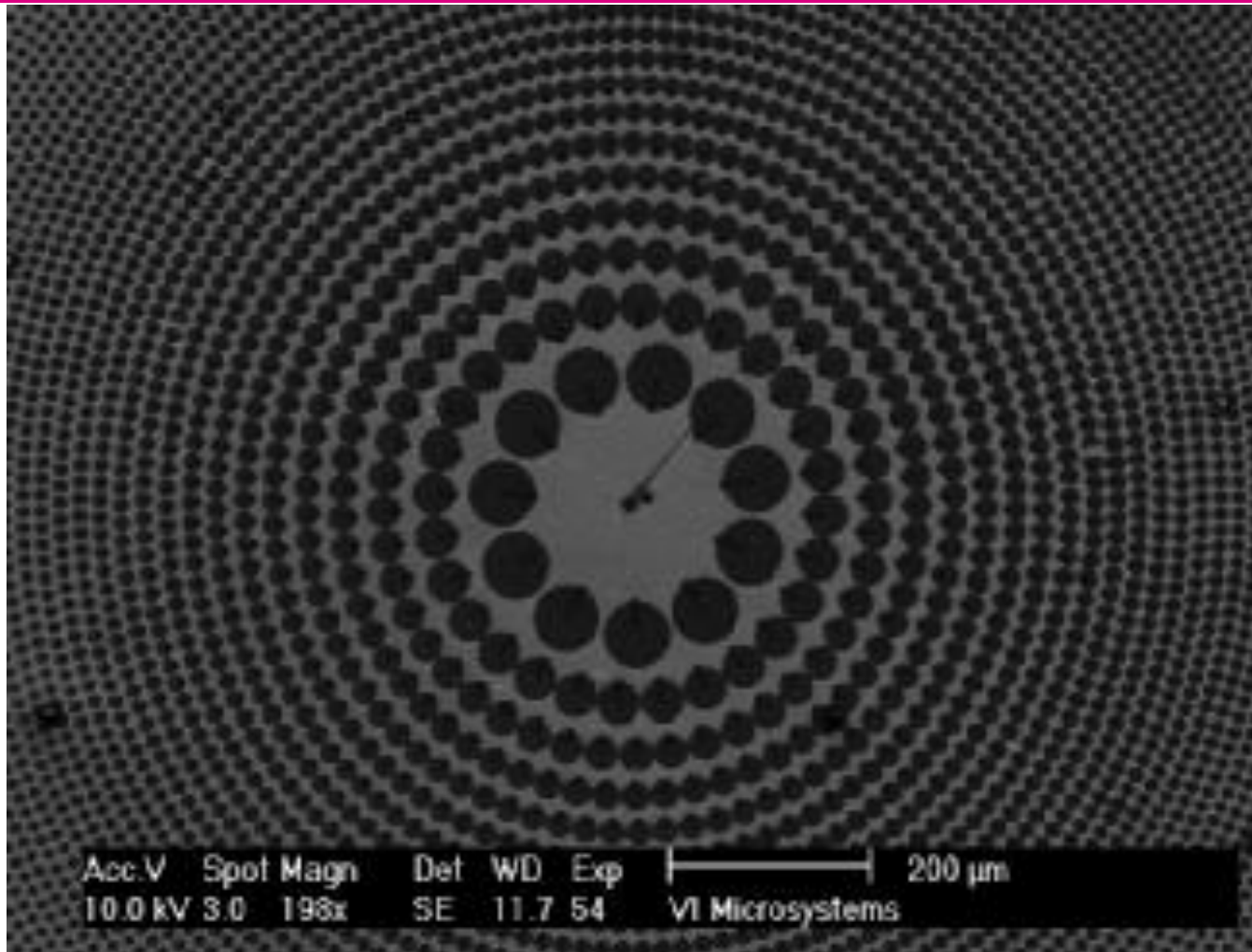
818 pinholes,
transmission 28.3%

\varnothing 1.0 mm,
f.l. 10 mm,
 $\lambda=650$ nm

Paraxial point spread function



Fabricated Lens



SEM of PS Pattern



New Physics Building



Filtered and greyscaled



Compare depth of field

- 50 mm focal length, photon sieve designed for $\lambda = 500$ nm (weight below 1 gram) vs 50 mm focal length Canon lens (weight 400 gram)
- Both set to 3 mm aperture (f/16)
- Sieve images adjusted for color, contrast in photoshop, and 1 level unsharp mask applied.



Depth of field at 1 foot



PSF measurements

- Source is 540 nm light from monochromator.
- Light illuminates an 80 μm hole.
- Optic under test images this hole at 1:1 magnification on the CCD.

WinCamD™

The only way to get accurate results is to know the accuracy of the beam.



The WinCamD™ is a CCD-based, beam intensity, width, and position profiler. It displays rotatable 3D beam profiles as small as 50 μm in width, in real time (5-Hz update), with positional accuracy of 1 μm . WinCamD functions include pass/fail mode, Gaussian and top-hat profile fit, and relative power measurement — all at a low cost that makes it ideal for both scientific and industrial applications.

Applications

- Verify beam performance in all applications
- Set pass/fail parameters in lab or production
- Determine Gaussian and top-hat profile fit
- Graph the intensity profile for all beam shapes

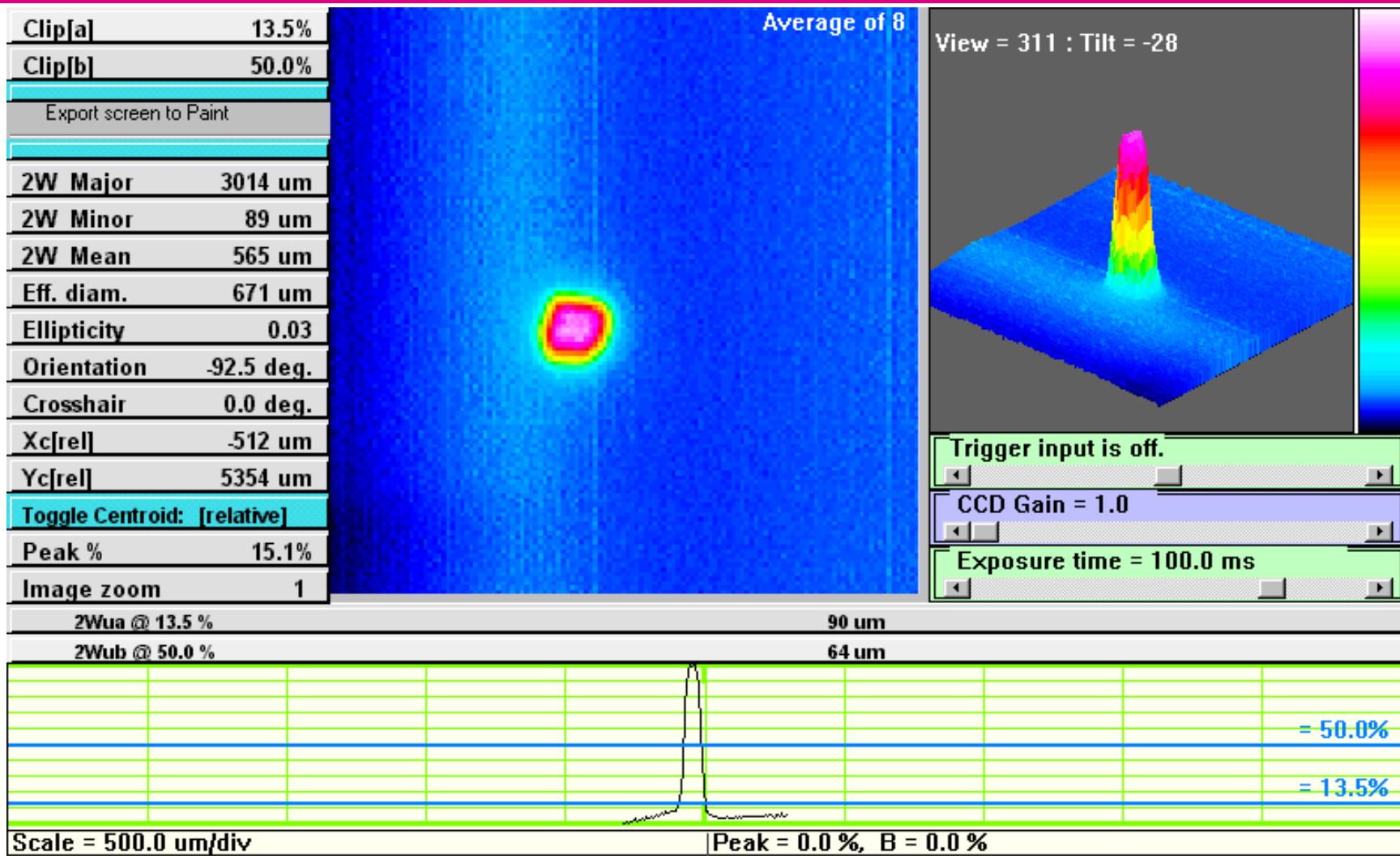
Features

- Provides high resolution with 1.39 million, 4.65- μm square pixels
- Resolves 60,000 intensity levels (with shutter) with a 14-bit ADC chip
- Measures pulsed (as low as 1 Hz) and continuous-wave beams
- Accepts beam sizes from 50 μm to 6.32 mm
- Measures power from 2 μW to 100 mW @ 633 nm (1-mm beam)

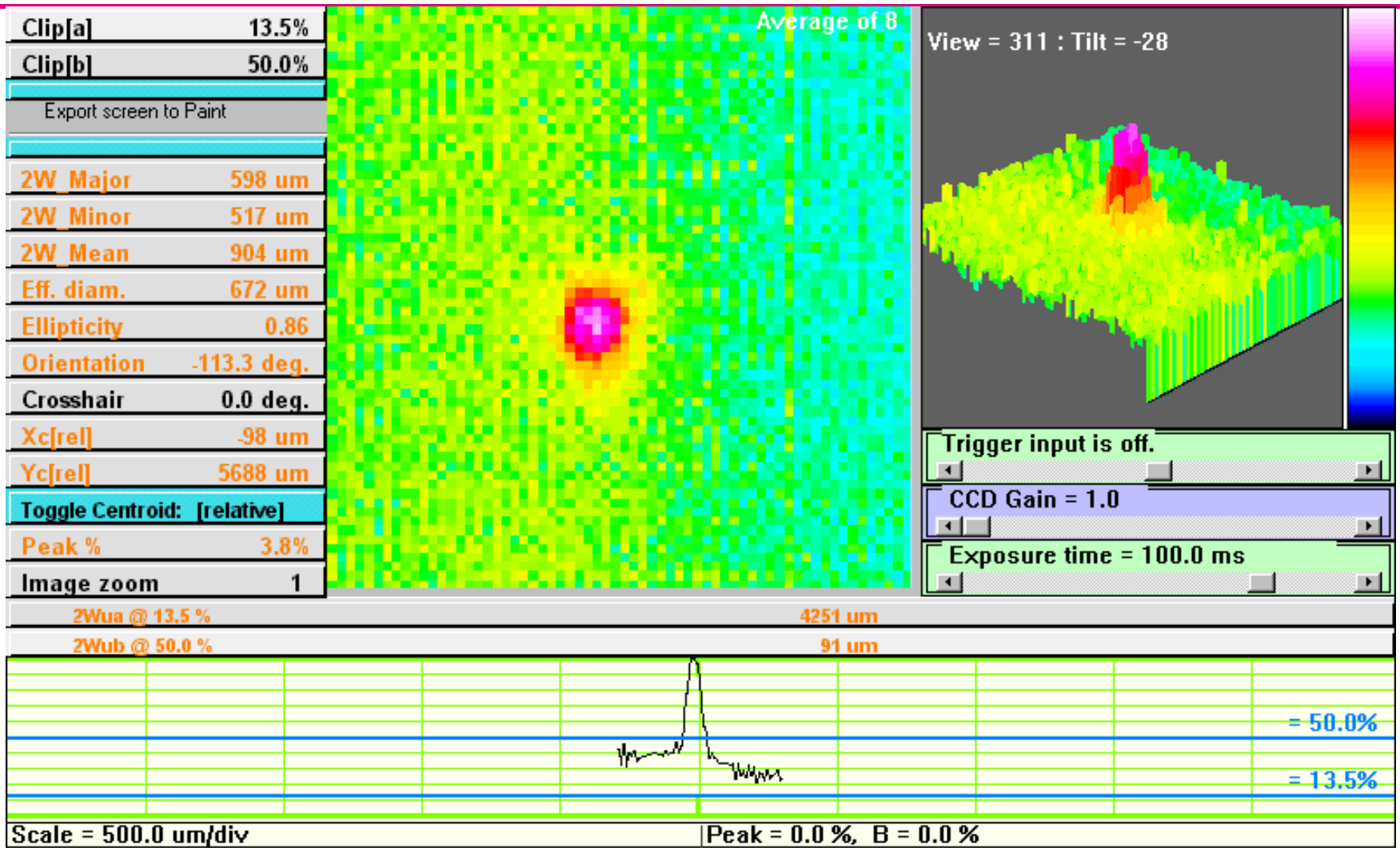
MELLES GRLOT



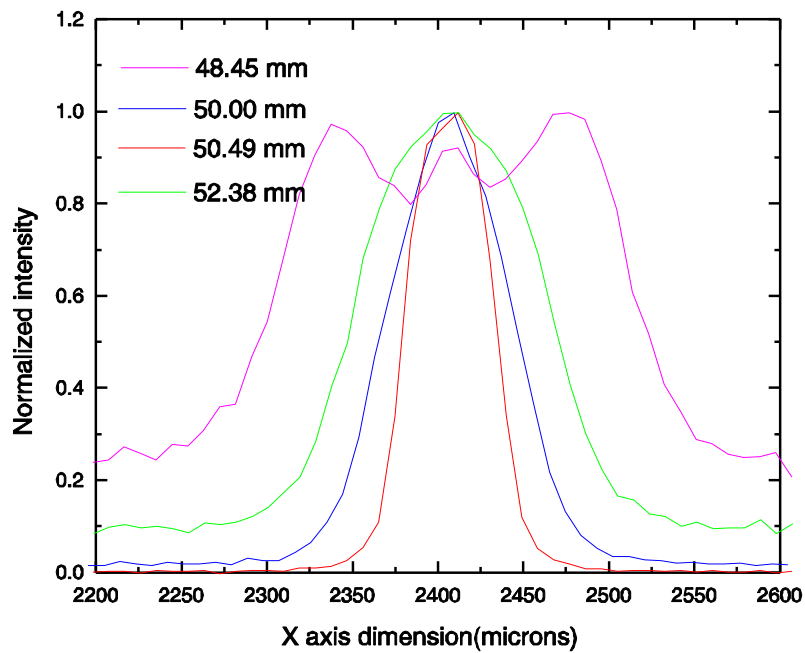
PSF of 50 mm lens



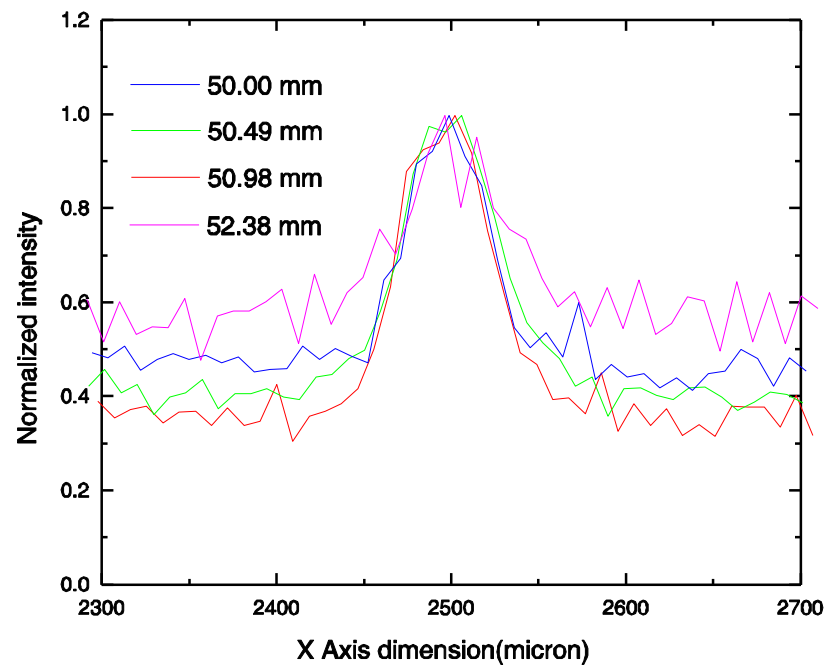
PSF of photon sieve



Effect of focusing



Lens

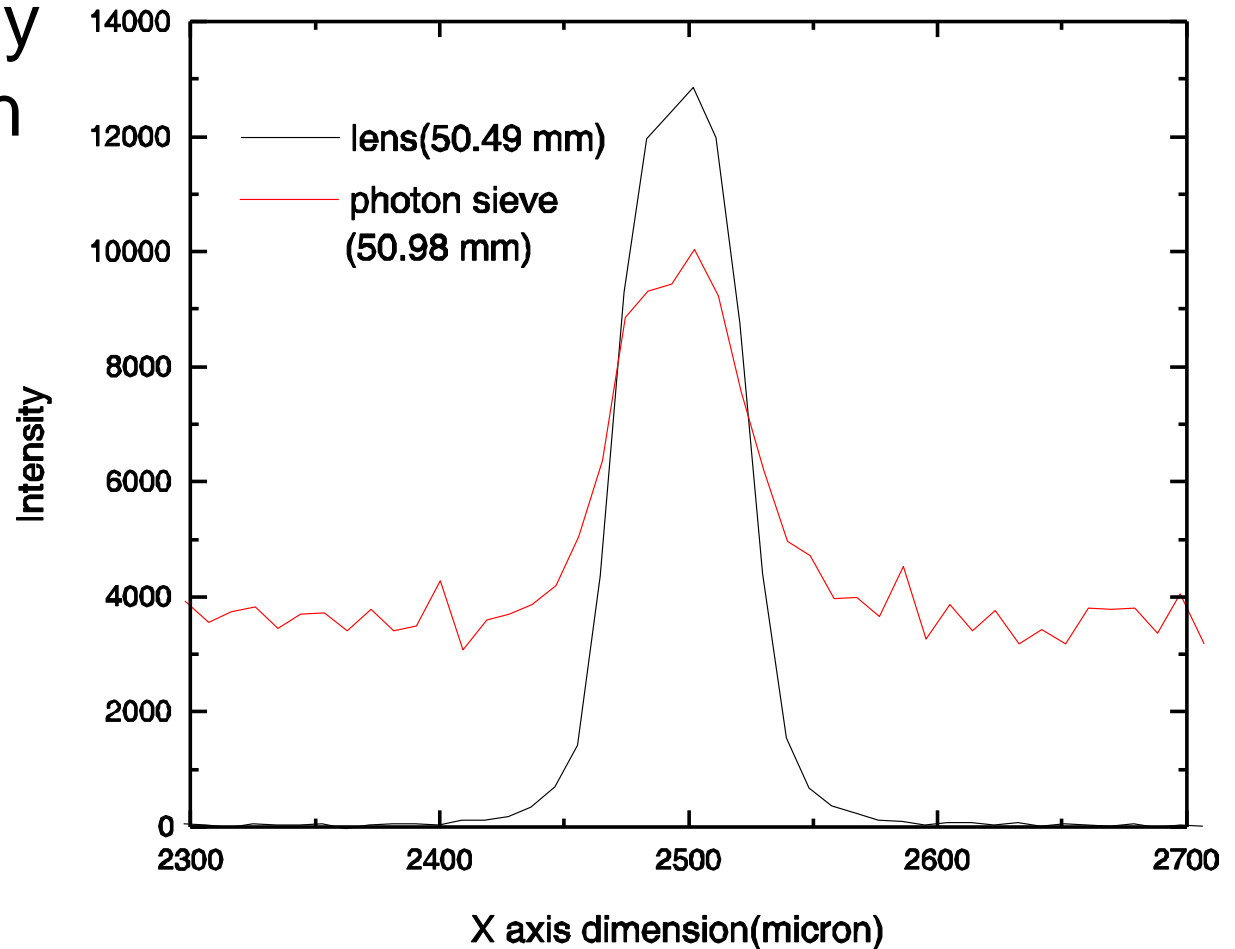


Photon sieve



Comparison – in focus

- Lens has slightly better resolution than PS
- PS has better depth of field
- PS has 75% transmission at peak
- PS has ~30% scattered light



Sieve has better depth of field

- Glass lens far superior in contrast, flare.
- However, it appears that some of the sieve's flare problems come from back reflection off the silver film.
- Sieve has better depth of field, from 1 ft to infinity vs about 10 ft to infinity for the glass lens.



Summary

- Diffraction and diffractive devices have remarkable properties
 - Unexpected phase relation
 - Enhanced transmission by periodic arrays
 - Unusual effects in corrugated metal structures
 - Imaging with ultra-light-weight diffractive optics
 - Can be designed for any wavelength band
- Geometry governs their performance
- Simulations require full electromagnetic theory
 - Polarization and phase matters



THE END



Yanbei's solution

- Gratings bestow a phase factor on the light of

$$e^{ikG(x)} = \sum_m C_m e^{imgx} \approx e^{-igx} \quad \text{and} \quad e^{-ig(x-x_o)}$$

where $G(x)$ is the periodic grating profile, $g = 2\pi/d$, $m = -1$, $C_{-1} = 1$, and x_o is the offset of the second grating wrt the first.

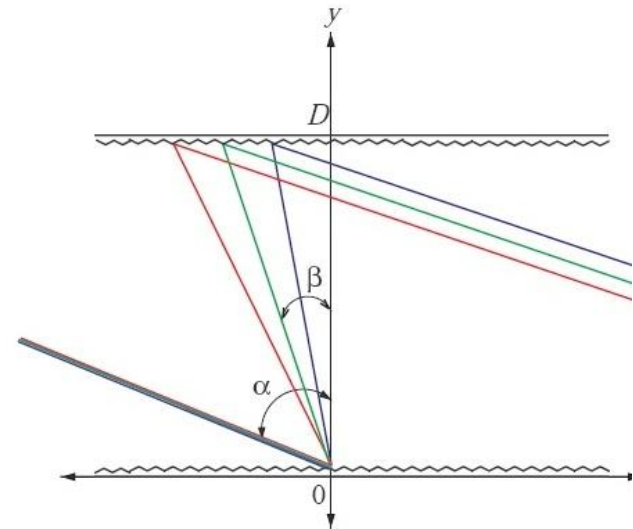
- Then

$$E_{1,in} = E_o e^{ik(x \sin \alpha - y \cos \alpha)} \quad (1)$$

$$E_{1,out} = E_o e^{i[(k \sin \alpha - g)x + ky \cos \beta]} \quad (2)$$

$$E_{2,out} = E_o e^{i[k(x \sin \alpha + D \cos \beta) - gx_o]} \quad (3)$$

$$E_{em} = E_o e^{i[k\{x \sin \alpha - (y-D) \cos \alpha + D \cos \beta\} - gx_o]} \quad (4)$$



Phase

- The phase $\Phi(\omega, x, y)$ is

$$\Phi = \frac{\omega}{c} [x \sin \alpha - (y - D) \cos \alpha + D \cos \beta] - g x_o$$

so that

$$\frac{\partial \Phi}{\partial \omega} = \frac{1}{c} [x \sin \alpha - (y - D) \cos \alpha] + \frac{D}{c} \left(\cos \beta - \omega \frac{\partial \beta}{\partial \omega} \sin \beta \right).$$

- Using $\frac{\partial \beta}{\partial \omega}$ from the grating equation and the (wavelength-dependent) geometric path length $L(\omega)$ from the first grating (at the origin) to the end mirror, we find

$$\frac{\partial \Phi}{\partial \omega} = \frac{L(\omega)}{c},$$

making it clear that the variation of phase with frequency cannot be set to zero.



Summary: enhanced transmission

- Transmission of perforated silver films can be quite high at certain wavelengths
- Novel computational algorithm (vector diffraction) produces computed results in good agreement with measurements
- Closer to CDEW than SPP explanation
- Would get enhanced transmission even for perfect metal
- Future plans
 - Look at reflection ($1 - R - T = A$) to learn about plasma contribution direct
 - Groove structures: control of phase of trapped mode to interfere constructively with the direct transmission
 - Find diffracted beams in the short wavelength regime for periodic structure



Surface Plasmon Coupling via 2-Dimensional Grating

Momentum conservation for 2-d grating

$$k_{sp} = k_x + k_y + ig_x + ig_y \quad (g_x = g_y = \frac{2\pi}{D})$$

Dispersion relation of surface plasmon (p-pol.)

$$k_{sp} = k_0 \left(\frac{\epsilon_d \epsilon_m}{\epsilon_d + \epsilon_m} \right)^{1/2}$$

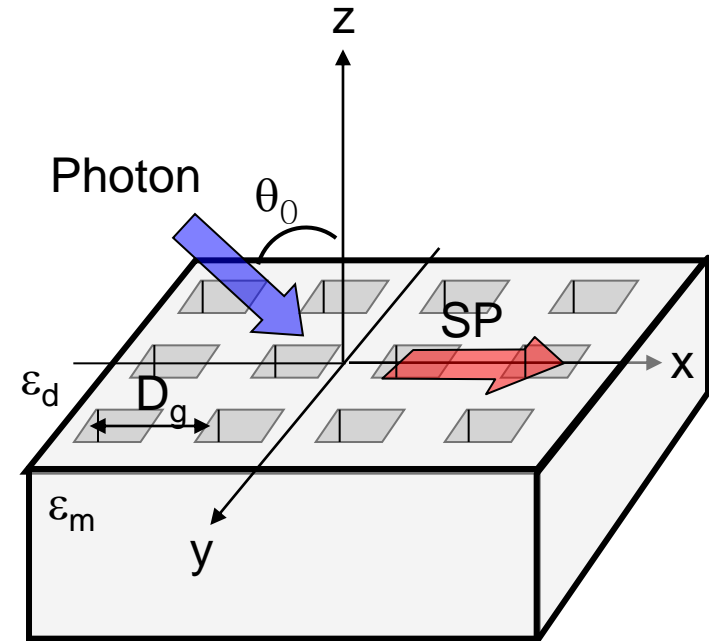
Equations for position of SP resonant peak

Normal incidence ($\phi_0 = 0, \theta_0 = 0$)

$$\lambda_{\max} = \frac{D_g}{\sqrt{i^2 + j^2}} \sqrt{\frac{\epsilon_d \epsilon_m}{\epsilon_d + \epsilon_m}}$$

Oblique incidence ($\phi_0 = 0$ but $\theta_0 \neq 0$)

$$\lambda_{\max} = \frac{D_g}{i^2 + j^2} \left\{ -i \sin \theta_0 + \sqrt{(i^2 + j^2) \frac{\epsilon_d \epsilon_m}{\epsilon_d + \epsilon_m} - j^2 \sin^2 \theta_0} \right\}$$



Diffraction minima at

$$\lambda_{\min} = \frac{D_g}{i^2 + j^2} \left\{ -i \sin \theta_0 + \sqrt{(i^2 + j^2) \epsilon_d - j^2 \sin^2 \theta_0} \right\}$$

- 2-dimensional diffraction channels open at these wavelengths
- Diffracted beam is parallel to the surface of the film
- R. W. Wood, Phys. Rev. **48**, 928 (1935)
- Compare to SPP eqn for max:

$$\lambda_{\max} = \frac{D_g}{i^2 + j^2} \left\{ -i \sin \theta_0 + \sqrt{(i^2 + j^2) \frac{\epsilon_d \epsilon_m}{\epsilon_d + \epsilon_m} - j^2 \sin^2 \theta_0} \right\}$$



Dispersion relation of surface plasmon

p-polarization

$$\mathbf{E}_1 = (A, 0, B)e^{i(k_x x - \omega t)} e^{-\alpha_1 z} \quad z > 0$$

$$\mathbf{H}_1 = (0, C, 0)e^{i(k_x x - \omega t)} e^{-\alpha_1 z} \quad z > 0$$

$$\mathbf{E}_2 = (D, 0, E)e^{i(k_x x - \omega t)} e^{\alpha_2 z} \quad z < 0$$

$$\mathbf{H}_2 = (0, F, 0)e^{i(k_x x - \omega t)} e^{\alpha_2 z} \quad z < 0$$

$$\mathbf{E}_{1x}|_{z=0} = \mathbf{E}_{2x}|_{z=0}$$

boundary conditions

$$\mathbf{H}_{1x}|_{z=0} = \mathbf{H}_{2x}|_{z=0}$$

$$\nabla \times \mathbf{H} = \frac{\epsilon}{c} \frac{\partial \mathbf{E}}{\partial t} \quad \text{Maxwell's equation}$$

$$\Rightarrow \frac{\alpha_1}{\alpha_2} = -\frac{\epsilon_1}{\epsilon_2} \quad \text{condition for surface plasmon mode}$$

$$\nabla \times \mathbf{H} = \frac{\epsilon}{c} \frac{\partial \mathbf{E}}{\partial t} \quad \nabla \times \mathbf{E} = -\frac{1}{c} \frac{\partial \mathbf{H}}{\partial t}$$

$$\nabla \times (\nabla \times \mathbf{E}) = -\frac{1}{c} \frac{\partial}{\partial t} (\nabla \times \mathbf{H}) = -\frac{\epsilon}{c^2} \frac{\partial^2 \mathbf{E}}{\partial t^2}$$

$$\nabla \times (\nabla \times \mathbf{E}) = \nabla(\nabla \cdot \mathbf{E}) - \nabla^2 \mathbf{E} \quad \nabla \cdot \mathbf{E} = 0$$

$$\nabla^2 \mathbf{E} = \frac{\epsilon}{c^2} \frac{\partial^2 \mathbf{E}}{\partial t^2} \quad \text{transverse wave equation}$$

$$\Rightarrow k_x = \frac{\omega}{c} \sqrt{\frac{\epsilon_1 \epsilon_2}{\epsilon_1 + \epsilon_2}}$$



Dispersion relation of surface plasmon

s-polarization

$$\mathbf{E}_1 = (0, A, 0)e^{i(k_x x - \omega t)} e^{-\alpha_1 z} \quad z > 0$$

$$\mathbf{H}_1 = (B, 0, C)e^{i(k_x x - \omega t)} e^{-\alpha_1 z} \quad z > 0$$

$$\mathbf{E}_2 = (0, D, 0)e^{i(k_x x - \omega t)} e^{\alpha_2 z} \quad z < 0$$

$$\mathbf{H}_2 = (E, 0, F)e^{i(k_x x - \omega t)} e^{\alpha_2 z} \quad z < 0$$

$$\mathbf{E}_{1x}|_{z=0} = \mathbf{E}_{2x}|_{z=0}$$

boundary conditions

$$\mathbf{H}_{1x}|_{z=0} = \mathbf{H}_{2x}|_{z=0}$$

$$\Rightarrow A = D \text{ and } B = E$$

$$\nabla \times \mathbf{E} = -\frac{1}{c} \frac{\partial \mathbf{H}}{\partial t} \quad \text{Maxwell's equation}$$

$$B = \frac{c\alpha_1}{i\omega} A \quad z > 0$$

$$C = \frac{k_x c}{\omega} A \quad z > 0$$

$$E = -\frac{c\alpha_2}{i\omega} D \quad z < 0$$

$$F = \frac{k_x c}{\omega} D \quad z < 0$$

$$\Rightarrow \frac{c}{i\omega} (\alpha_1 + \alpha_2) A = 0$$

With α_1 and α_2 positive, all of constants A, B, C, E and F become zero which means there is no surface wave.



Longitudinal wave and transverse wave

Longitudinal wave: field oscillation and propagation are in the same direction

Transverse wave: field oscillation direction is perpendicular to propagation direction

If there is no external charge, $\nabla \cdot \mathbf{D} = 0 \Rightarrow \epsilon \mathbf{k} \cdot \mathbf{E} = 0$

For longitudinal wave, $\mathbf{k} \cdot \mathbf{E} \neq 0$, therefore $\epsilon = 0$

For transverse wave, $\mathbf{k} \cdot \mathbf{E} = 0$. To determine ϵ for transverse wave,

$$\nabla \times \mathbf{E} = -\frac{1}{c} \frac{\partial \mathbf{H}}{\partial t}$$

$$\nabla \times \nabla \times \mathbf{E} = -\frac{1}{c} \frac{\partial (\nabla \times \mathbf{H})}{\partial t}$$

$$\nabla \times \mathbf{H} = \frac{1}{c} \frac{\partial \mathbf{D}}{\partial t} \quad (\text{if } \mathbf{J}_f = 0)$$

$$\nabla \times \nabla \times \mathbf{E} = \nabla(\nabla \cdot \mathbf{E}) - \nabla^2 \mathbf{E} = -\frac{1}{c^2} \frac{\partial^2 \mathbf{D}}{\partial t^2}$$

$$\nabla \cdot \mathbf{E} = 0$$

$$\nabla^2 \mathbf{E} = \frac{1}{c^2} \frac{\partial^2 \mathbf{D}}{\partial t^2}$$

$$\left(k^2 - \frac{\epsilon \omega^2}{c^2} \right) \mathbf{E} = 0$$

$$k = \frac{\omega}{c} \sqrt{\epsilon}$$



Bethe's theory for transmission of sub-wavelength hole

Transmittance of a single hole in a infinite conducting screen which is very thin, but optically opaque with $d \ll \lambda$.

$$A = \frac{\int |\vec{S}| r^2 \sin \theta d\theta d\phi}{|\vec{S}_i|} \quad \begin{array}{l} \text{diffraction} \\ \text{cross section} \end{array}$$

$$\vec{S} = \vec{E} \times \vec{H} \quad \text{for diffracted field}$$

$$\vec{S}_i = \vec{E}_i \times \vec{H}_i \quad \text{for incident field}$$

$$A_s = \frac{64}{27\pi} k^4 \left(\frac{d}{2}\right)^6 \cos \theta \quad \text{for s-polarization}$$

$$A_p = \frac{64}{27\pi} k^4 \left(\frac{d}{2}\right)^6 \left(1 + \frac{1}{4} \sin^2 \theta\right) \quad \text{for p-polarization}$$

normalized cross sections

$$\frac{A}{\pi \left(\frac{d}{2}\right)^2} = \frac{64}{27\pi^2} \left(\frac{kd}{2}\right)^4 \approx 23 \left(\frac{d}{\lambda}\right)^4$$

for circular hole

$$\frac{A}{D^2} = \frac{64}{27\pi} \frac{(kD)^4}{2^6} \approx 18 \left(\frac{D}{\lambda}\right)^4$$

for square hole



Penetration depth of surface plasmon

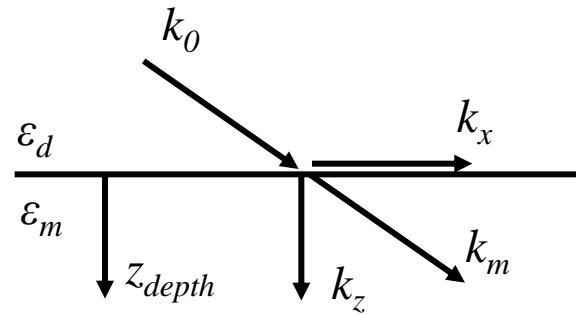
$$E = e^{-|k_z|z} = e^{-1} \Rightarrow z = \frac{1}{|k_z|}$$

$$\vec{k}_m = \vec{k}_x + \vec{k}_z$$

$$|k_m| = \frac{\omega}{c} \sqrt{\epsilon_m} \quad \text{and} \quad |k_x| = \frac{\omega}{c} \sqrt{\frac{\epsilon_d \epsilon_m}{\epsilon_d + \epsilon_m}}$$

$$|k_z| = \frac{\omega}{c} \sqrt{\frac{\epsilon_m^2}{\epsilon_d + \epsilon_m}}$$

$$z_{\text{depth}} = \frac{\lambda}{2\pi} \sqrt{\frac{\epsilon_d + \epsilon_m}{\epsilon_m^2}}$$



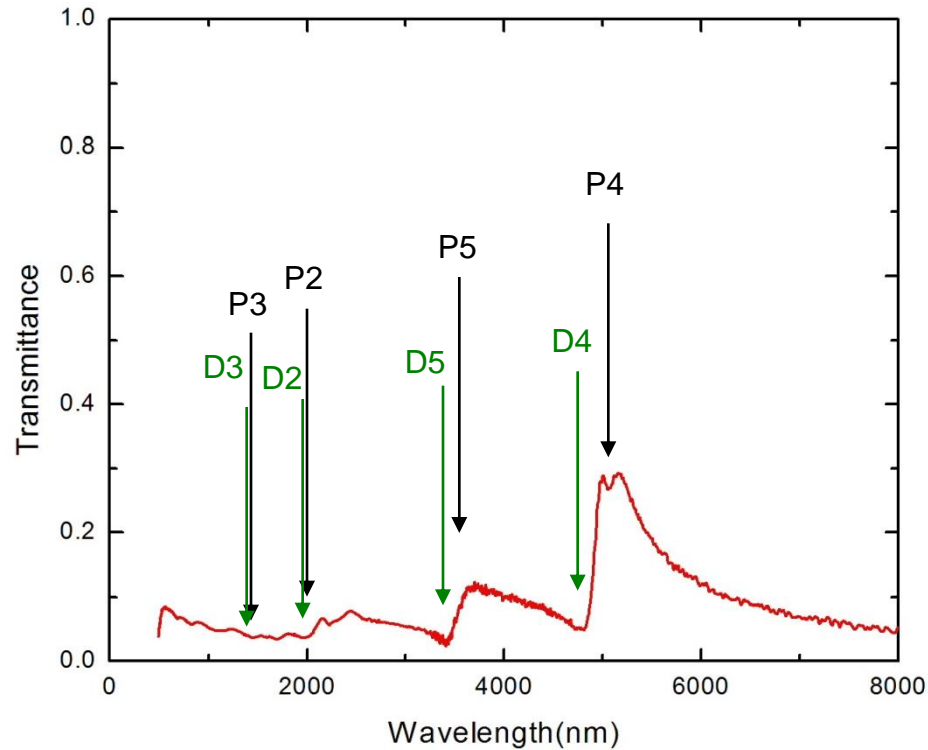
For air-silver interface, z_{depth} at $\lambda = 3000 \text{ nm}$ is about 50 nm .

$$\text{Skin-depth } \delta = \sqrt{\frac{2}{\mu_0 \sigma_c \omega}} = \sqrt{\frac{\lambda}{\pi \mu_0 \sigma_c c}}$$

For $\lambda = 3000 \text{ nm}$, δ is about 10 nm .



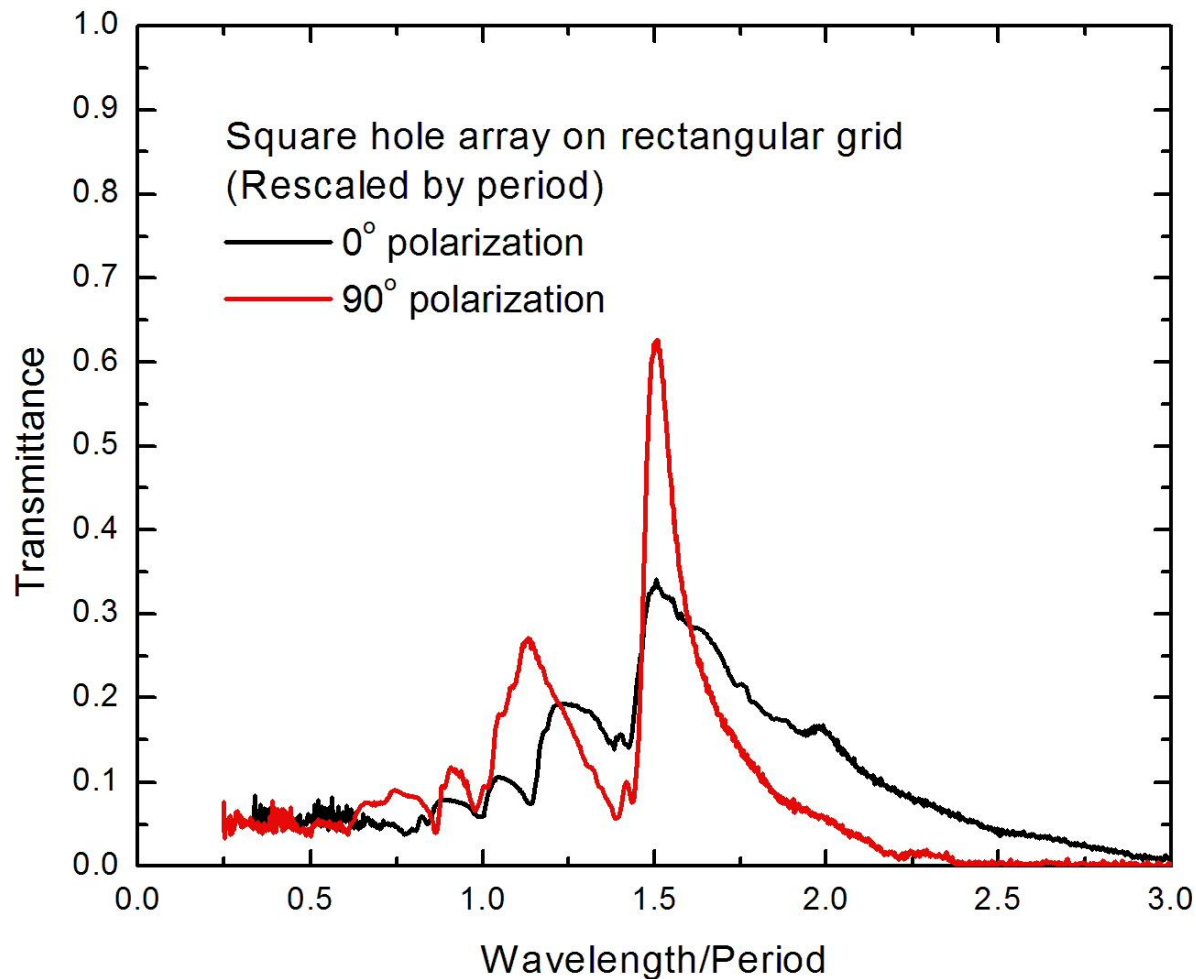
Peak and dip positions for ZnSe substrate



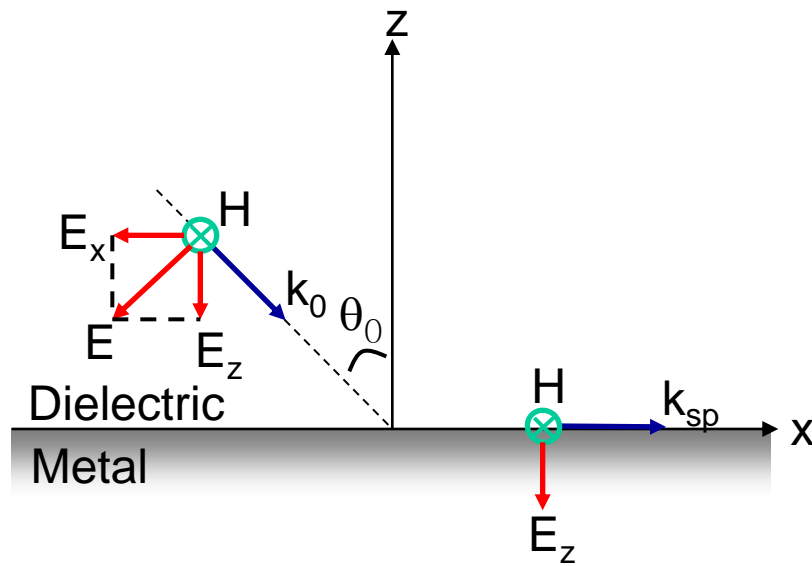
(i, j)	peak	dip
(0, ± 1), (± 1 , 0)	5080 nm (P4)	4900 nm (D4)
(± 1 , ± 1)	3590 nm (P5)	3460 nm (D5)



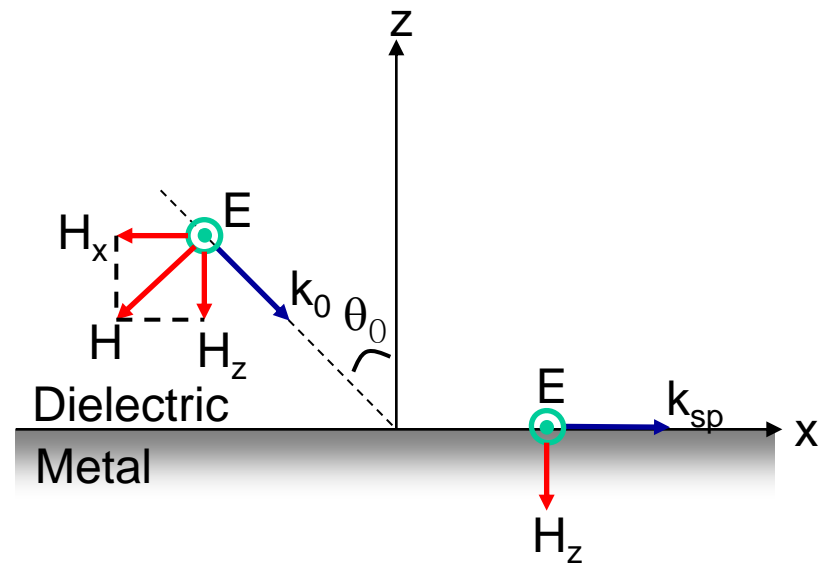
Scaling in the transmittance of a square hole array on a rectangular grid



p-polarization and s-polarization of incident light on dielectric/metal interface



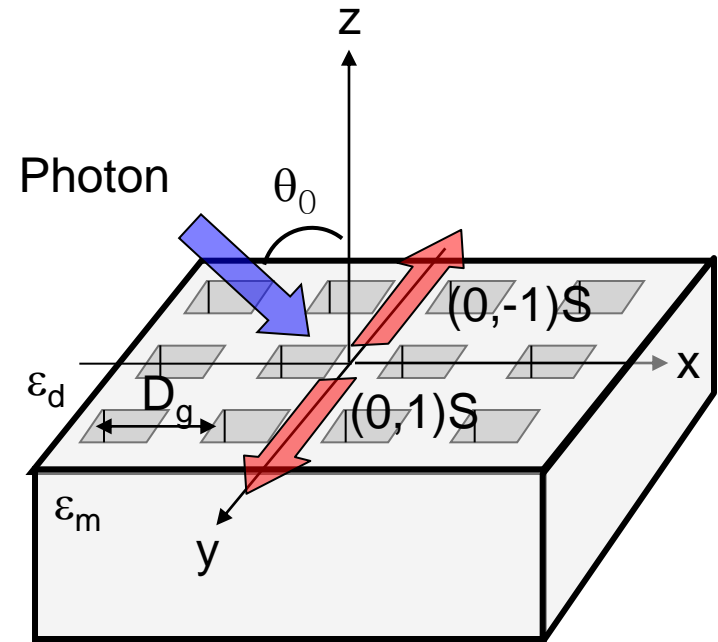
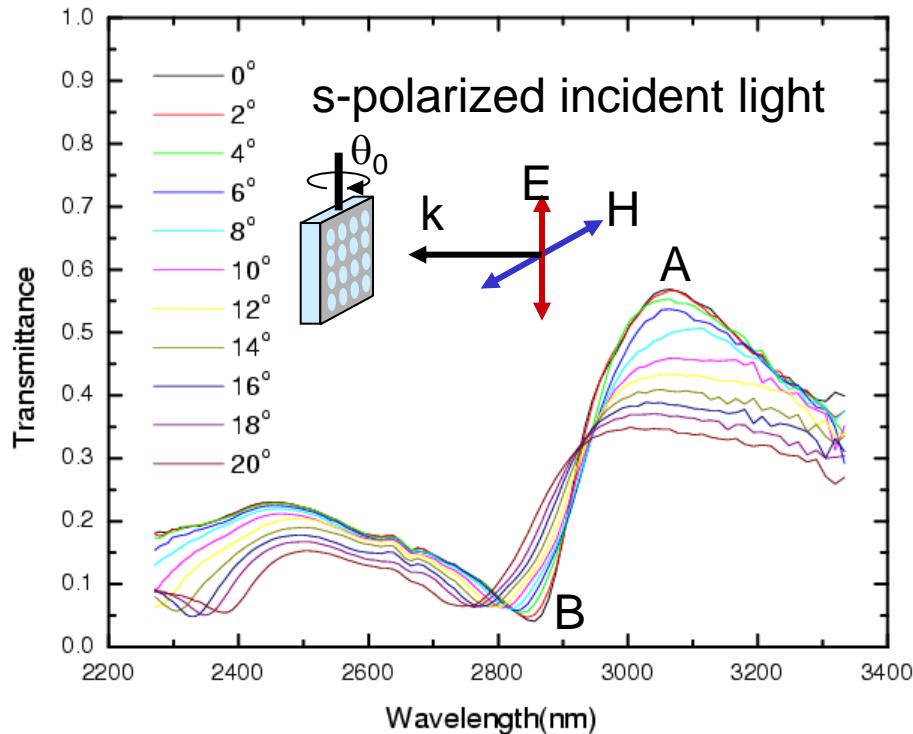
p-polarization (TM)



s-polarization (TE)



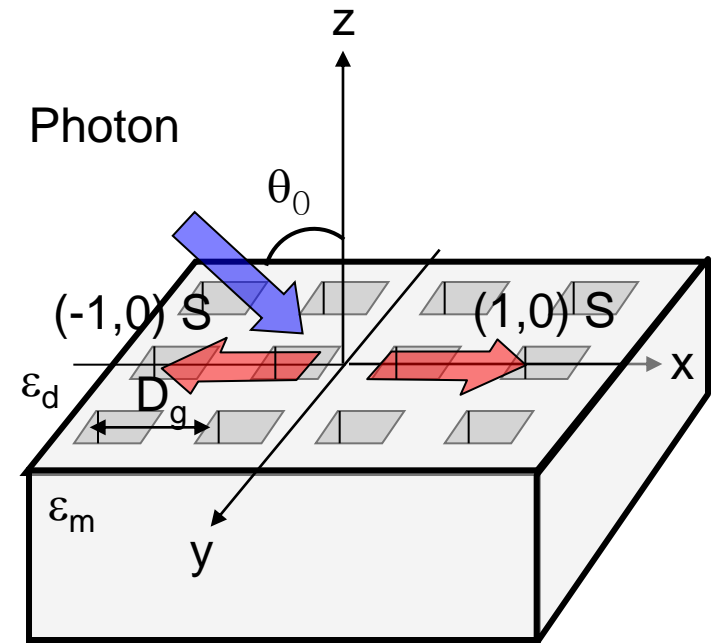
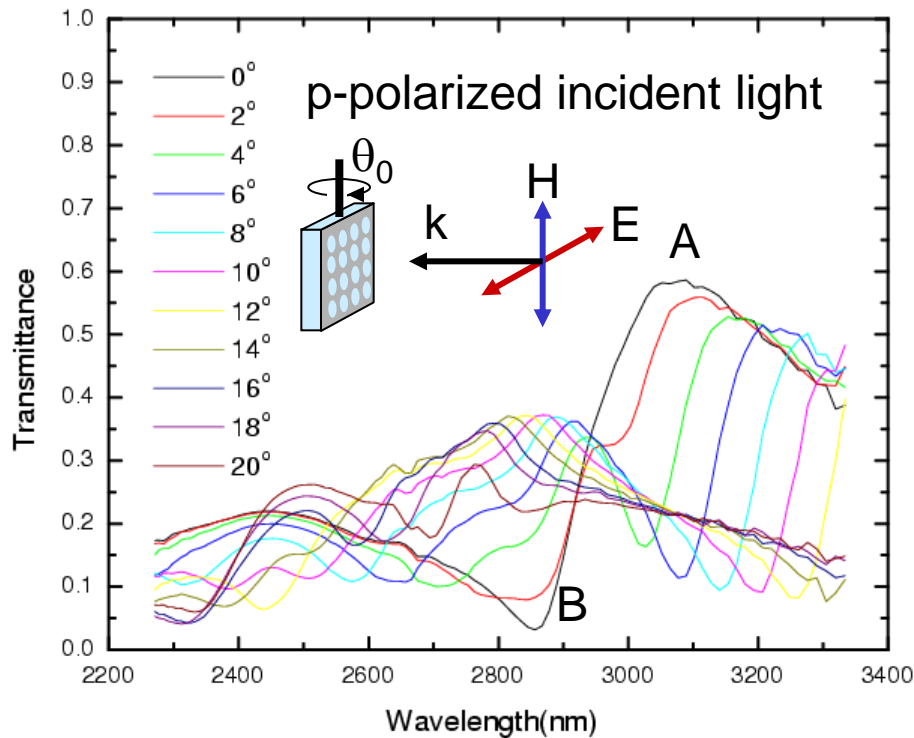
Transmittance with s-polarized light



1. Only $(0, j)$ modes ($j \neq 0$) will be excited because the E-field is parallel to the y-axis on the metal surface.
2. Peak A and dip B are due to the degenerate $(0,1)$ and $(0,-1)$ modes at the film-silica interface.



Transmittance with p-polarized light



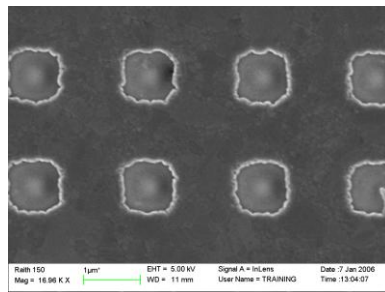
1. Only $(i, 0)$ modes ($l \neq 0$) will be excited because there is an E-field component parallel to the x-axis on metal surface, but no component parallel to the y-axis.
2. Peak A and dip B are due to $(1,0)S$ and $(-1,0)S$ modes which are split by the “ $-i\sin\theta_0$ ” term.



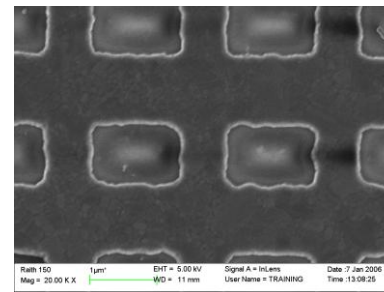
Aspect Ratio Experiment

1. All arrays are made in a 100 nm-thickness silver film on a fused silica substrate (refractive index $n = 1.4$)

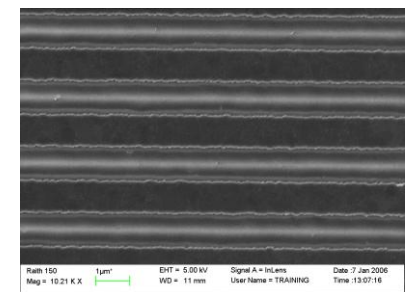
Square hole array



Rectangular hole array



Slit array



Hole size (μm^2) : 0.84 X 0.84

Period (μm) : 2.0

Open fraction: 0.18

1.3 X 0.9

2.0

0.29

1 μm width

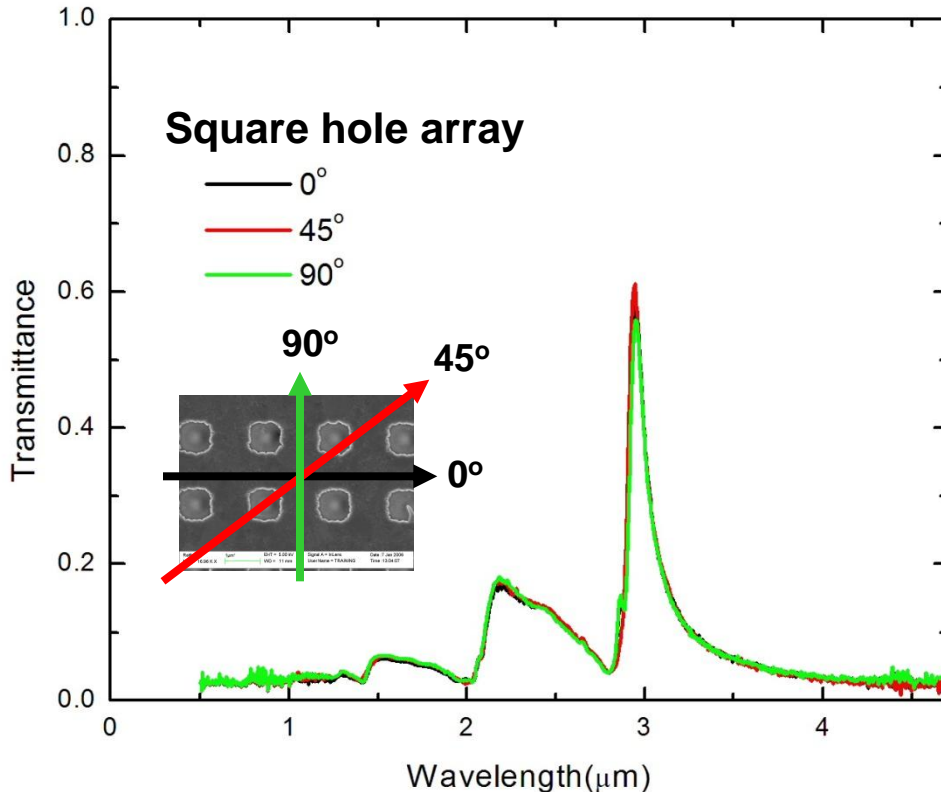
2.0

0.50

2. We measured the polarized transmittance vs. wavelength ($0.5 \mu\text{m} - 5 \mu\text{m}$)
3. The transmission of the sample is normalized by transmission of open hole of the same size as the sample, and corrected for the absorption in the fused silica



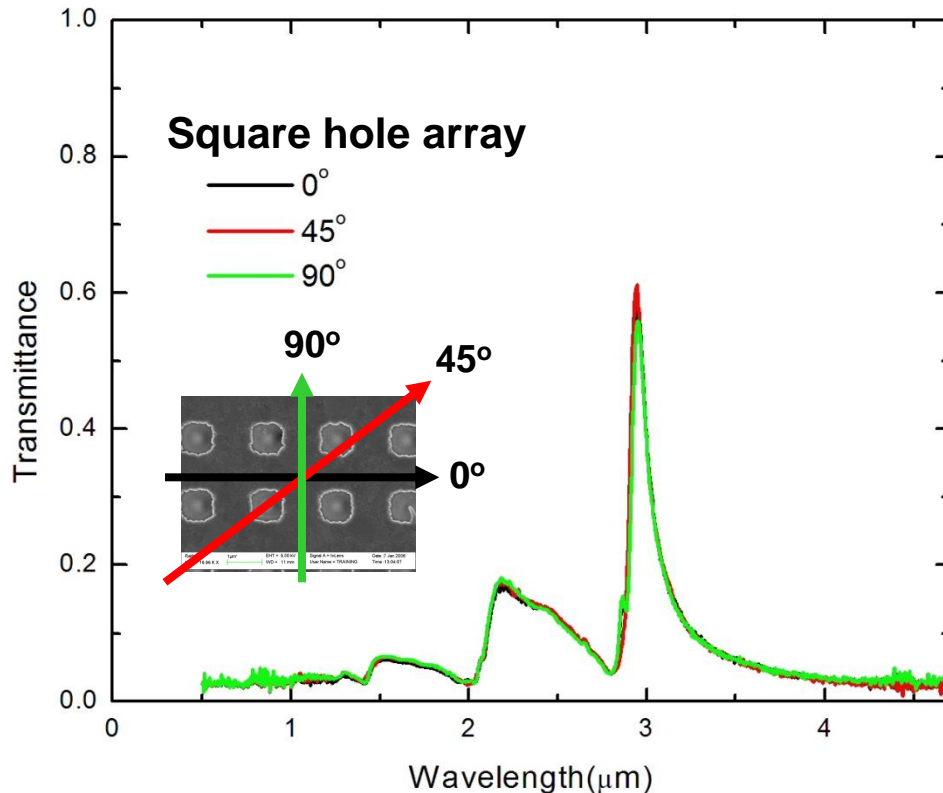
Square hole array



1. Maximum transmission is 61% at $\lambda = 2.94 \mu\text{m}$
2. All spectra (0° , 45° and 90° polarization) are the same
3. Decomposition of E field of 45° into 0° and 90° directions
4. Peak at $\lambda = 2.94 \mu\text{m}$ shows Fano profile
5. Second peak at $\lambda = 2.18 \mu\text{m}$



Square hole array



6. Transmission dips at $\lambda = 2.8$ μm , 2.0 μm and 1.4 μm correspond to diffraction to grazing angles at quartz and air interfaces, respectively

$$\lambda_{\min} = \frac{a_0}{\sqrt{i^2 + j^2}} \sqrt{\epsilon_d}$$

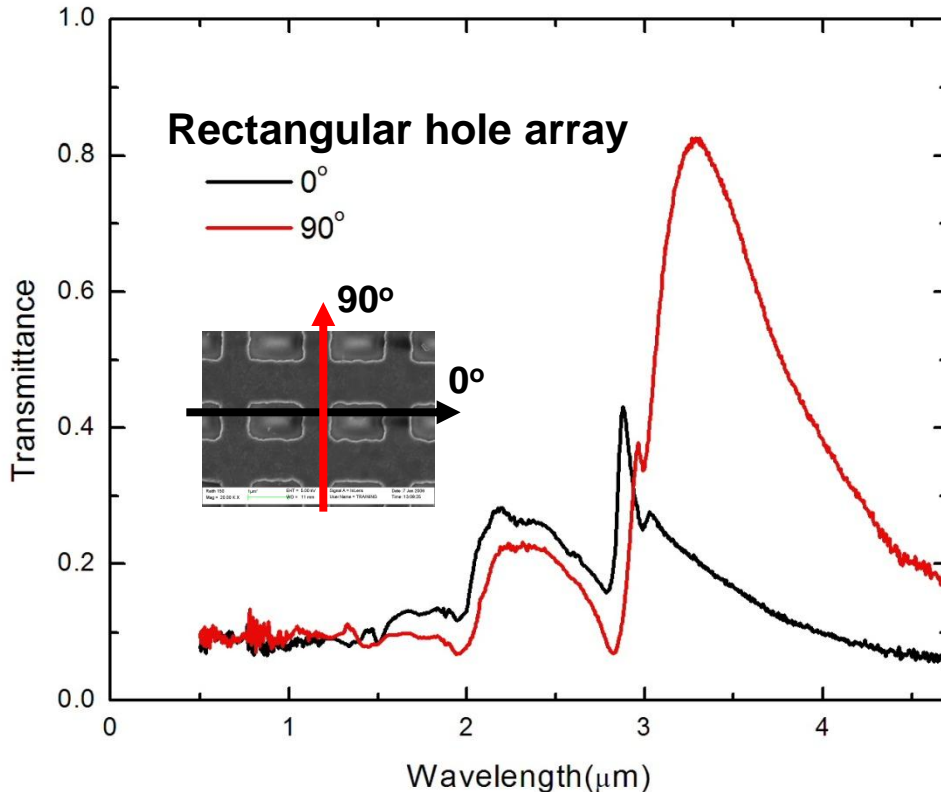
2.8 $\mu\text{m} \rightarrow (1,0)$ silica

1.4 $\mu\text{m} \rightarrow (1,0)$ air,
(1,1) silica

1.4 $\mu\text{m} \rightarrow (1,1)$ air,
(2,0) silica



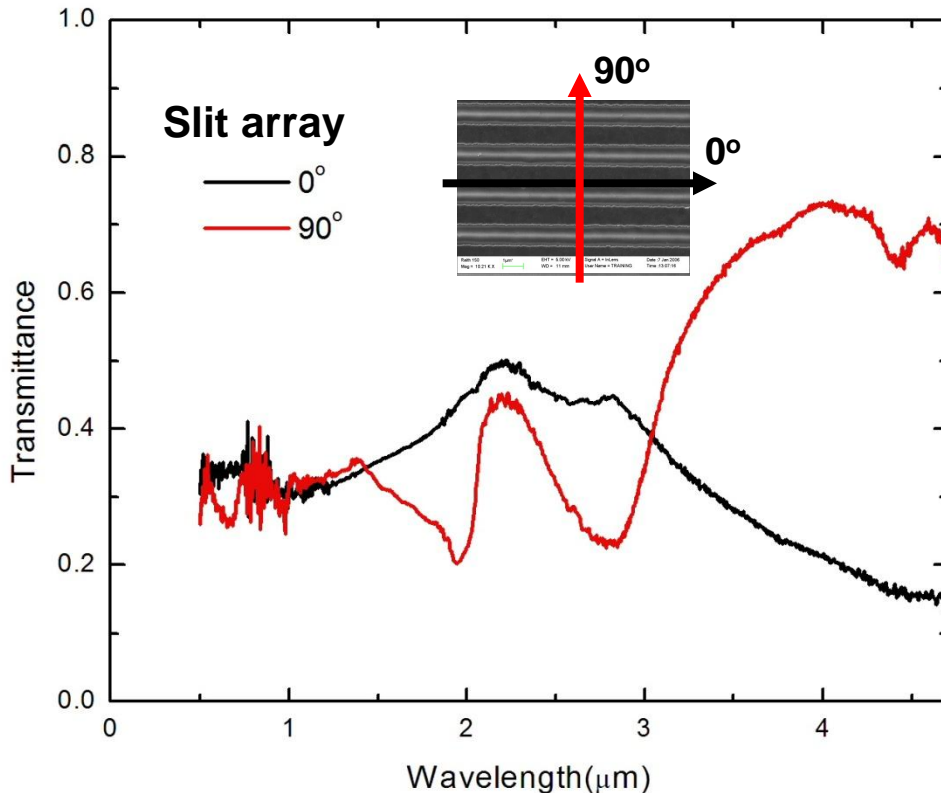
Rectangular hole array



1. Transmission maximum of 83% at $\lambda = 3.3 \mu\text{m}$ for 90° polarization
2. Another transmission maximum occurs at $\lambda = 2.9 \mu\text{m}$ for 0° polarization
3. The position of maximum transmission peak strongly depends on polarization direction due to the asymmetry of hole shape



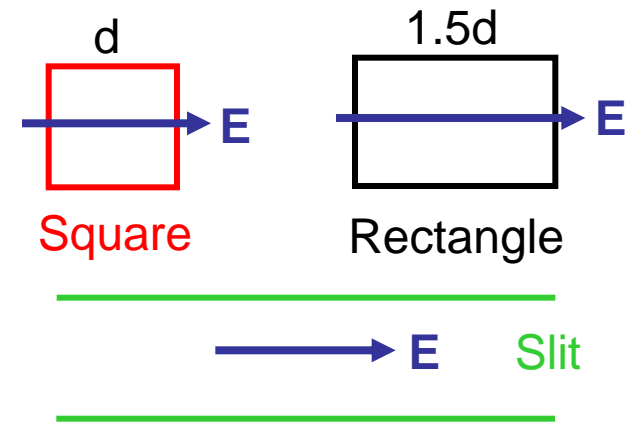
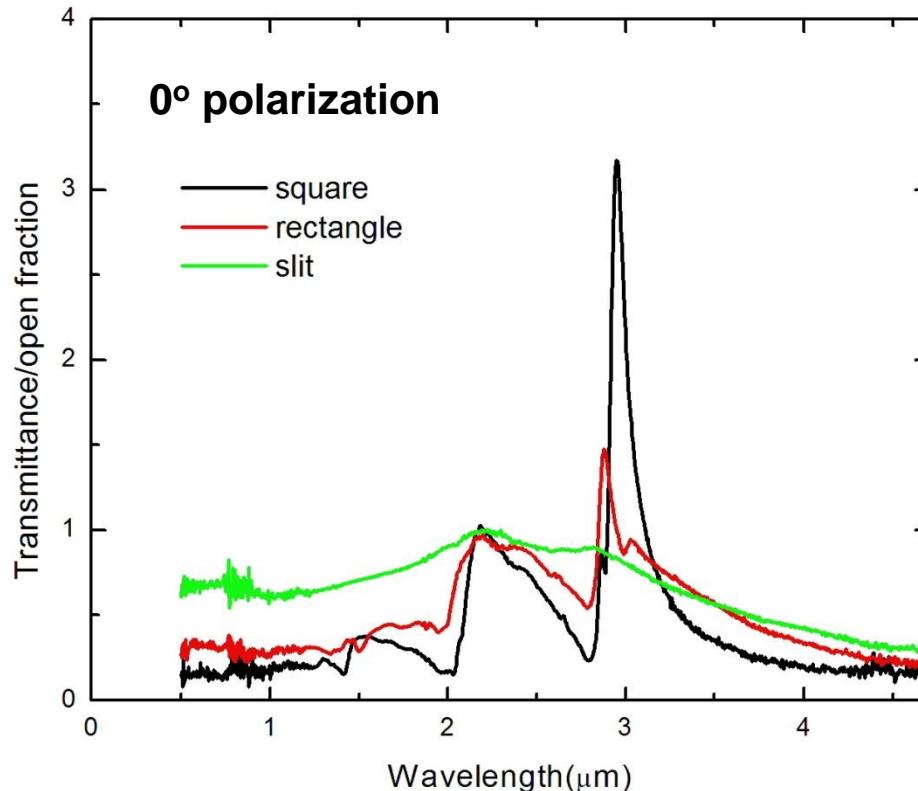
Slit array



1. Maximum intensity is 73% at $\lambda = 4.0 \mu\text{m}$ for 90° polarization
2. Maximum transmission peak disappears for 0° polarization
3. This is the expected result as the slit array is a wire grid polarizer



Transmission / open fraction for 0° polarization

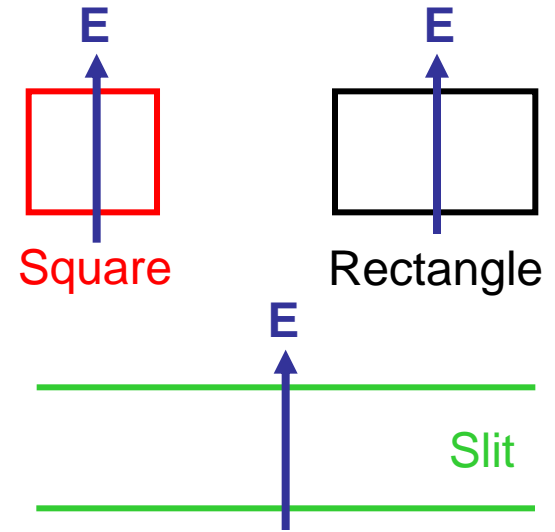
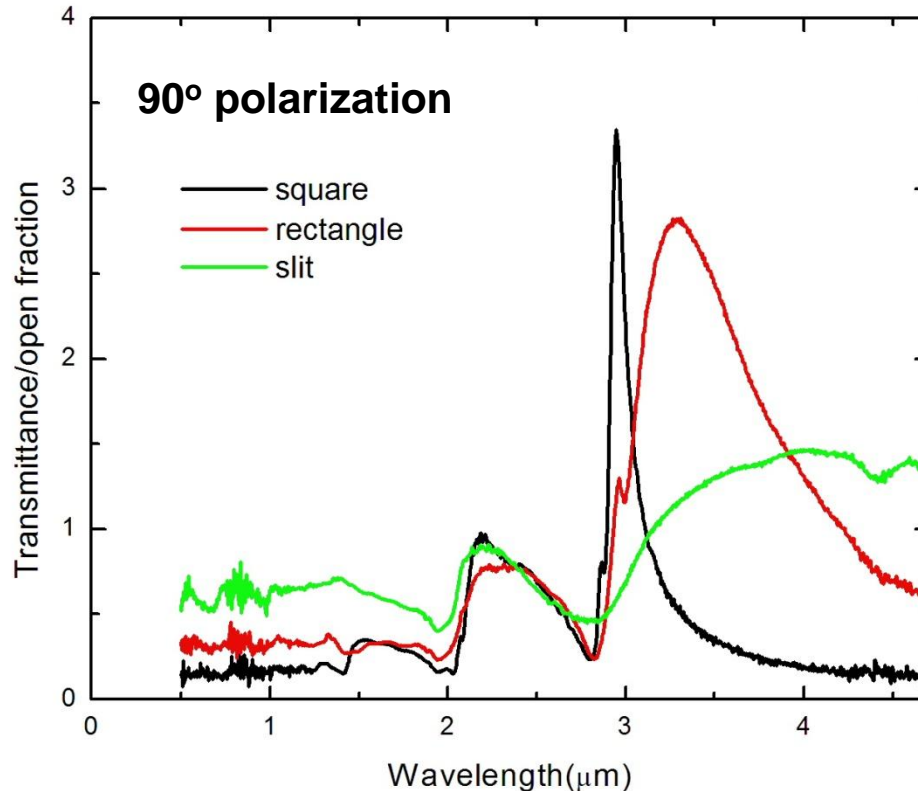


When the edge parallel to polarization becomes longer:

1. The largest peak shifts to shorter wavelengths
2. The maximum intensity decreases, and finally disappears for slit array



Transmission / open fraction for 90° polarization

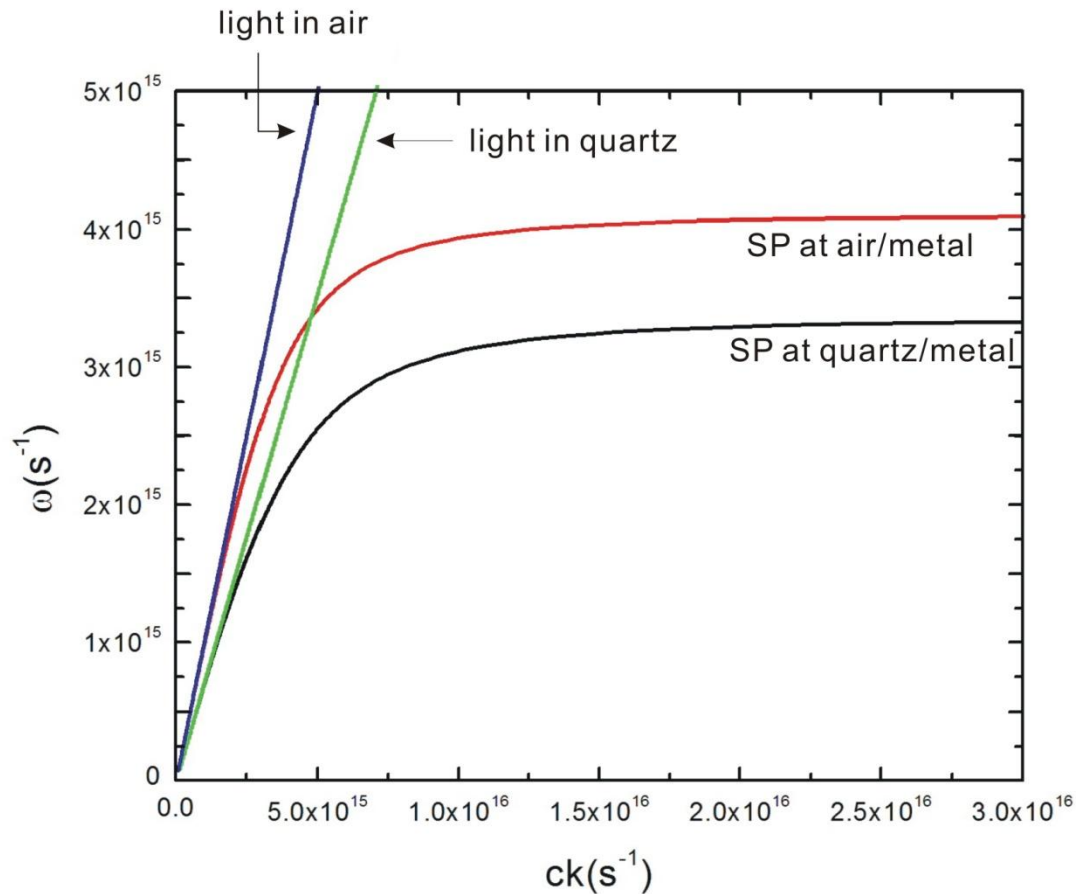


When the edge perpendicular to polarization becomes longer:

1. The largest peak shifts to longer wavelengths
2. The maximum intensity decreases, while the line-width becomes broader



Dispersion curves for surface plasmon and light lines for air-metal and fused silica-metal interfaces



CDEW (Composite Diffractive Evanescent Wave)

Evanescent wave at $z = 0$

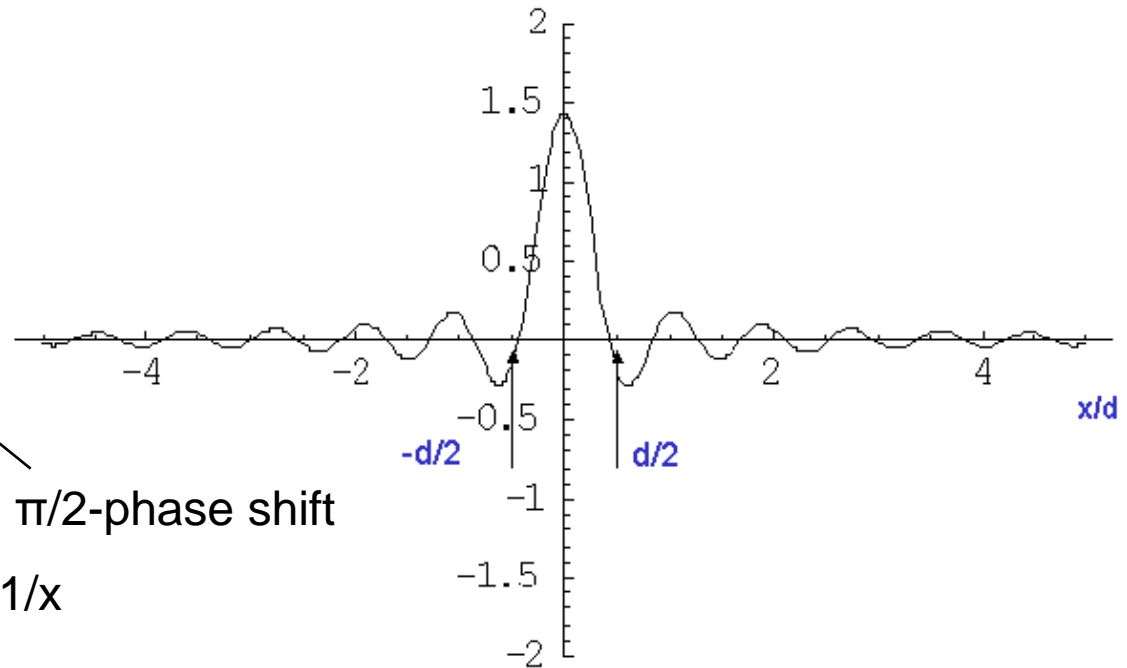
$$E_{ev}(x,0) = -\frac{E_0}{\pi} \left\{ \text{Si} \left[k_0 \left(x + \frac{d}{2} \right) \right] - \text{Si} \left[k_0 \left(x - \frac{d}{2} \right) \right] \right\} \quad \text{for } |x| > \frac{d}{2} \quad \text{Si}(\beta) \equiv \int_0^\beta \frac{\sin t}{t} dt$$

↓ approximation

$$E_{ev} \approx \frac{E_0}{\pi} \left(\frac{d}{x} \right) \cos \left(k_0 x + \frac{\pi}{2} \right)$$

CDEW has a $\pi/2$ -phase shift

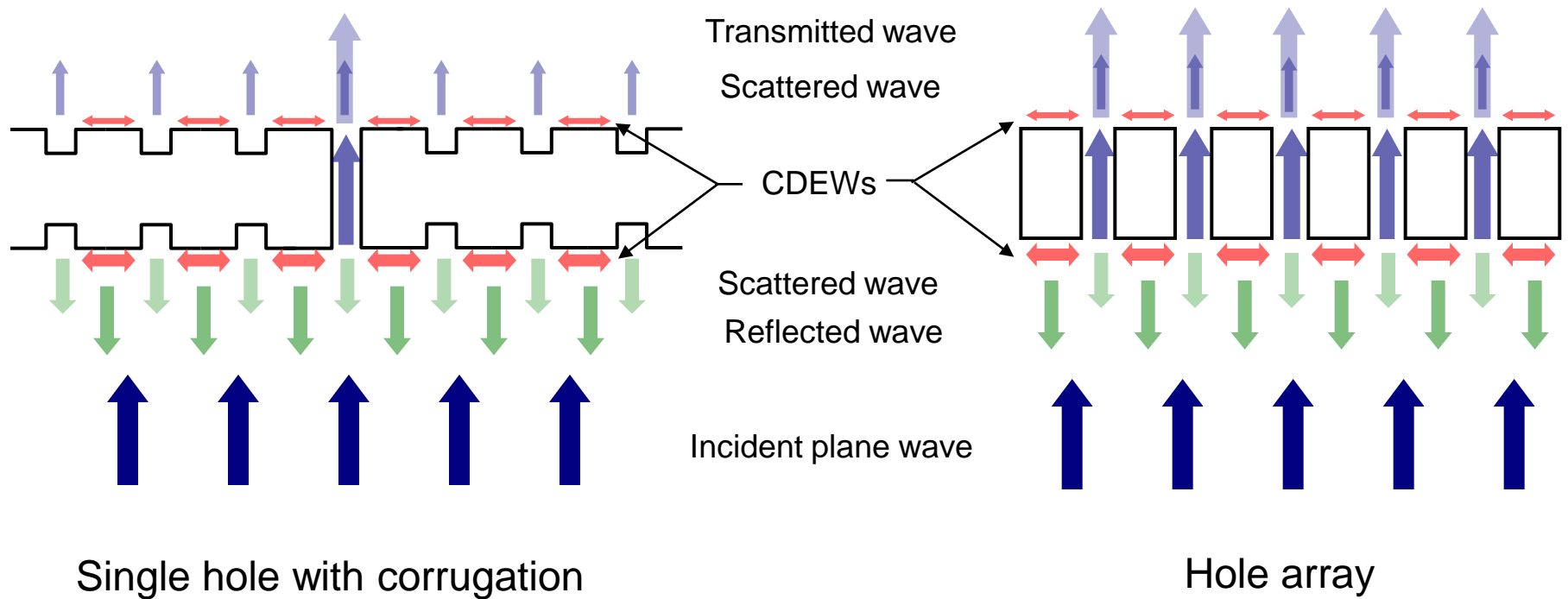
CDEW intensity decreases as $1/x$



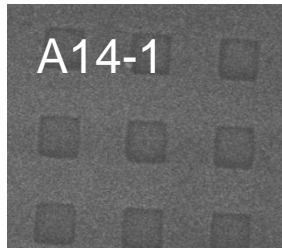
G. Gay et al., *J. Phys.: Conference series* **19**, 102 (2005)



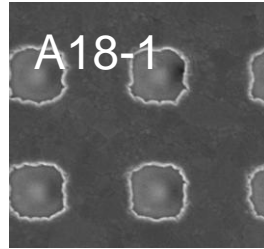
Transmission with CDEWs



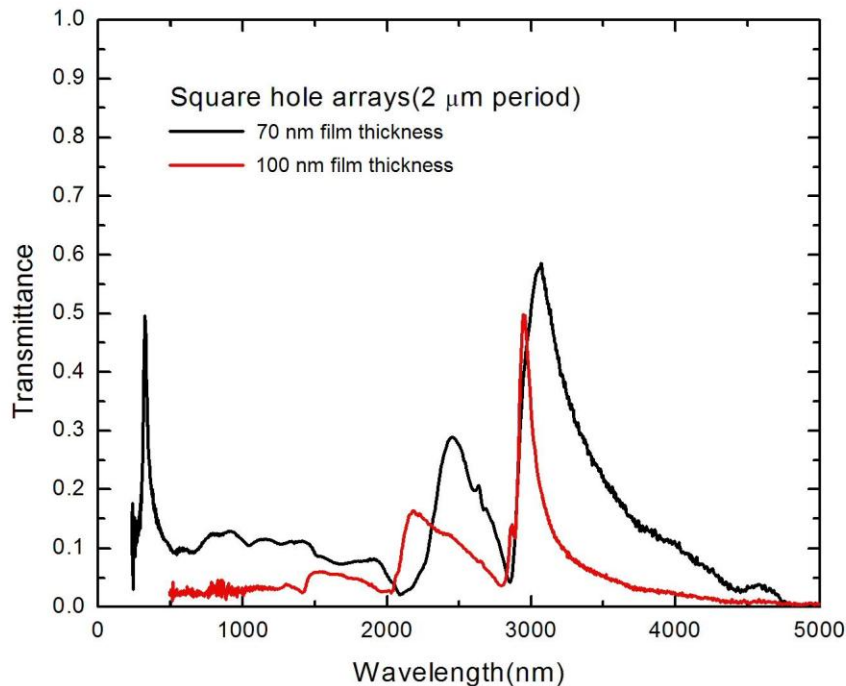
Dependence of transmittance on film thickness



70 nm



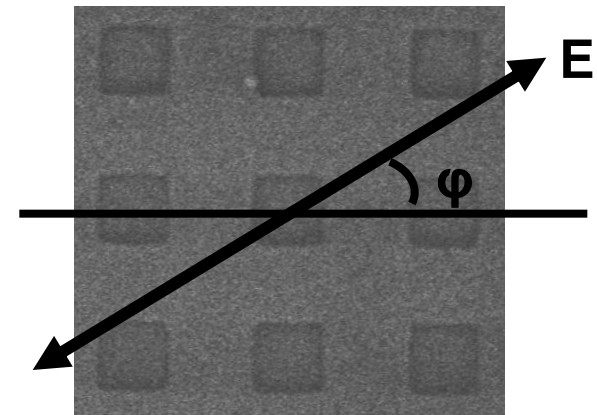
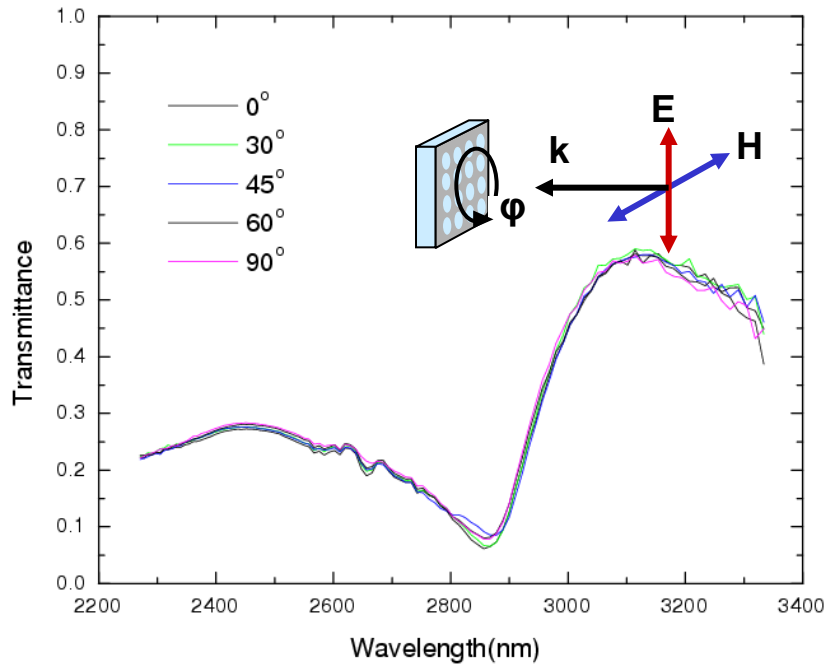
100 nm



- Reasons for difference between two spectra with the same period
 - Different thickness
 - Possible imperfection in the 70 nm-thickness hole array
 - Hole shape effect in the 100 nm-thickness hole array
 - Effective hole size difference



Dependence of transmission on azimuthal angle

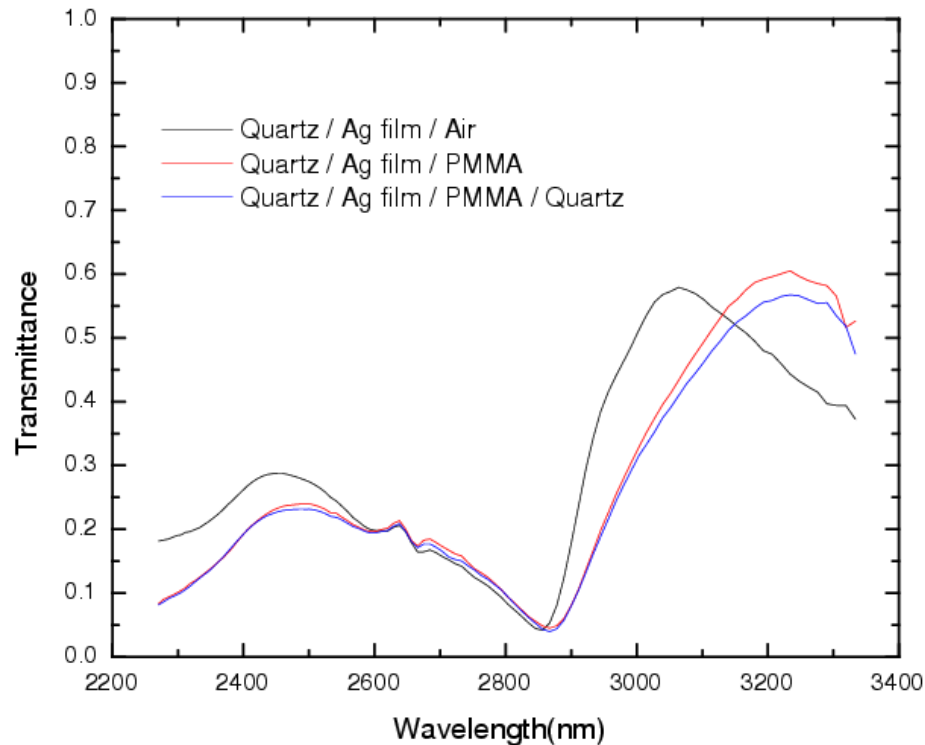


θ_0

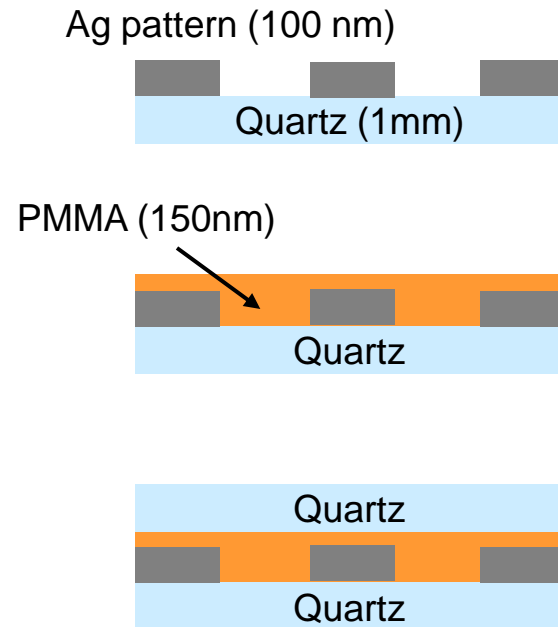


Effect of refractive index of top layer

A14-1



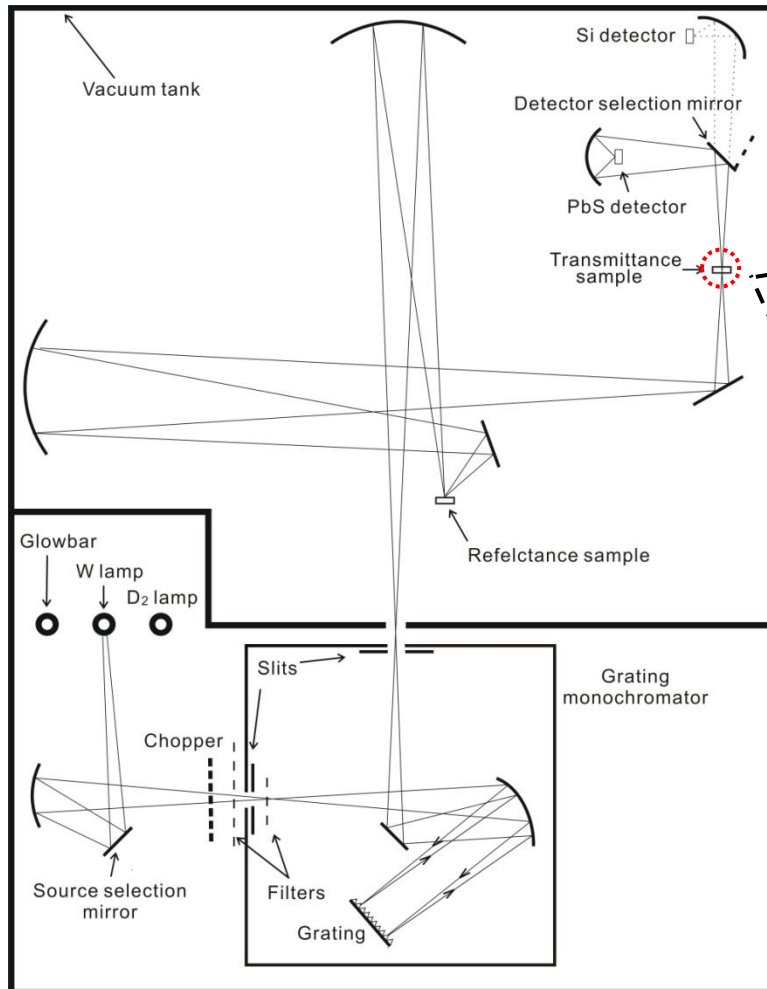
- Peak at 3070 nm shifts to longer wavelengths due to change of refractive index of top layer.



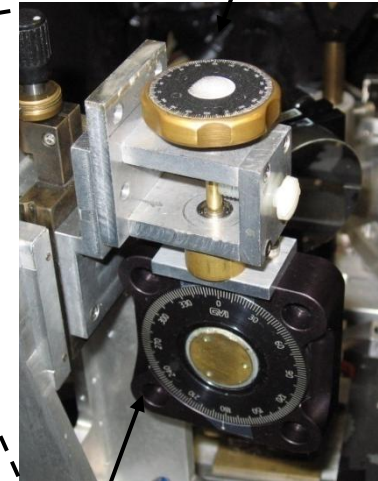
$$\lambda (i^2 + j^2)^{1/2} = D_g \left[\frac{\epsilon_d \epsilon_m}{\epsilon_d + \epsilon_m} \right]^{1/2}$$



Perkin-Elmer 16U monochromatic spectrometer



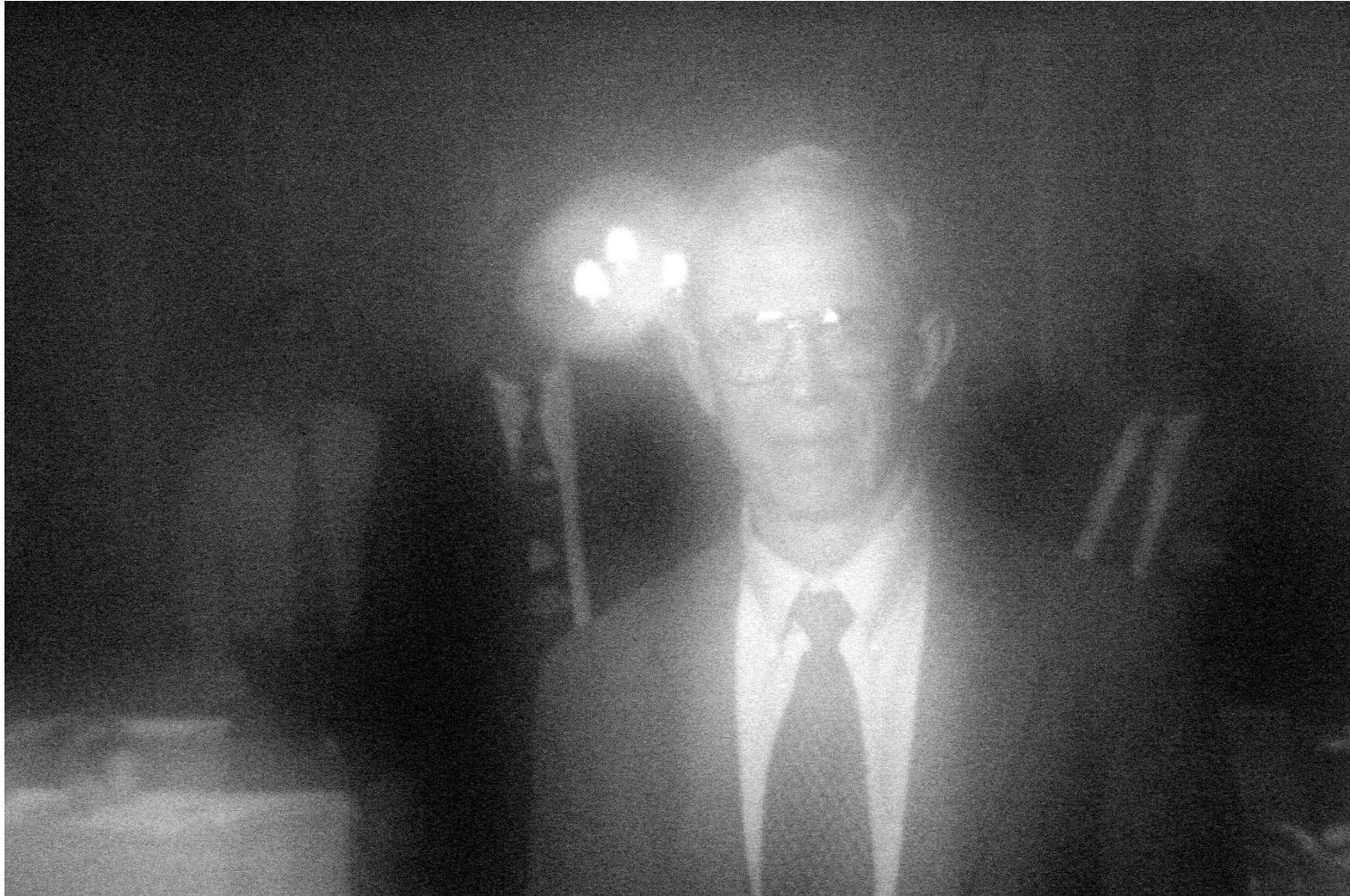
Incident angle rotator



In-plane polarization angle rotator



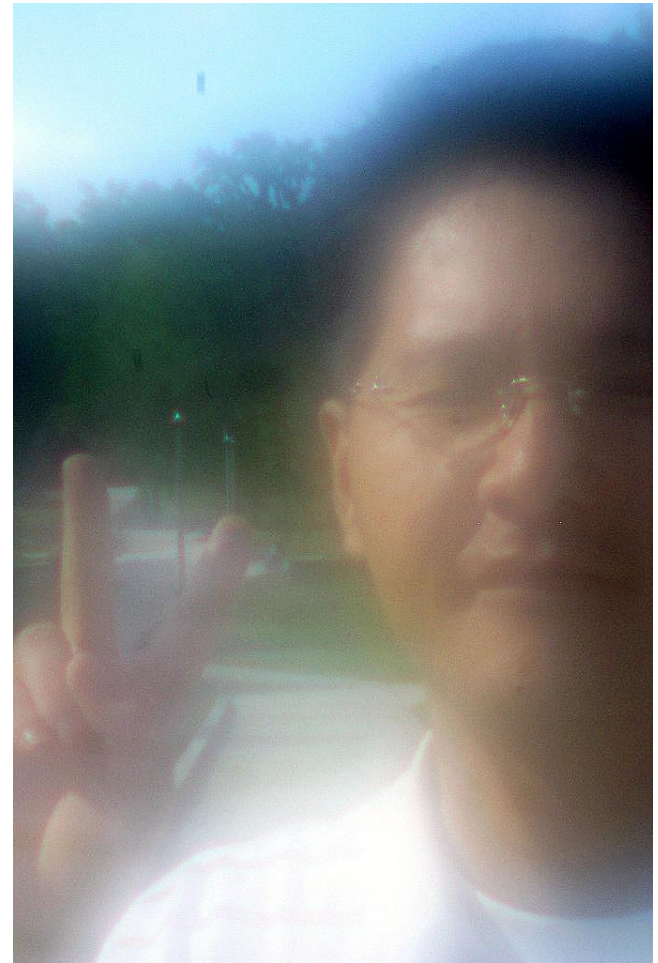
Indoor picture



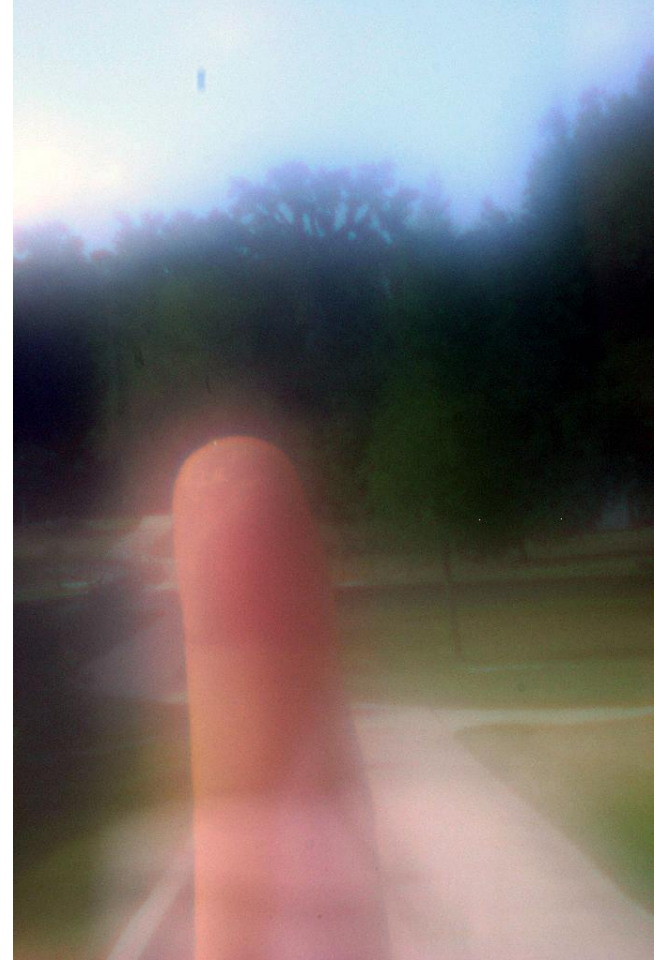
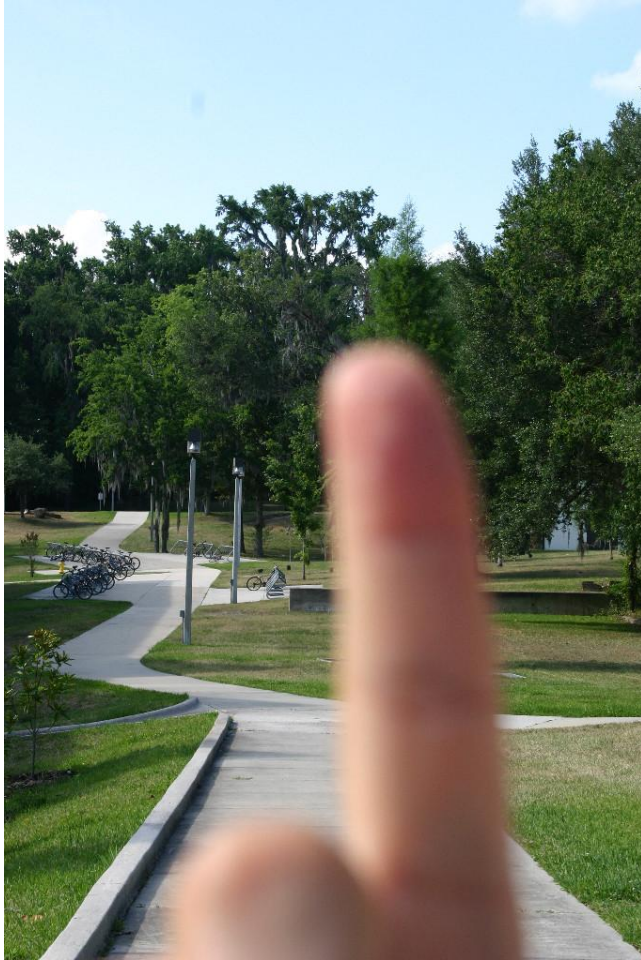
Depth of field at 2.5 feet



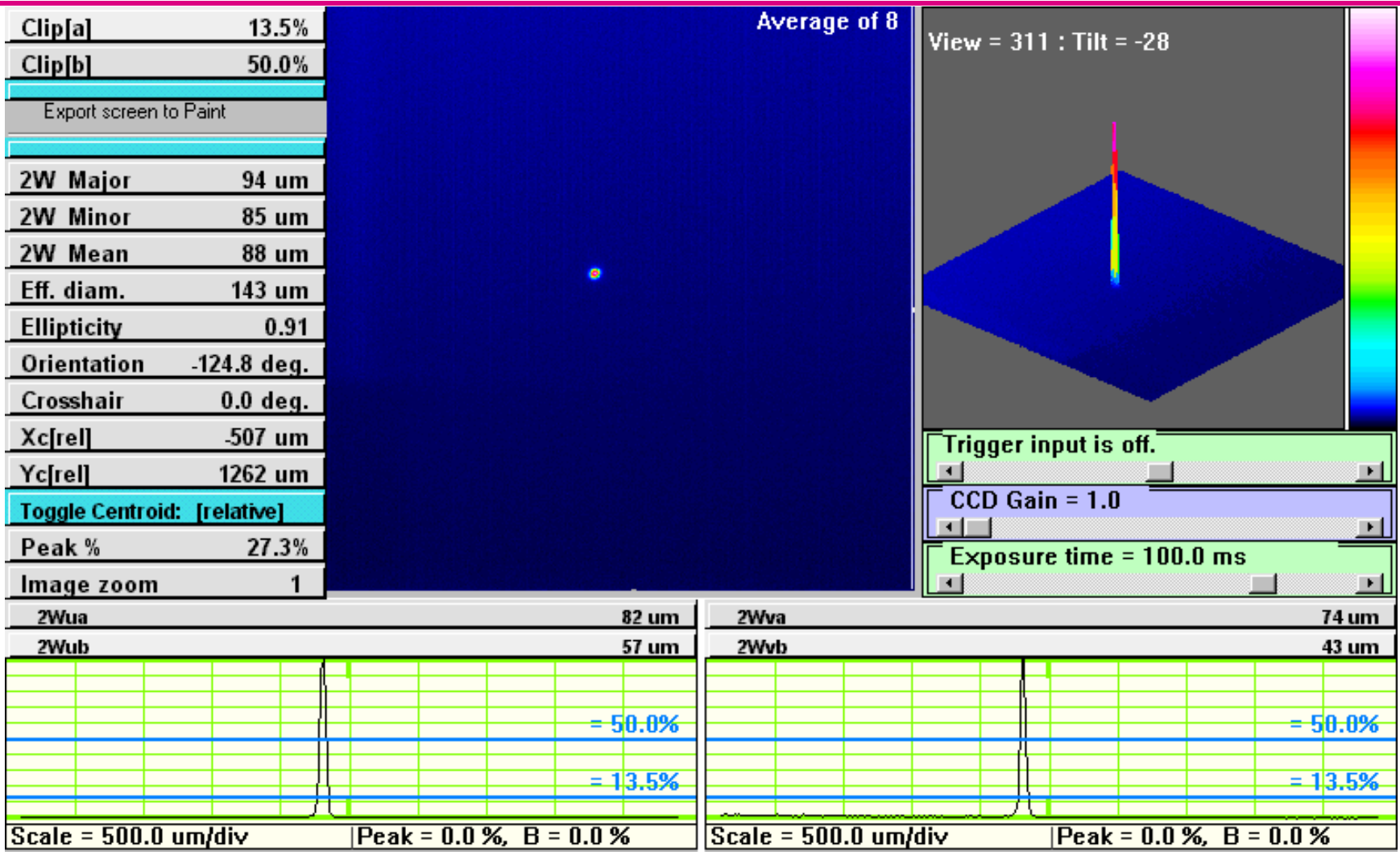
Depth of field at 2.5 feet



Depth of field at 1 foot



PSF of 50 mm lens



PSF of photon sieve

